

Lukas Schober BSc

Biocatalytic intramolecular hydroacylation via Tishchenko-like reaction catalysed by alcohol dehydrogenases

MASTER'S THESIS

to achieve the university degree of

Master of Science

Master's degree programme: Chemistry

submitted to

Graz University of Technology

Supervisor

Hall, Melanie, Ass.-Prof. Priv.-Doz. Dr.rer.nat.

Department of Chemistry

Organic/Bioorganic Chemistry

8010 Graz, Heinrichstraße 28/II

Graz, April 8 2021

Lukas Schober BSc

Biocatalytic intramolecular hydroacylation via Tishchenko-like reaction catalysed by alcohol dehydrogenases

MASTER'S THESIS

to achieve the university degree of

Master of Science

Master's degree programme: Chemistry

submitted to

Graz University of Technology

Supervisor

Hall, Melanie, Ass.-Prof. Priv.-Doz. Dr.rer.nat.

Department of Chemistry

Organic/Bioorganic Chemistry

8010 Graz, Heinrichstraße 28/II

Graz, April 8 2021

AFFIDAVIT

I declare that I have authored this thesis independently, that I have not used other than the declared sources/resources, and that I have explicitly indicated all material which has been quoted either literally or by content from the sources used. The text document uploaded to TUGRAZonline/KFUonline is identical to the present master's thesis.

08.04.21



Date, Signature

Acknowledgments

First of all, I would like to thank Univ.-Prof. Dipl.-Ing. Dr.techn Wolfgang Kroutil and Ass.-Prof. Priv.-Doz. Dr.rer.nat.Melanie Hall, who gave me the possibility for this thesis in the first place. My gratitude especially belongs to Ass.-Prof. Priv.-Doz. Dr.rer.nat.Melanie Hall for her supervision and help with everything in general from administrative problems, over problems during the lab time to writing this thesis.

Special thanks also to every elk, moose, and deer of the Elkcrew for the amazing working conditions, help and fun we had together. Moreover, I have to thank our technician Ing. Tarama Reiter for her help in enzyme expression and cell cultivation. Furthermore, gratitude to my dear lab colleagues and good friends Florian and Victor as well as my new lab buddy Tarek. All three of them helped a lot during my work with their ideas and opinions, collaborate well together and we were able to learn from each other.

Last, but not least I would like to thank all my friend and my whole family, especially my father Michael Schober and his wife Karin, as well as my mother Sabine Mitteregger for their support and making studying for me possible in the first place.

Abstract

A biocatalytic synthesis of several dihydrodibenzoxepinones and dihydrodibenzoxepinols was achieved via intramolecular hydroacylation from biaryllic compounds containing ketone and aldehyde moieties by employing wild-type and engineered alcohol dehydrogenases. Through NAD(P)H dependent short-chain dehydrogenases/reductases (SDRs) substrate consumption of over 99% and high optical purity (up to >99% ee) have been achieved. Furthermore, a successful coupled-substrate recycling system using isopropanol was applied to shift the formation of product from 7-methyldibenzo[*c,e*]oxepin-5(7*H*)-one to 7-methyl-5,7-dihydrodibenzo[*c,e*]oxepin-5-ol and 5-methyl-5,7-dihydrodibenzo[*c,e*]oxepin-5-ol and increase the conversion to 88 % and 90 %, respectively. Moreover, the significance of this system was shown by increasing the amount of substrate to a 50 mg scale.

Key words: biocatalysis; enzymes, alcohol dehydrogenases; disproportionation; lactonisation; hydroacylation; Tishchenko reaction; cofactor recycling

Abstract

Eine biokatalytische Synthese von Dihydrodibenzooxepinonen und Dihydrodibenzooxepinolen wurde erreicht durch intramolekulare Hydroacylierung von biarylischen Verbindungen mit Keton und Aldehyd Gruppen mithilfe Verwendung von natürlichen und modifizierten Alkoholdehydrogenasen. Durch den Einsatz von NAD(P)H abhängigen kurzkettigen Dehydrogenasen/Reduktasen (SDRs) konnten ein Substratverbrauch von über 99% und eine hohe optische Reinheit (bis zu >99% ee) erreicht werden. Weiters, wurde erfolgreich ein Substrat-gekoppeltes Recyclingsystem, das Isopropanol verwendet, implementiert um das Produkt von 7-methyldibenzo[*c,e*]oxepin-5(7*H*)-one zu 7-methyl-5,7-dihydrodibenzo[*c,e*]oxepin-5-ol und 5-methyl-5,7-dihydrodibenzo[*c,e*]oxepin-5-ol zu verschieben und den Umsatz auf 88 %, beziehungsweise 90 % zu erhöhen. Außerdem wurde die Relevanz des Systems durch die Erhöhung der eingesetzten Substratmenge zu 50 mg gezeigt.

Schlüsselwörter: Biokatalyse; Enzyme; Alkoholdehydrogenasen; Disproportionierung; Lactonisierung; Hydroacylierung; Tishchenko Reaktion; Cofaktor Recycling

Inhalt

1. Introduction	11
1.1. Biocatalysts.....	11
1.2. ADHs as biocatalysts.....	12
1.2.1. Aldo-keto reductases (AKRs)	13
1.2.2 Short-Chain Dehydrogenases/Reductases (SDR)	14
1.2.3 Medium-Chain Dehydrogenases/Reductases (MDR).....	14
1.2.4. Long-Chain Dehydrogenases/Reductases	15
1.2.5. Used ADHs	16
1.3. Prelog rule	18
1.4. Coupled substrate/ enzyme approach for recycling systems	19
1.5. Disproportionation	24
1.5.1. Cannizzaro reaction.....	24
1.5.2. Tishchenko reaction	26
1.6. Suzuki coupling.....	29
1.7. Hydroacylation reactions.....	31
2. Goals	33
3. Results and discussion	35
3.1. Docking study	37
3.1.1. [1,1'-biphenyl]-2,2'-dicarbaldehyde	44
3.1.2. 2'-acetyl-[1,1'-biphenyl]-2-carbaldehyde	50
3.1.3. 2'-(2,2,2-trifluoroacetyl)-[1,1'-biphenyl]-2-carbaldehyde.....	53
3.1.4 2'-benzoyl-[1,1'-biphenyl]-2-carbaldehyde	56
3.2 Screening.....	60
3.2.1. [1,1'-biphenyl]-2,2'-dicarbaldehyde	60
3.2.2. 2'-acetyl-[1,1'-biphenyl]-2-carbaldehyde	61
3.2.3. 2'-(2,2,2-trifluoroacetyl)-[1,1'-biphenyl]-2-carbaldehyde.....	68
3.2.4. 2'-benzoyl-[1,1'-biphenyl]-2-carbaldehyde	74

3.3. Up-Scale.....	80
3.3.1. Up-scale entry 2-Biotransformation of 1b with Lk-ADH Lica under reductive conditions..	81
3.3.2. Up-scale entry 3-Biotransformation of 1b with Kp-ADH under reductive conditions	83
3.3.3. Up-scale entry 4-Biotransformation of 1c with Lk-ADH Lica under reductive conditions ..	84
3.3.4. Up-scale entry 5-Biotransformation of 1c with TR I under reductive conditions	85
3.3.5. Up-scale entry 6-Biotransformation of 1c with TR II under redox-neutral conditions	86
3.3.6. Up-scale entry 9-Biotransformation of 1d with Sy-ADH under reductive conditions.....	87
4. Experimental section	89
4.1 General information	89
4.2. Synthesis General	90
4.3. Biotransformation	91
4.4. Product characterisation	92
4.5. Synthesis.....	95
4.6. Enzyme expression	99
4.6.1. Enzyme solubility test of TRII	99
4.6.2. Activity test of TRI and TRII	104
5. Conclusion & Outlook	105
6. Reference:	108
7. Appendix	120

1. Introduction

1.1. Biocatalysts

One of the most important applications of chemistry is catalysis, a subject allowing a plethora of modern chemical reactions. Catalysis enables reactions to yield the desired products in the first place and accelerates reactions to a useable degree by lowering the activation energy. By definition a catalyst must take part in a reaction but cannot be used up in this reaction. Biocatalysts, catalyst directly produced by living organisms, or to be more specific enzymes, are still emerging in the last several decades and can replace several important key-steps in synthesis, thanks to lower costs, better environmental sustainability, and general efficiency.

Several biocatalytic reactions have already been able to evolve from an interesting academic synthetic tool towards an industrially feasible technology. Examples are the synthesis of (*S*)-Dulox alcohol, a key precursor for the antidepressant Duloxetine^[1], the synthesis of the diabetes drug Sitagliptin via transamination^[2] and biocatalytic cascade for vanillin production.^[3] The use of enzymes as catalysts also gives several advantages. Enzymes have the possibility to be excellent and effective catalysts for suitable substrates, typical reactions can be accelerated by a factor of 10^8 - 10^{10} and higher in special cases, such as with catalase, which catalyses the decomposition of hydrogen peroxide to water and oxygen up to 10^{12} -fold compared to the non-catalysed process. Therefore, enzymes are usually employed in lower concentrations compared to most chemical catalysts that have to be used in the range of 0.1 to 10 mol%, while enzymes are able to perform at even 10^{-4} mol%.^[4,5] Enzymes are not only used in very low concentration but also under mild conditions. For example, the optimal temperature range for many enzymes is from 20 to 40 °C, while most enzymes show the best stability and activity in a pH range between pH 5-8. While a plethora of catalysts depend on different heavy metals for the catalytic activities and therefore, exhibit several environmental challenges regarding qualities such as difficult disposal and toxic waste, biocatalysts are well environmentally acceptable since they are effortlessly and completely degraded under natural conditions.

Another advantage of biocatalysts is the capability of enzymes to display three major types of selectivity, such as chemoselectivity that allows the enzyme to act specifically on one single type of functionality and preserve other functional groups in the molecule leading to less side reactions. This may lead to higher conversions and less purification steps. The regioselectivity exhibited by biocatalysts allows to distinguish identical functional moieties in different positions of the compound, due to the specific fit of the substrate in the 3-dimensional structure in the active site, leading to very specific products with transformed and retained functional groups. Stereoselectivity is also a very important aspect, due to their structure enzymes can recognise and act specifically on chiral

compounds leading to pure chiral products, perform deracemization of mixtures and may introduce new stereo centres, when acting on prochiral molecules. These specific ways an enzyme can mediate reactions contribute to the properties of the biocatalysts and are some of the most important factors in selective and asymmetric synthesis.^[6]

The chirality of products has great importance for example in pharmaceutical compounds and industrial chemistry, since different enantiomers show vastly different properties. While one enantiomer has a pleasant odour, the other form may exhibit a terrible scent, or while one enantiomer can have medical applications, the other enantiomer could be toxic. One of the most infamous examples for the different effects an enantiomer can have is probably the disaster caused by “thalidomide”, a drug that was administered to treat mild cases of pain and nausea mainly in pregnant women during the 1960s. The sedative effect residing in the (*R*)-enantiomer have been well know at the time, while the highly teratogenic effects of the (*S*)- enantiomer still had to be discovered. Due to cases like this and the resulting policy changes regarding this issue, the demand of accessible asymmetric processes steadily increased.^[7] One solution to ensure simple access to products in high enantiomeric purity is therefore, the use of biocatalysts.

1.2. ADHs as biocatalysts

Alcohol dehydrogenases (ADHs) are some of the most important and most broadly applied enzymes of the oxidoreductase class. All oxidoreductases are grouped in EC 1. This refers to Enzyme Commission number, an enzyme cataloguing system based on the reactions they catalyse. ADHs catalyses the transformation of a carbonyl-group into the reduced alcohol functionality. When dealing with a prochiral substrate, ADHs can especially excel in carrying out such reductions in a stereoselective fashion, to create a chiral centre in the product.^[8]

ADHs are biologically very important enzymes and have been found and identified in almost every organism, both prokaryotic and eukaryotic microorganisms as well as multicellular organisms such as plants and animals. Therefore, a huge number of ADHs exist and even more are expected to be found. In general, the family of ADHs serves for the reversible oxidation and reduction of a wide scope of alcohols, aldehydes, and ketones. This reduction is coupled with the stoichiometric consumption of NADH or NADPH as a cofactor for the reduction, while a stoichiometric amount of NAD⁺ or NADP⁺ is needed for the reverse oxidative reaction.

Alcohol dehydrogenases can be divided into 4 different superfamilies: Aldo-keto reductases (AKRs), short-chain dehydrogenases/reductases (SDR), medium-chain dehydrogenases/reductases (MDR)^[9] and long-chain dehydrogenases/reductases.

1.2.1. Aldo-keto reductases (AKRs)

Usually AKRs are monomeric proteins and possess a characteristic $(\alpha/\beta)_8$ -barrel structure. The typically length of enzymes in this superfamily is in the range of approximately 325 amino acids, resulting in a molecular mass of about 37 kDa. A characteristic feature of AKRs is the total lack of Rossmann-fold motif for binding of the cofactor. Members of this superfamily in general possess a capability to use a number of aliphatic and aromatic aldehydes and ketones, including sugars, steroids, and xenobiotics as substrates.^[10,11]



Figure 1 Mechanism of reduction (left) and oxidation (right) of an aldehyde or ketone by an Aldo-keto reductase

All AKRs use a catalytic tetrad at the active site consisting of tyrosine, lysine, aspartate, and histidine for binding the substrate. When reducing a substrate, the hydride of the cofactor attacks the carbonyl carbon and the hydroxyl-group of the tyrosine serves as an acid to protonate the substrate. The effectivity of this acid–base catalyst is enhanced by the surrounding histidine and lysine that lower the pK_a of the tyrosine. While the protonated histidine serves to donate an H^+ to the OH-group, when reducing a substrate, the lysine is responsible for deprotonating the OH-group in the oxidation reaction. In this case, the acid moiety of the asparagine deprotonates the ϵ -amino group of the lysine that regains a proton by removing the hydrogen of the hydroxy group leaving it capable of acting as a base and deprotonating the substrate.^[11] This mechanisms is displayed in Figure 1 above.

The superfamily of AKRs can be divided into 14 different families named systematically AKR1 to AKR14. All the families are further subdivided into subfamilies by adding a letter to the code. For example, the family AKR1 contains AKR1A (Aldehyde reductase), AKR1B (aldose reductase), AKR1C (hydroxysteroid dehydrogenase) and AKR1D (Steroid dehydrogenase).

1.2.2 Short-Chain Dehydrogenases/Reductases (SDR)

The SDR superfamily is the largest of the three ADH superfamilies and one of the largest enzyme superfamilies in general, consisting of over 46000 members. An important feature of dehydrogenases of this superfamily is the presence of a Rossmann-fold motif that serves to bind the nicotinamide-based cofactor. There are two different types of SDR, the around 250 amino acid long enzyme, regarded as the “classical” short variant and an extended one with an additional residue domain in the C-terminal region of the protein containing additional 100 amino acids.^[9]

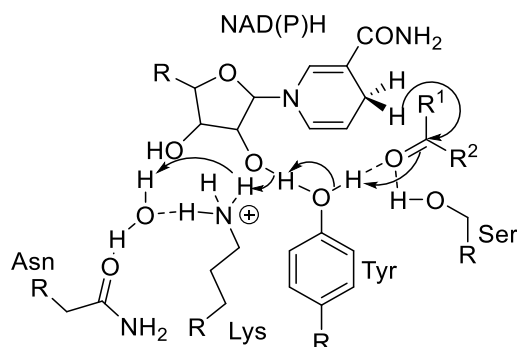


Figure 2 Mechanism of reduction of an aldehyde or ketone by an SDR

A characteristic that SDRs possess is a catalytic triad consisting of a serine, a tyrosine and a lysine that often also have an additional fourth amino acid, an asparagine, therefore, extending the catalytic triad of Ser-Tyr-Lys to a tetrad of Asn-Ser-Tyr-Lys. After the hydride of the cofactor attacks the substrate, the tyrosine moiety of the catalytic centre serves as an acid–base catalyst. The hydroxy group of this amino acid is able to accept or donate a proton from or to the substrate, when it is reduced or oxidised. This ability to act as a catalytic acid/base can be enhanced by an adjacent lysine and the oxidized, positively charged nicotinamide-based cofactor. Both factors contribute to lower the pK_a value of the hydroxy group of the tyrosine, allowing a much easier protonation/ deprotonation. The tyrosine can be reprotonated by the 2'-hydroxygroup of the ribose of the NAD(P)H, the lysine can donate one of the protons of its ϵ -amino group to the sugar of the cofactor. The ϵ -amino group of the lysine can then regain a proton of a water molecule, this is enhanced by the asparagine of the tetrad by activation and fixation of one single water molecule.^[9] Mechanism is shown in Figure 2.

1.2.3 Medium-Chain Dehydrogenases/Reductases (MDR)

The MDR superfamily contains over 10000 different ADHs with a typical size of around 350 amino acid residues, among these are some of the best investigated ADHs like the class I type mammalian ADH, also called horse liver dehydrogenase (HLADH; EC 1.1.1.1) which primary structure was solved already in 1970^[12]. Another example is the human ADH1^{[13][14]} that is one of the key enzymes in the human alcohol metabolism. Members of the MDR display a large variety in quaternary structures, possessing

monomers, dimers, trimers, and tetramers. Furthermore, several families can possess 1 or 2 zinc ions that play either a role as a catalytic centre or for structural purposes. In total each subunit can have 0, 1 or 2 zinc ions. In general, MDRs are made of 2 domains: on the C-terminal, there is a Rossmann-fold motif that binds the cofactor and a 6-stranded parallel β -sheet sandwiched between α -helices on each side, while the N-terminal domain consists of a core of antiparallel β -strands with α -helices positioned at the surface. This N-terminal domain serves for the binding of the substrate. Both domains are separated by a cleft containing a deep pocket.^[15] The MDR superfamily can be separated into following families. The zinc-dependent ADH family is with approximately 1000 members the largest of the families in the MDR superfamily and consists of dimeric proteins that possess at least one zinc ion. To this family belong some of the most important ADHs like for example liver ADHs.^[16] Due to also being zinc dependent tetrameric ADH^[17], TADH for short, was contained in the zinc-dependent ADH, before becoming an own separate subfamily. Their structure is like the name implies tetrameric and common yeast ADHs^[18] are found in this family. The cinnamyl ADH family^[19] (CAD) consists of monomeric enzymes that bind 2 zinc ions and use NAD(P)H as cofactor, and their main uses is in lignin biosynthesis in plant cell walls. However, CADs seem to be not limited to plant, for example YMR318C (ADH6) of *Saccharomyces cerevisiae* display a high catalytic activity for cinnamaldehyde as a substrate, although yeast is unable to synthesize lignin.^[20]

1.2.4. Long-Chain Dehydrogenases/Reductases

Overall, LDRs are considered as a widely heterogeneous family and are not discerned regarding molecular similarities, in contrast to the situation for several short-chain and medium-chain dehydrogenases, but coenzyme-binding segments are discernible. An important member of the LDRs for example, is glucose-6-phosphate dehydrogenase, an enzyme of the pentose phosphate pathway. Variants of this ADH exhibit about 20% strictly conserved residues, with overrepresented amount of glycine.^[21] The polyol-specific long-chain dehydrogenases/reductases (PSLDRs) are clustered into 7 sub-families which in turn are defined by a minimum of 30% internal amino acid identity. PSLDRs typically fold into monomers, sizing between 380 and 550 amino acid residues, and catalyse oxidation of secondary alcohol groups in polyol substrates using NAD(P)⁺ as the coenzyme. A common structural organization was suggested for PSLDRs where the active site is located in a cleft formed by two domains: a N-terminal Rossmann-fold domain required for binding the coenzyme, and a largely α -helical C-terminal domain that allows recognition and binding of substrates.^{[22][23]} Polyol dehydrogenases, PDH for short, like for example, sorbitol DH display a tetrameric structure, but in contrast to the tetrameric ADH PDHs possess only one zinc ion in the catalytic centre per subunit and none for structural purposes. Members of this group are specialised to act on sugar alcohols. Sorbitol dehydrogenase catalyses the isomerisation of L-idoitol and L-sorbose, D-glucitol and D-fructose and other related sugar alcohol substrates.^[20]

1.2.5. Used ADHs

In total 11 ADHs, listed in Table 1 below were used for investigation in this work.

Table 1 Information of ADHs used in this work

entry	PEG	Name	Organism	Cofactor
1	10	ADH-A	<i>Rhodococcus ruber</i> DSM 44541	NADH
2	53	Sy-ADH	<i>Sphingobium yanoikuyae</i> DSM 6900	NADPH
3	105	Ras-ADH	<i>Ralstonia</i> sp. DSM 6428	NADPH
4	180	Lb-ADH	<i>Lactobacillus brevis</i>	NADPH
5	326	Lk-ADH	<i>Lactobacillus kefir</i> DSM 20587	NADPH
6	474	Lk-ADH Montelukast	<i>Lactobacillus kefir</i> DSM 20587	NADPH
7	475	Lk-ADH Lica	<i>Lactobacillus kefir</i> DSM 20587	NADPH
8	478	Morphine dehydrogenase	<i>Pseudomonas putida</i>	NADH
9	587	Kp-ADH 50C10	<i>Kluyveromyces polysporus</i>	NADPH
10	585	Tropinone reductase I	<i>Datura stramonium</i>	NADPH
11	586	Tropinone reductase II	<i>Datura stramonium</i>	NADPH

ADH-A is an alcohol dehydrogenase from the bacterium *Rhodococcus ruber* DSM 44541, that can be employed for ketone–alcohol conversions in both the oxidative and reductive directions and prefers NADH and NAD⁺ respectively as a cofactor. This ADH is well known to be a potent enzyme with high tolerance towards temperature, pH, and solvents. Systems using this ADH can display thermostability of up to 60°C and pH stability of up to pH 11^[24]. The purified enzyme tolerates acetone at a concentration of up to 50 vol% and isopropanol up to 80 vol%^[25] and could even successfully be used in 99 vol% hexane.^[26] Sy-ADH from *Sphingobium yanoikuyae* DSM 6900 and Ras-ADH from the strain DSM 6428 of *Ralstonia* sp. are both NADPH dependent enzymes that excel at the recognition and reduction of sterically demanding or bulky-bulky ketones.^[27] Sy-ADH is a dimer and each monomer features a characteristic Rossmann-type fold, again a central β -sheet of seven strands surrounded by seven α -helices, while Ras ADH is considered tetrameric displaying also a Rossmann fold, a central β -sheet of seven strands that is only surrounded by six α -helices.^[28] Other promising and well established enzymes are the wild type ADH from *Lactobacillus brevis* and *Lactobacillus kefir*, as well as its variants Lk-ADH Montelukast^[29] and Lk-ADH Lica.^{[30][31]} Lk-ADH Montelukast and Lk-ADH Lica have been developed to especially excel in the use of bulky-bulky substrates. Both wild type ADHs represent two quite homologous enzymes, that are valuable biocatalysts for the preparation of (*R*)-hydroxy compounds^{[9][32]} while on the other hand, Lk-ADH Montelukast and Lk-ADH Lica tend to produce the (*S*)-hydroxy product from of both their intended substrates (*E*)-methyl 2-(3-(3-(2-(7-chloroquinolin-2-

yl)vinyl)phenyl)-3-oxopropyl)benzoate, a key intermediate of montelukast sodium, and oxcarbazepine, respectively. All ADHs from *Lactobacillus* used in this work are NADPH dependent. Morphine dehydrogenase^{[33][34]} is a NADH dependent ADH from *Pseudomonas putida* with high specificity of oxidizing only the C-6 hydroxy group of morphine and morphine derivatives. Another specially developed and novel enzyme is Kp-ADH 50C10^[35], an NADPH/NADP⁺ dependent alcohol dehydrogenase from *Kluyveromyces polysporus* (variant 50C10). In the development of this ADH was the focus on creating an enzyme with high stereoselectivity for “hard-to-reduce” considered ketones, especially compounds such as (4-Chlorophenyl)(pyridin-2-yl)methanone (CPMK) and the production of its chiral alcohol products. Moreover, the two wild type ADHs Tropinone reductase I (TR I) and Tropinone reductase II (TR II)^[36] that are both NADPH/NADP⁺ dependent ADHs originally found in *Datura stramonium*, are investigated. Both enzymes use Tropinone as the substrate, but TR I (EC 1.1.1.206) reduces tropinone to tropine and TR II (EC 1.1.1.236) produces pseudotropine, respectively.

1.3. Prelog rule

In the reduction of a prochiral ketone to a secondary alcohol the hydride is delivered preferentially from one site in the active site by the enzyme. So, the hydride attacks from the so-called *Si*- or the *Re*-side of the ketone to yield the corresponding (*R*)- or (*S*)-alcohol. Whether the hydride adds to the *Si*- or the *Re*-face of the substrate depends on the steric requirements of the compound^[5] and can be explained by a simple model referred as the “Prelog’s rule” as illustrated in Figure 3 below.

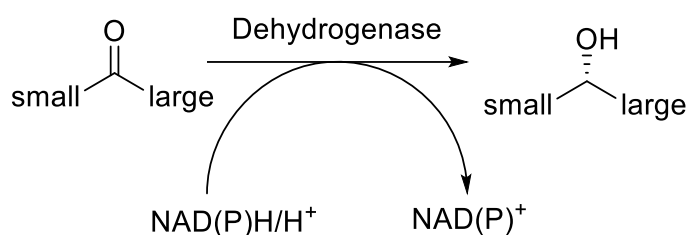


Figure 3 The Prelog’s rule in the reduction of carbonyl by dehydrogenases

This model is based on the ketone possessing a large substituent such as an aromatic ring or ring system and a small substituent such as, a methyl-group, each fitting in one larger and one smaller pocket at the active site of the enzyme respectively. This fit in the binding pocket allows the cofactor to specifically transfer a hydride to the prochiral substrate. In this model enzymes adding the hydride to the *Si*-face and therefore, producing the (*S*)-alcohol follow this “Prelog rule” and are consequently called Prelog’s specific enzymes, while other enzymes following the opposite to this rule are called anti-Prelog. A selection of dehydrogenases with their specificity is given in Table 2.

Table 2 Specificity regarding the Prelog’s rule of several prominent ADHs

Dehydrogenase	Specificity
Yeast-ADH	Prelog
Horse liver-ADH	Prelog
<i>Thermoanaerobium brockii</i> -ADH	Prelog
Hydroxysteroid-DH	Prelog
<i>Candida parapsilosis</i> -ADH	Prelog
<i>Lactobacillus kefir</i> -ADH	Anti-Prelog
<i>Mucor javanicus</i> -ADH	Anti-Prelog
<i>Pseudomonas</i> sp.-ADH	Anti-Prelog

1.4. Coupled substrate/ enzyme approach for recycling systems

Reduction and oxidation reactions are coupled with the stoichiometric consumption of NADH or NADPH for the reduction or NAD^+ or NADP^+ for the oxidation, but since these cofactors are too expensive reducing/oxidising agents for stoichiometric usage, a common practice is to add a recycling system that regenerates the cofactor by coupling the reaction with a second process that in situ oxidised or reduced the cofactor again.^{[5][20]}

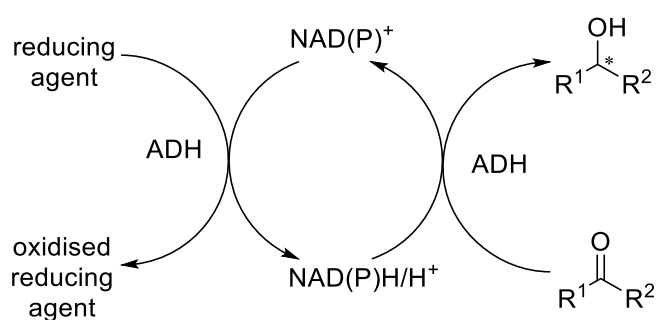


Figure 4 Concept of a general cofactor recycling system for reducing ketones/ aldehydes

For this different concepts and systems have been developed and employed. The general concept of such a system for reductions is shown in Figure 4. Two different approaches to achieve such kinds of systems exist, the coupled-substrate and coupled-enzyme cofactor-recycling.

For the coupled-substrate cofactor-recycling system an ADH is used that is able to reduce the substrate and oxidise a cost-effective alcohol. One very often used alcohol for this is isopropanol that is widely and easily commercially available to a reasonable price and serves as a cheap reducing agent. In this process the cosolvent isopropanol is oxidised to yield acetone as a side product. For the oxidation of a substrate the same already developed system can be used by switching the cosolvent from isopropanol to acetone. This makes the coupled-substrate cofactor-recycling system a quite simple, but also very variable concept.

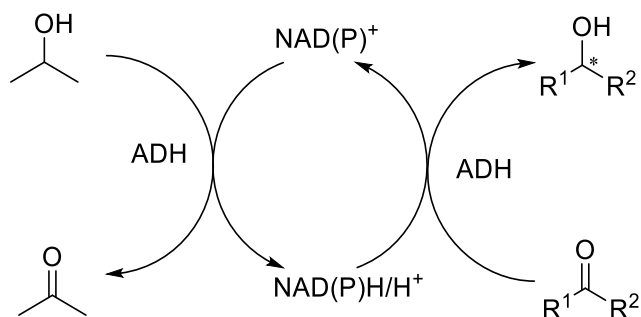


Figure 5 Concept of a cofactor recycling system for reducing ketones/ aldehydes using isopropanol as a reducing agent

One of the largest advantages of this concept is that just one enzyme is needed to catalyse both reactions, the reduction of the ketone or aldehyde containing substrate and the oxidation of

isopropanol as displayed in Figure 5. But this is also one of this system's greatest limitations, since the ADHs must have the capability to accept the target compound and isopropanol/acetone as a substrate. Although there is a vast quantity of enzymes that exhibit capabilities to both process substrates, there might be specific cases where screened enzymes show promising results with the substrate regarding conversion and selectivity but possess an incapability to oxidise isopropanol or reduce acetone. Another disadvantage of the coupled-substrate cofactor-recycling system is the reversibility of both reactions. Therefore, an equilibrium between the ketone and desired alcohol product is reached, where an additional force is needed to push the equilibrium to the side of the product. A common solution to overcome this limitation is the removal of one of the products, for example the formed acetone/isopropanol is likely the most volatile component in the reaction, so the solvent could be removed by shifting it to the gas phase. Another widely used method is the use of an excess of isopropanol/acetone that has also the positive side effect of increasing the solubility of hydrophobic and water-immiscible ketones or aldehydes in the reaction mixture.^[37]

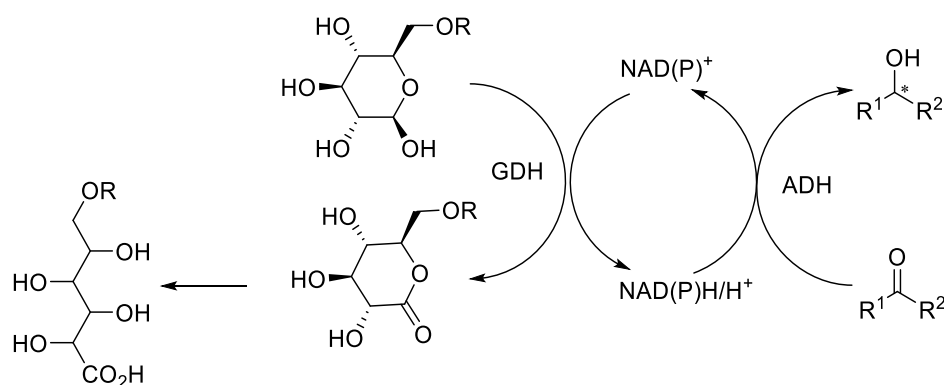


Figure 6 Concept of a cofactor recycling system for reducing ketones/ aldehydes using glucose as a reducing agent

Another possible solution for recycling the cofactor is the coupled-enzyme approach, where an additional second enzyme is used to reduce the oxidised form of the cofactor. Similar to the coupled-substrate system here also another more reasonably priced compound is oxidised in the regeneration. The second enzyme and the reducing agent have to be compatible with each other. One example for this system would be D-glucose as the reducing agent that is oxidised by glucose dehydrogenase (GDH) to D-gluconolactone. This compound is not stable in aqueous solutions, which leads to spontaneous hydrolysis of the lactone to D-gluconic acid. This system is shown in Figure 6. The generation of an acid can lead to problems in high concentrations since activity of enzymes can be harshly influenced by the pH of the solution. Therefore, the D-gluconic acid can be easily neutralised by a buffer solution or by adding a base. Both will lead to the precipitation of the corresponding gluconate salt. This removal of the oxidised reagent ensures pushing the reaction towards reducing the cofactor.^[38,39]

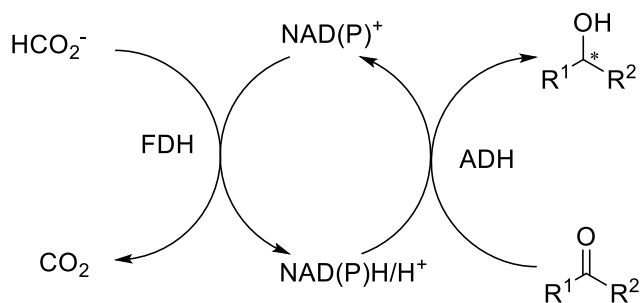


Figure 7 Concept of a cofactor recycling system for reducing ketones/ aldehydes using formate as a reducing agent

Another often used pair of agent and enzyme is formate and formate dehydrogenase (FDH) as displayed in Figure 7, here the dehydrogenation of the formate forms carbon dioxide that will almost completely remove itself by transitioning into the gas-phase. This removal of the gas serves to shift the equilibrium of the reaction to the product side.

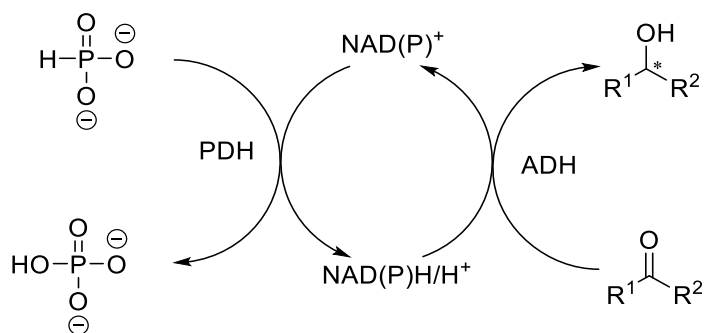


Figure 8 Concept of a cofactor recycling system for reducing ketones/ aldehydes using phosphite as a reducing agent

A third not as widely used, but still well-developed example for a coupled-enzyme cofactor-recycling system displayed in Figure 8 is comprised of a phosphite dehydrogenase (PDH) that oxidizes phosphite to phosphate to reduce NAD(P)⁺ to NAD(P)H.^[9]

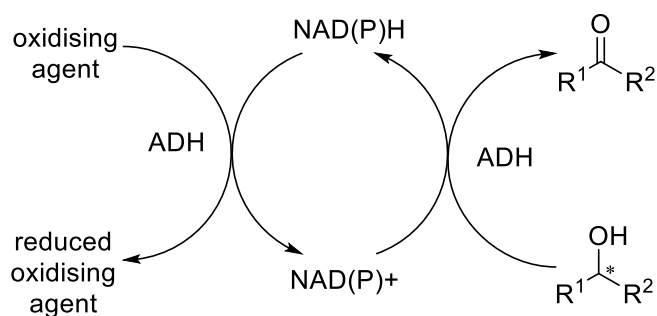


Figure 9 Concept of a general cofactor recycling system for oxidising alcohols

Due to having irreversible reaction to regenerate the cofactor the same systems cannot be used for regenerating the oxidised cofactors, but completely new enzymes and chemicals have to be used for oxidising NAD(P)H. The general scheme of a system for oxidation is illustrated in Figure 9 above.

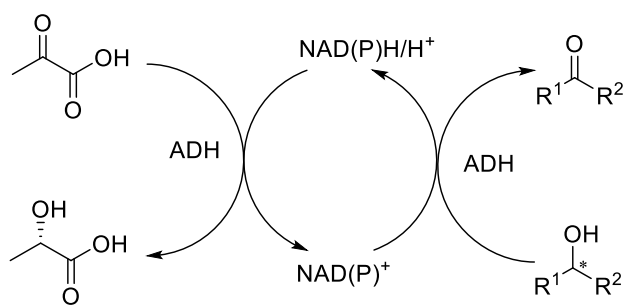


Figure 10 Concept of a cofactor recycling system for reducing ketones/aldehydes using pyruvate as an oxidising agent

One such system is a lactate dehydrogenase paired with pyruvate. Here the hydride can be transferred to the pyruvate that is reduced to L-lactate as seen in Figure 10.^[40]

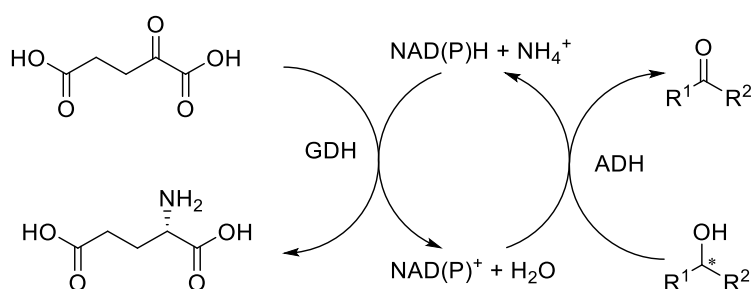


Figure 11 Concept of a cofactor recycling system for reducing ketones/ aldehydes using α -ketoglutarate as an oxidising agent

A bit more complicated system consists of a glutamate dehydrogenase (GDH) and α -ketoglutarate displayed in Figure 11. In this system the α -ketoglutarate is reduced to L-glutamate by reductive animation.^[41] For this a source of ammonia is additionally needed, which is usually added in form of ammonia or as an ammonium salt in the buffer solution.

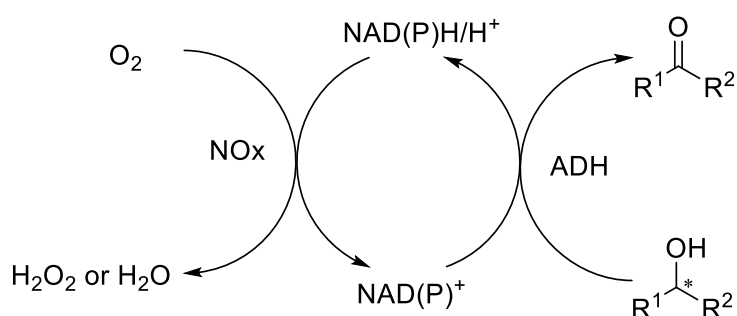


Figure 12 Concept of a cofactor recycling system for reducing ketones/ aldehydes using oxygen as an oxidising agent

Another interesting approach for a NAD(P) oxidation system is the direct use of molecular oxygen. For this nicotinamide oxidase (NOx) is used to oxidise the cofactor and reduce the oxygen to hydrogen peroxide or water as shown in Figure 12 above.^[42] The formed hydrogen peroxide can also spontaneously deteriorate to water or this reaction can be aided by catalase. The most unique advantage here is the reagent used for oxidation, since the oxygen present in the air is sufficient for

this reaction and therefore, is the most cost-effective method. However, the usage of air/oxygen results in some also unique challenges such as the formation of hydrogen peroxide, a compound well known for its tendencies of decomposing other compounds such as enzymes needed both for the reaction and the recycling system. One common solution could be using an additional third enzyme, catalase, to neutralise all produced peroxides by converting them to water. A further complication resulting from using a gas as reagent is to ensure proper saturation of the solution. This can be achieved in small scale application by shaking the reaction vessel, while in larger scale a more complex solution such as mixers or direct injection of the gas is needed.

A coupled-enzyme recycling system has the beneficial use of a low-value chemical such as formic acid or even oxygen as reducing/oxidising agent in stoichiometric amount. But the main advantages of the coupled enzyme approach compared to the coupled-substrate approach is to avoid reaching an equilibrium, since the side products like carbon dioxide and D-gluconic acid are removed from the reaction. This also yields the advantage that due to the removal of this compounds eventual downstream-processing or work-up steps are simplified. Potential problems for this kind of system are too different optima for reaction conditions, because of different enzymes present. Ideally the enzyme for NAD(P)H regeneration and the ADH for substrate reduction should be compatible and possess the same or at least a similar optimum range in terms of temperature and pH. In reality there is in most cases an overlap in the ranges of all enzymes and a compromise can be found that ensures the best possible activity of both enzymes combined. Additionally, substrate or product inhibition effects with the enzyme used for the cofactor recycling and the ADH used on the substrate can occur. This phenomenon might significantly reduce the total reaction speed.^{[38][9]}.

1.5. Disproportionation

Disproportionation reactions are reactions where species with the same oxidation state combine to yield one of higher oxidation state and one of lower oxidation state. As a more general term, disproportionation can also be used to describe desymmetrising reactions with the form shown in Figure 13, regardless whether a redox reaction occurs.^[43] This type of reactions is regarded as effective reactions with a high atom efficiency.

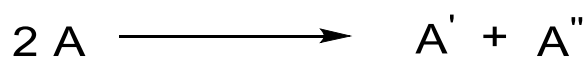


Figure 13 General scheme of a disproportionation

1.5.1. Cannizzaro reaction

A common disproportionation reaction is the Cannizzaro reaction, that reduces and oxidises two molecules of a non-enolisable aldehyde to produce a primary alcohol and a carboxylic acid in the same ratio as displayed in Figure 14 below.^[44] The substrate cannot possess a hydrogen on the α -carbon, since the produced enolate would lead to an aldol product as the preferred product. Due to this limitation, the majority of substrates are aromatic aldehydes.^[45]

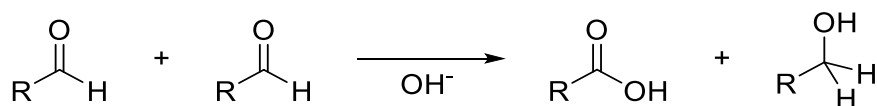


Figure 14 The Cannizzaro reaction

The mechanism of this reaction starts by the attack of a strong base (e.g. alkali metal hydroxide) usually under high temperature to result into a tetrahedral intermediate. The intermediate transfers a hydride to another aldehyde as shown in Figure 15, while the intermediate is oxidised to the corresponding carboxylic acid, while the transferred hydride reduces the aldehyde to the primary alcohol.^[46]

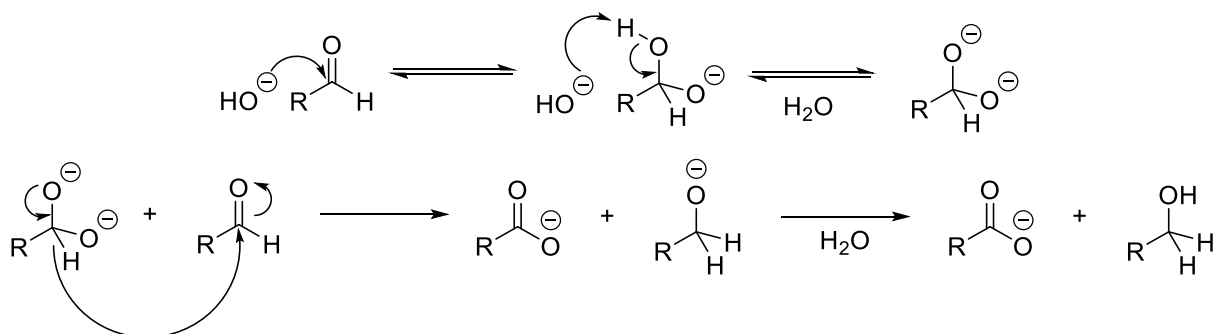


Figure 15 Mechanism of the Cannizzaro reaction

Since this reaction yields an equimolar mixture of alcohol and carboxylic acid and therefore, exhibits a theoretical maximum conversion of 50% for each product, a common approach is the crossed Cannizzaro reaction to enhance the reaction. This will not increase any conversion neither to the alcohol nor the carboxylic acid, but rather used a cheap sacrificial aldehyde such as formaldehyde to reduce another more valuable aldehyde to the alcohol as the product. Alternatively, both the regular Cannizzaro reaction and the crossed variant can be also catalysed by biocatalysts like ADHs.^[47] This reaction relies on the spontaneous hydration of the aldehyde to the geminal diol that can be oxidised by the ADH as illustrated in Figure 16. The removed hydride is transferred by the ADH to the aldehyde reducing it to the alcohol.

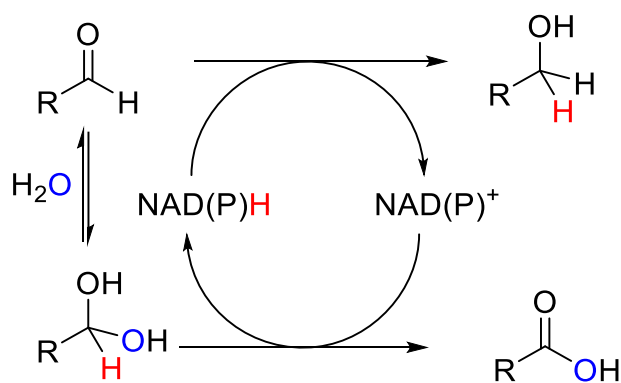


Figure 16 Biocatalytic Cannizzaro reaction catalysed by alcohol dehydrogenase (ADH)

This approach is based on the concurrent oxidative and reductive activity of nicotinamide-dependent alcohol dehydrogenases (ADHs) to perform the dismutation of aldehydes in a redox-neutral fashion. The system relies on the recycling the NAD(P)H/NAD(P)⁺ similar to the coupled-substrate approach by transferring a hydride from a molecule to another molecule using the same ADH for the reduction and the oxidation, but unlike the coupled-substrate approach the substrate itself is used to regenerate the cofactor, so no sacrificial auxiliary substrate is necessary.^{[47][48]}

1.5.2. Tishchenko reaction

Another well-known and widely used example for disproportionation reactions is the Claisen–Tishchenko reaction or also just called Tishchenko reaction.^{[49][50]} Similar to the Cannizzaro reaction it also uses aldehydes as a substrate, but in the case of the Tishchenko reaction an ester or a lactone are yielded as a product. This scheme is displayed in Figure 17. Another dissimilarity is a larger substrate scope compared to Cannizzaro reaction, because the process is not just limited to nonenolizable compounds. Since Tishchenko reactions can be regarded as a formal inter- or intramolecular hydride transfer, this type of reaction possesses a high atom efficiency and is regarded as an effective and relevant syntheses. An example for this is industrial scale production of ethyl acetate from ethanal. This method uses an acceptorless dehydrogenation of ethanol to generate ethanal that combines to give rise to ethyl acetate.^[51]

For this usually a Lewis acid like aluminium alkoxides or aluminium oxide is used for mediating the reaction. The empty orbital of the aluminium ion coordinates with the oxygen of the aldehyde that allows another aldehyde to perform a nucleophilic substitution on the carbonyl carbon. Furthermore, the low pH value of aluminium alkoxides has the added effect of reducing the production of aldols as side product.^[49]

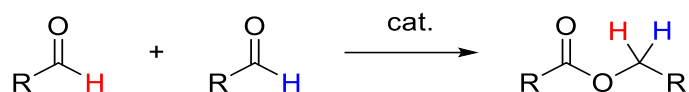


Figure 17 The Tishchenko reaction

The Ogata–Kawasaki model seen in Figure 18 below, is recognized as the most likely correct mechanism of the Tishchenko reaction catalysed by aluminium alkoxides.^[49] The aldehyde coordinates to the free space at the aluminium, where the alkoxide can attack the carbonyl carbon resulting in the formation a new alcoholate bound between the metal and the previously bound alkoxide. This insertion creates a new free coordination place, where another aldehyde can coordinate. A hydride shift from the alkoxide to the aldehyde reducing it to the alcoholate equivalent. This hydride shift forms the ester and release the product. Furthermore, the reduction of the aldehyde to the alcoholate regenerates the aluminium alkoxide catalyst.^[52]

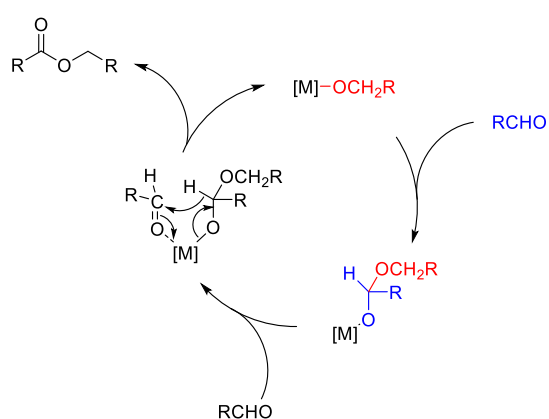


Figure 18 Mechanism and catalytic cycle of a general Tishchenko reaction after the Ogata–Kawasaki model

The Tishchenko Reaction: A Classic and Practical Tool for Ester Synthesis

Also, like in the case of the Cannizzaro reaction, the Claisen–Tishchenko reaction can be performed biocatalytically with ADHs. Similar to the Cannizzaro reaction the enzyme has an oxidation and reduction step that regenerates the cofactor as shown in Figure 19 below. This allows good performance with very low amounts of biocatalyst and a high atom efficiency. In the first step one substrate molecule is reduced to a primary alcohol that is able to nucleophilic attack the carbonyl-carbon of another unreduced molecule of the substrate. This attack links both molecules and forms a hemiacetal. The hydroxyl group of this hemiacetal can be oxidised by the same ADH that reduced the substrate to yield an ester as a final product. This oxidation in turn allows the recycling of the cofactor.^[53]

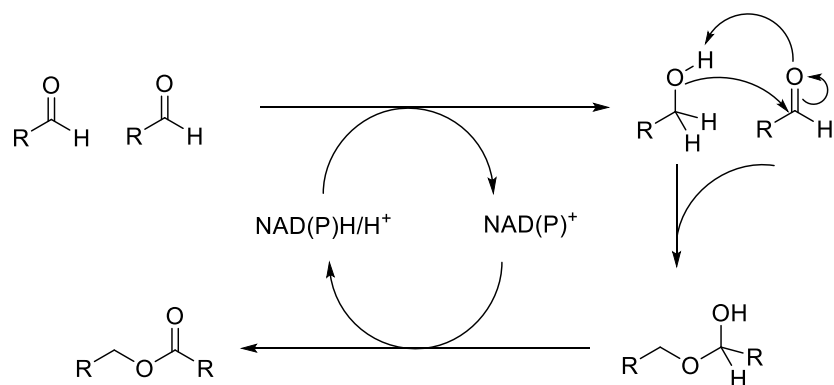


Figure 19 Biocatalytic Tishchenko reaction catalysed by alcohol dehydrogenase (ADH)

A special case is the intramolecular Tishchenko-like reactions, where dialdehydes are used to form the cyclic equivalent of hemiacetals and esters, that are lactols and lactones as displayed in Figure 20. The size of the produced ring depends on the position of the aldehyde moieties to each other, for example 1,4- and 1,5-dialdehydes are preferred substrates, since they form γ - and δ -lactones respectively.

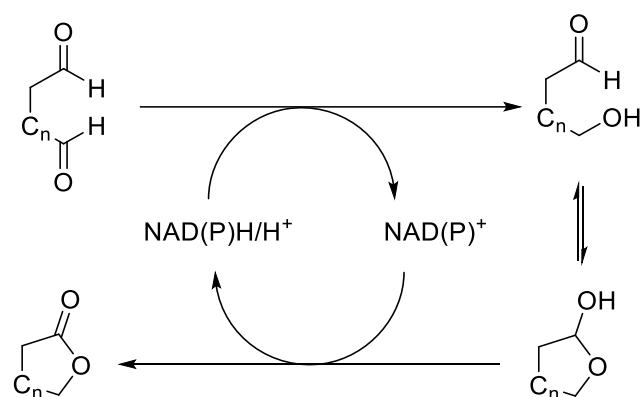


Figure 20 Biocatalytic intermolecular Tishchenko reaction

1.6. Suzuki coupling

Suzuki-Miyaura reactions or also simply called Suzuki coupling are organic coupling reactions that are used for coupling a boronic acid and an organohalide. The reagent scope includes alkyls, alkenyls and alkynyls, but most notable is the application in linking aryls. In general, Suzuki coupling reactions also accept several functional groups such as amines, aldehydes, and ketones. This cross-coupling reaction is catalysed by a palladium catalyst and a base has to be used for activation of the boronic acid.^{[54][55]} The general scheme is shown in Figure 21 below.

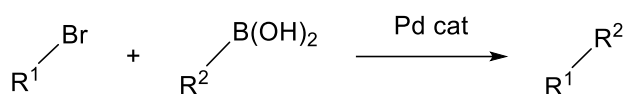


Figure 21 The Suzuki-Miyaura reaction

The three steps for the cross coupling are displayed in Figure 22 and consist of an oxidative addition to the halide, while oxidising the palladium to Pd^{II}, a transmetalation to exchange the base coordinated to the metal with the organic substituent of the activated boronic acid and finally a reductive elimination that yields the final coupled product and reduces the catalyst back to the original state.

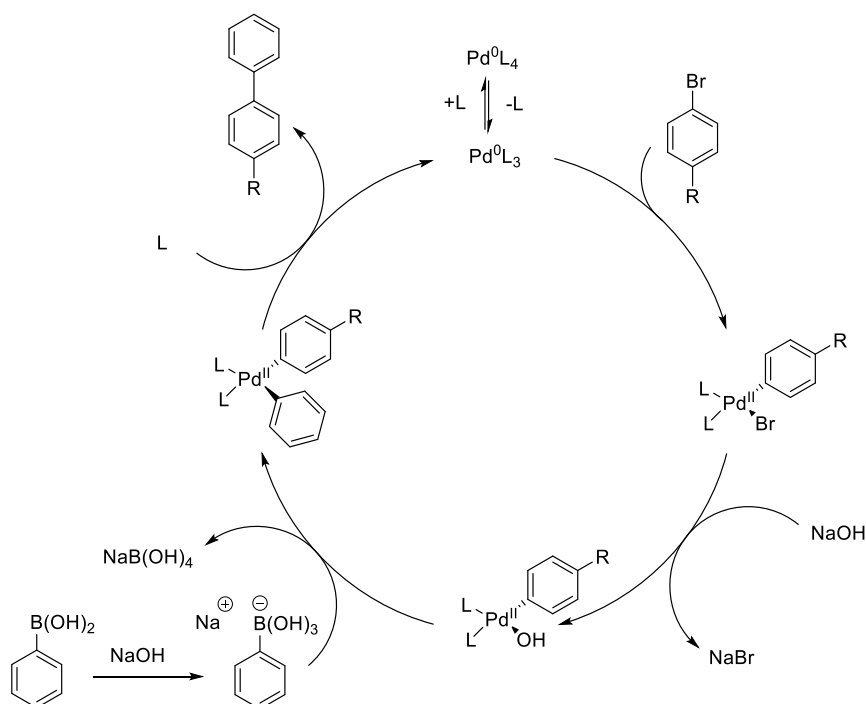


Figure 22 Mechanism/ Catalytic cycle of a Suzuki-Miyaura reaction

First the oxidative addition occurs, where the C-X is broken and both coordinate to the palladium complex, while the catalyst is oxidized from palladium(0) to palladium(II). Though the original complex being after the oxidative addition is in *cis* form, the complex rapidly isomerises into the more stable *trans*-complex, where the distance between halide and the R group is increased as much as possible shown in Figure 23.^[56]



Figure 23 The *cis/trans* isomerisation of the palladium complex

Additional information of R regarding *trans/cis* configuration is retained as displayed in Figure 24.^[57] The oxidative addition is usually the rate determining step of the catalytic cycle.^[56]

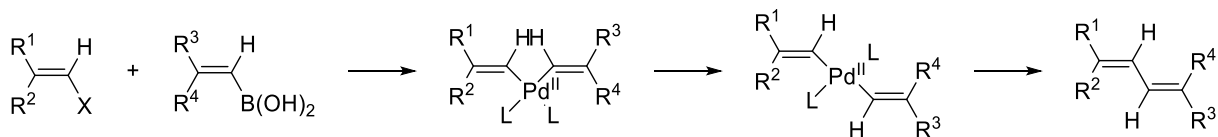


Figure 24 Conservation of *cis/trans* configuration in Suzuki-Miyaura reactions

Before the transmetalation takes place, the halide of the complex is replaced by the added base. The halide precipitates usually as a salt after removal. For example, when using NaO^tBu as a base, the alcoholate coordinates to the metal, while sodium and the halide forms NaX . Now the activated organoboron species exchanges the organic substituent with the base added in the prior step, to give rise to a new palladium(II) complex containing both R^1 and R^2 . The final step is the reductive elimination of the product to regenerate palladium(0). For this R^1 and R^2 have to be in *cis* position. The product keeps retention of stereochemistry from the substrate^[58].

1.7. Hydroacylation reactions

Hydroacylation reactions are reactions in which a double bond of usually an alkene performs a nucleophilic attack on an aldehyde to yield a saturated ketone. This reaction is usually performed with a homogeneous rhodium or ruthenium-based catalyst.^[59] This reaction can either be used to link two different molecules, one with an aldehyde moiety and an alkene to form a longer chained ketone or be used intramolecularly to give rise to a cyclic product. Both described reactions are shown in Figure 25.^[60]

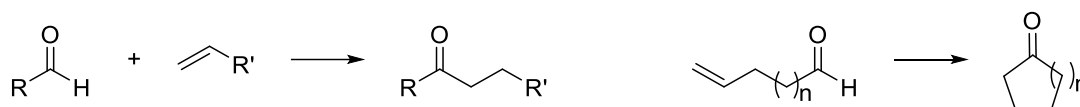


Figure 25 The hydroacylation reaction(left) and intramolecular hydroacylation reaction(right)

A special case for intramolecular hydroacylation reactions exists where not an alkene but a ketone moiety attacks the aldehyde forming 7 or 6 membered lactones as a product as displayed in Figure 26. In general, decarbonylation is considered a competing side reaction in both cases.^[61]

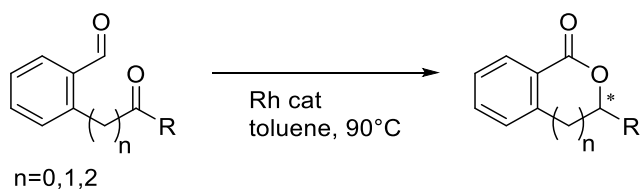


Figure 26 The intramolecular hydroacylation reaction forming a lactone

The proposed mechanism adds the aldehyde to the metal-catalyst by oxidative addition and the double bond can coordinate the metal centre. The coordinated alkene inserts via migratory insertion into either the metal-acyl or the metal-hydride bonds forming in case of an aldehyde with an unsaturated chain a metalo-cycle. As a last step a reductive elimination occurs to yield a ketone as a product and recycle the catalyst. The catalytic cycle is shown in Figure 27. A competing side-reaction is decarbonylation of the aldehyde.^[62]

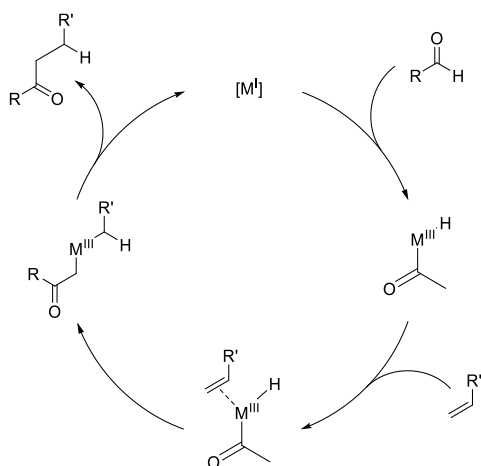


Figure 27 Mechanism and catalytic cycle of hydroacylation reactions

Analogue to this is also the mechanism of the intramolecular hydroacylation reaction. The substrate performs an oxidative addition with the aldehyde moiety, oxidising the Rh^I to a $Rh^{III}H$, afterwards the complex undergoes a hydroacylation hydrometallation of ketone to form organo-rhodium intermediate, where the carboxy-functionality is also coordinated to the metal centre. The hydrogen in the aldehyde coordinates after the oxidative addition on the metal catalyst and can determine the chirality of the R substituent on the ketone. For longer chained ketones, especially with an electron withdrawing group such as oxygen in the chain, the aldehyde and the ketone are in *trans*-position in the complex. In this transition state is the metal centre sandwiched between the aldehyde and ketone moiety. In case of a present electron-rich heteroatom, this atom can also serve as a ligand. In a molecule with shorter distance between both functionalities like exhibited in 2-acetylbenzaldehyde both groups are in *cis* position to each other. Afterwards, an insertion occurs, where the hydride is transferred to the carbonyl carbon that is therefore, reduced. As a last step a reductive elimination occurs to yield a ketone as a product and recycle the catalyst.^{[63][64]}

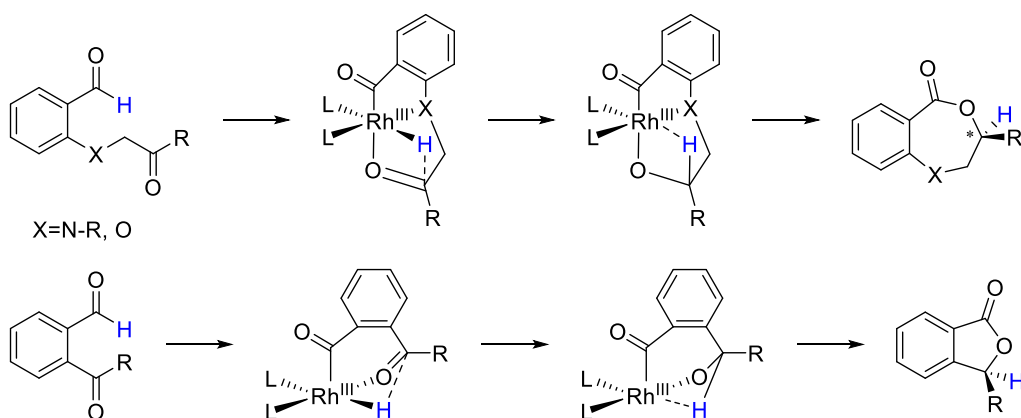


Figure 28 Mechanism of intramolecular hydroacylation reaction with a long chain on the ketone (top) and a short chain on the ketone (bottom)

2. Goals

Primary objectives of this work are regarded as follows:

- Developing a platform for lactone synthesis based on keto-aldehyde substrates
 - Vary the substituent on the ketone-group
- Investigating several different ADHs for the system
 - New enzymes for this reaction (TR I, TR II and Kp-ADH)

Since several studies about bio-Tishchenko-like reactions with molecules containing two aldehyde moieties have been conducted, a logical progression to broaden the substrate scope is to investigate substrates with a ketone and an aldehyde moiety to develop a biocatalytic formal hydroacylation protocol.

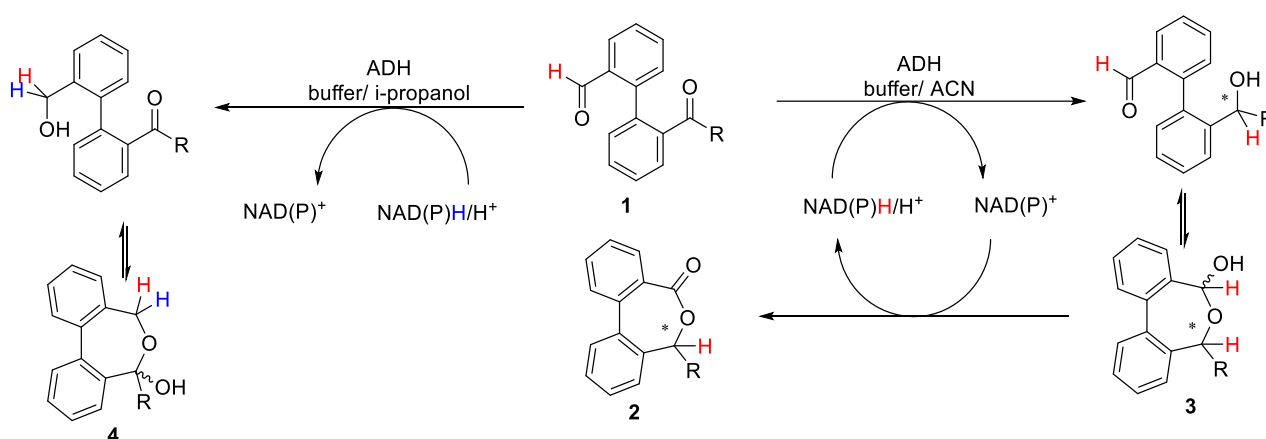


Figure 29 Reaction system for a keto-aldehyde substrate with reduction of the aldehyde(left) and the ketone(right) including the cofactor recycling system

Due to different groups capable of being reduced, a larger variety of products can be expected as seen in Figure 29 above. The ketone being reduced allows a nucleophilic attack on the aldehyde to yield a lactol via ring closure that possesses a secondary alcohol functionality. This secondary alcohol is able to be oxidised to the analogue lactone and recycle the cofactor allowing the catalytic use of NAD(P)H. The reduction of the ketone can introduce a steric centre depending on the used ADH resulting in a chiral centre in product **3** and **2**. To shift the product more from **2** to **3** a cofactor recycling system is developed to use a cosolvent such as isopropanol instead of the intermediate product **3**. If the aldehyde of the substrate **1** is reduced, the produced hemiketal **4** possesses a tertiary alcohol functionality that cannot be oxidised and therefore, the cofactor cannot be recycled by an internal

hydride shuffling. Since the produced secondary alcohol lacks steric information, no chirality of **4** is predicted. To increase the yield of **4** a cofactor coupled substrate recycling system with isopropanol is implemented.

In development of further bi-aryl substrates, it was considered to substitute protons on the methyl-group to produce non enolisable compounds. Therefore, the methyl group is substituted by a trifluoromethyl (**1c**) and a phenyl-group (**1d**) as displayed in Figure 30 below.

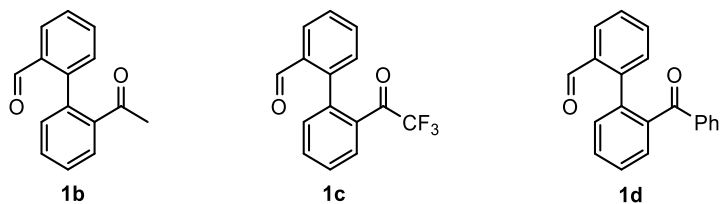


Figure 30 Substrates **1b**, **1c** and **1d**

Another aim in this work is not only to increase the scope of substrates and reactions for well-established enzymes, but also add and investigate new promising enzymes to increase the available tools. Therefore, two potential tools were tested for this purpose: tropinone reductase I and II (TR I and TR II) both from *Datura stramonium*. In total are 11 enzymes investigated in the scope of this work. The complete list of investigated ADHs, their organism of origin and their cofactor as well as several other details are shown in Table 1.

3. Results and discussion

The following substrates displayed in Figure 31 are the keto-aldehyde substrates investigated to perform bio Tishchenko-like hydroacylations.

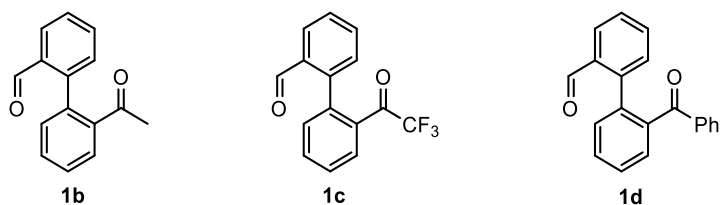


Figure 31 Tested substrates **1b**, **1c** and **1d**

In this study **1b** showed at first stability problems when synthesised in aqueous solution, since the ketone group tautomerizes to the enol and attacks the aldehyde to spontaneously perform a ring closure and an intramolecular aldol condensation to yield **5b**. This side reaction is shown in Figure 32. Therefore, all substrates are synthesised in dry organic solvents, mainly THF, and purified separately beforehand or used directly in a reaction cascade to minimise this reaction. Quantifications of **5b** in reactions using **1b** as substrate revealed **5b** as a minor side product of the reaction.

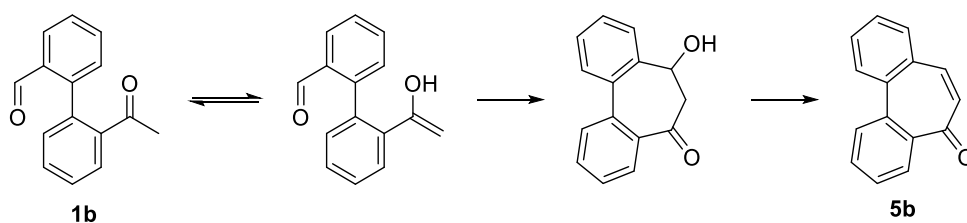


Figure 32 Aldol-condensation of **1b** to side product **5b**

Eleven different ADHs were investigated in this thesis, which are listed in Table 3. The natural diversity of the ADH enzyme class ensures that enzymes encompassing a broad range of catalytic characteristics have been made available for applications and offer characteristics like (*R*)- or (*S*)-selectivity, thermostability and tolerance to organic solvents. Among the chosen enzymes were several well-known and widely used enzymes such as ADH-A of *Rhodococcus ruber*, engineered ADHs like Lk-ADH Lica, a mutant variant of *Lactobacillus kefir* as well as enzymes that are still quiet novel and not investigated yet for use in biocatalysis such as tropinone reductase I and II from *Datura stramonium*. Several investigated enzymes are already established as biocatalysts as they catalyse the transformation of sterically challenging or ‘bulky–bulky’ substrates such as Sy-ADH, Ras-ADH and the before named Lk-ADH Lica.

Table 3 List of used enzymes

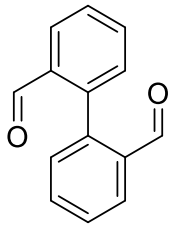
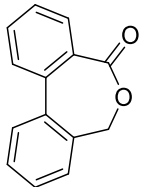
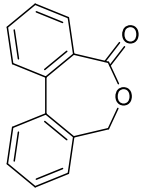
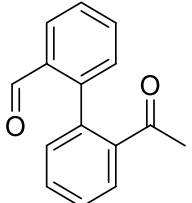
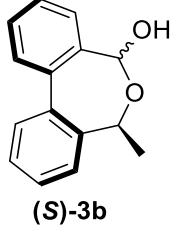
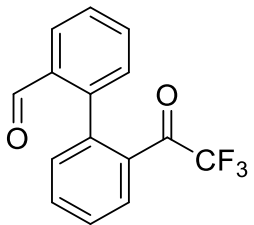
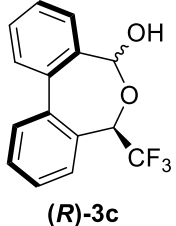
entry	ADHs
1	ADH-A
2	Sy-ADH
3	Ras-ADH
4	Lb-ADH
5	Lk-ADH
6	Lk-ADH Montelukast
7	Lk-ADH Lica
8	Morphine dehydrogenase
9	Kp-ADH 50C10
10	Tropinone reductase I
11	Tropinone reductase II

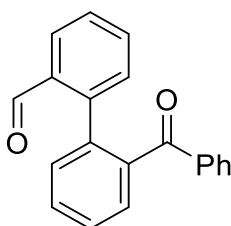
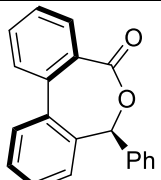
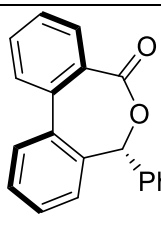
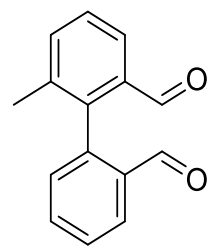
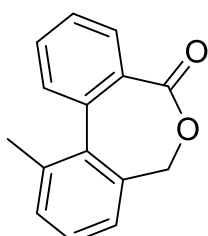
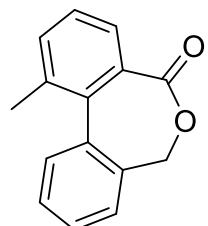
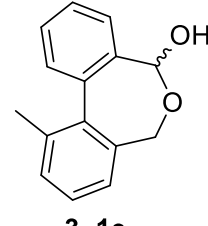
3.1. Docking study

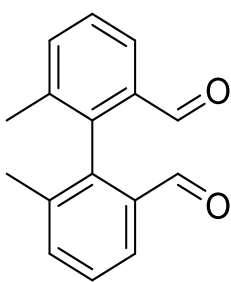
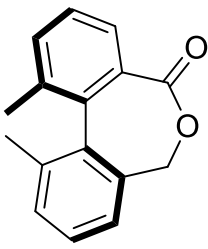
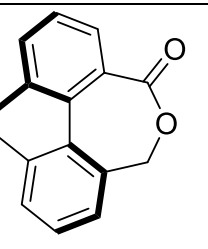
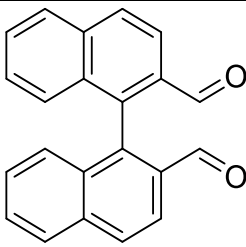
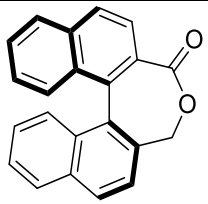
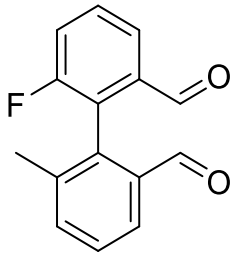
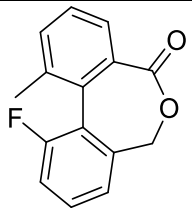
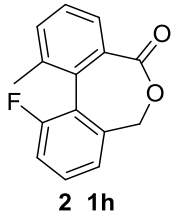
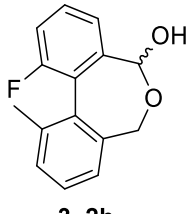
A theoretical docking study was conducted using YASARA^[65] and Pymol^[66] to investigate the scope of the substrate binding pocket present in TRI and TRII for several possible substrates and to explore the capability for performing the expected redox reaction. For qualifying as a potential substrate, the compound has to possess at least two carbonyl functionalities like a ketone or an aldehyde or two aldehydes. The functional groups also have to be in a position and orientation to each other to allow a ring closure and yield a stable ring with ideally between 5 and 8 atoms in the ring. Furthermore, this project only focuses on compounds with at least one aromatic ring to investigate especially the capability for sterically challenging substrates.

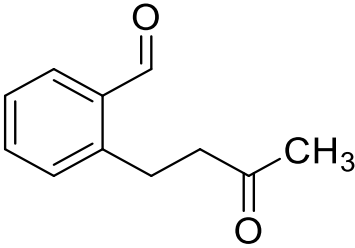
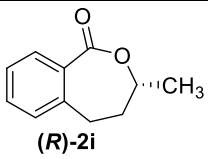
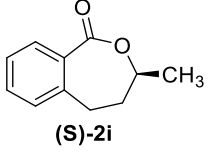
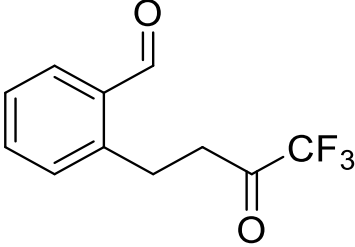
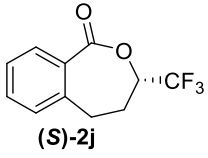
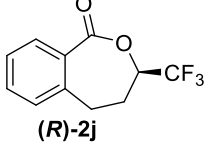
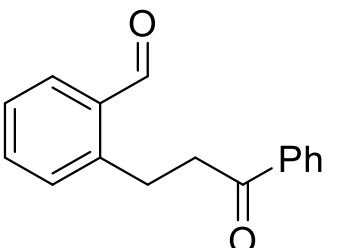
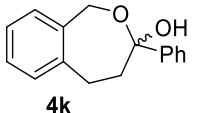
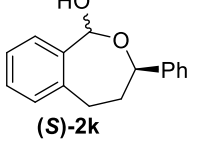
The following substrates and their possible intermediates are fitted into the enzyme regarding their spacious orientation towards the cofactor. In general, first the substrate was docked to the enzyme with an altered cofactor. Since there was no data of the enzyme structure with reduced cofactor (NADPH) available, the oxidised cofactor, NADP⁺ present in the structural data was exchanged in YASARA with the reduced form. For the oxidation step the enzyme structure was used as received and the intermediate structures **(R)-3** and **(S)-3** were fitted into the binding pocket. For this docking all isomeric forms and axial chirality are considered by also determining their fit in the binding pocket. All substrates and their predicted products with predictions are listed in Table 4. Compounds **1a** to **1d** are tested in biotransformations and are compared to the predictions in Table 5.

Table 4 Overview of reaction prediction for substrates **1a-k** based on docking using YASARA and PyMOL
Distance of substrate to cofactor is measured between the carbonyl carbon and the hydride of the cofactor (NADPH)

Substrate	AD H	Distance of Substrate to cofactor [Å]		Structure of the predicted product	Prediction
 1a [1,1'-biphenyl]-2,2'-dicarbaldehyde	TRI	4.3		 2a	Reduction with a distance of 4.3 Å seems likely and oxidation of the intermediate 3a distance of 5.9 Å the formation of 2a seems difficult, but possible. Therefore, formation of 2a is predicted.
	TRII	2.9		 2a	A cofactor substrate distance of 2.9 Å indicate a probable reduction and a distance of 6.0 Å the formation of 2a seems difficult, but possible for oxidation. Therefore, formation of 2a is predicted.
 1b 2'-acetyl-[1,1'-biphenyl]-2-carbaldehyde	TRI	CHOCH ₃	3.9	 (S)-3b	The formation of 4b (hemiketal) or (S)-3b approximately equal probable (maybe (S)-3b slightly favoured), but the oxidation to (S)-2b appears unlikely (5.9 Å distance cofactor-substrate)
		CHO	3.9		
	TRII	CHOCH ₃	3.3		No conversion should occur, since despite the near proximity, the angle of the hydride attack is impossible in both cases
		CHO	3.4		
 1c 2'-(2,2,2-trifluoroacetyl)-[1,1'-biphenyl]-2-carbaldehyde	TRI	CHOCF ₃	3.6	 (R)-3c	Reduction to (R)-3c should occur easily, but oxidation to 2c is improbable (6.3 Å distance cofactor-substrate)
	TRII	CHOCF ₃	3.2		No conversion should occur, since despite the near proximity, the angle of the hydride attack is impossible in both cases.
		CHO	3.2		
2'-(2,2,2-trifluoroacetyl)-[1,1'-biphenyl]-2-carbaldehyde					

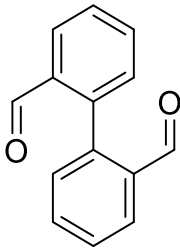
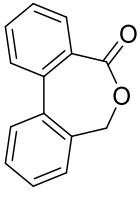
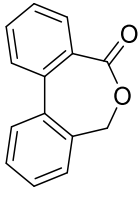
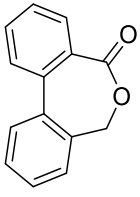
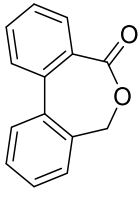
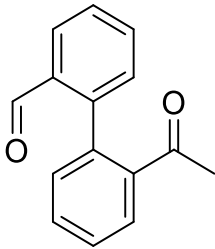
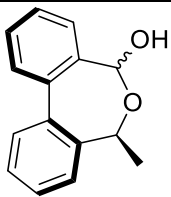
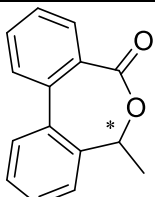
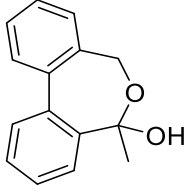
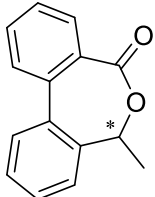
 <p>1d</p>	TRI	CHOPh	3.7	 <p>(R)-2d</p>	With a cofactor substrate distance of 3.6 Å is (R)-2d expected with 4d as a possible side product	
		CHO	4.2			
	TRII	CHOPh	3.0	 <p>(S)-2d</p>	As a product (S)-2d is expected (3.5 Å distance cofactor-substrate), but since fitting problems with reduction of the ketone occur is 4d also possible.	
		CHO	4.5			
2'-benzoyl-[1,1'-biphenyl]-2-carbaldehyde						
 <p>1e</p>	TRI	CHO on the Me substituted ring	4.3	 <p>2_1e</p>	The oxidation to yield 2_1e should occur more easily due to a cofactor-substrate distance of 3.6 Å, but the reduction of the other aldehyde on the unsubstituted ring is with 3.8 Å preferred	
		CHO on the ring with no Me substitution	3.8			
	TRII	CHO on the Me substituted ring	3.7	 <p>2_2e</p>	Reduction is equally probable, but oxidation to 2_2e is with 4.7 Å cofactor-substrate distance favoured, but formation of 3_1e is also expected in some quantities	
		CHO on the ring with no Me substitution	3.7			
	6-methyl-[1,1'-biphenyl]-2,2'-dicarbaldehyde				 <p>3_1e</p>	

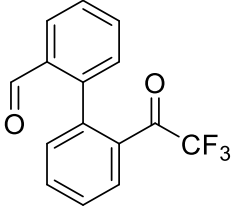
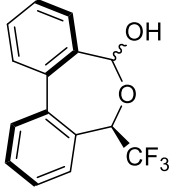
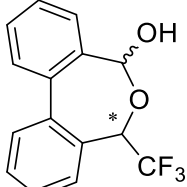
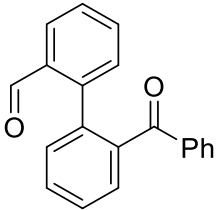
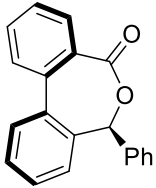
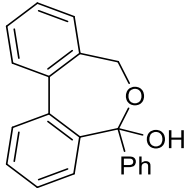
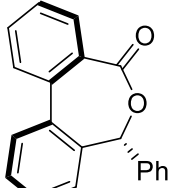
 <p>1f</p>	TRI	4.4		 <p>2f</p>	With a distance of also 4.9 Å of the intermediate to the cofactor the oxidation to 2f seems difficult, but possible.	
	TRII	4.2		 <p>2f</p>	With a cofactor-substrate distance of 2.7 Å the oxidation to 2f is expected	
6,6'-dimethyl-[1,1'-biphenyl]-2,2'-dicarbaldehyde						
 <p>1g</p>	TRI	5.1			With a cofactor substrate distance of 5.1 Å in the reduction step any substrate consumption appears improbable	
	TRII	4.2		 <p>(S)-2g</p>	The production of (S)-2g is with 3.7 Å cofactor-substrate distance predicted	
[1,1'-binaphthalene]-2,2'-dicarbaldehyde						
 <p>1h</p>	TRI	CHO on the Me substituted ring	4.2	 <p>2_1h</p>	Oxidation to this product is improbable but might be possible. With 5.5 Å over 5.6 Å a slight preference in axial chirality should be observable	
	TRII	CHO on the Me substituted ring	4.1	 <p>2_1h</p>	 <p>3_2h</p>	Oxidation to 2_1h (4.6 Å and 4.7 Å for both enantiomers) is likely but traces of 3_2h are also plausible
		CHO on the F substituted ring	4.1			
	6-fluoro-6'-methyl-[1,1'-biphenyl]-2,2'-dicarbaldehyde					

 1i 2-(3-oxobutyl)benzaldehyde	TRI	CHOMe	2.4	 (R)-2i	The oxidation to (R)-2i is with 4.1 Å cofactor substrate distance predicted. Both reduction and oxidation are specific to this chirality
	TRII	CHOMe	2.9	 (S)-2i	The formation of (S)-2i is quite likely. The oxidation does not show a strong selectivity regarding chirality (5.4 Å for R 5.3 Å for S), but (S)-3i is produced selectively
	CHO	4.0			
 1j 2-(4,4,4-trifluoro-3-oxobutyl)benzaldehyde	TRI	CHOCF ₃	2.6	 (S)-2j	The oxidation to (S)-2j is with 4.0 Å cofactor substrate distance predicted. Both reduction and oxidation are specific to this chirality
	TRII	CHOCF ₃	2.9	 (R)-2j	The formation of (R)-2j is difficult, but plausible with 5.0 Å cofactor substrate distance. Both reduction and oxidation are specific to this chirality
	CHO	4.1			
 1k 2-(3-oxo-3-phenylpropyl)benzaldehyde	TRI	CHO	2.9	 4k	Since CHO moiety is reduced selectively 4k is predicted as a main product
	TRII	CHOPh	2.9	 (S)-2k	Oxidation of (R)-2k would be expected very probable with 3.8 Å cofactor substrate distance, but TRII forms selectively (S)-2k
	CHO	3.2			

According to the simulation in this docking study tropinone reductase I and II should be quite capable of using bulky-bulky and bulky-non bulky substrates and forming selectively products with chiral preferences in many cases, while in some cases, the formation of enantiomeric products by TRI and TRII can be expected.

Table 5 Comparison of the predicted and experimental data of substrates 1a to 1d

Substrate	ADH	Predicted product	Observed product(s)	Comparison
 <p>1a</p>	TRI	 <p>2a</p>	 <p>2a</p>	As predicted TRI is capable of producing 2a as the main product
	TRII	 <p>2a</p>	 <p>2a</p>	As predicted TRII is capable of producing 2a as the main product
[1,1'-biphenyl]-2,2'-dicarbaldehyde		2a	2a	
 <p>1b</p>	TRI	 <p>(S)-3b</p>	 <p>2b</p>  <p>4b</p>	Formation of 2b and 4b occurs approximately in same amounts (around 20%), but in a reductive environment is 4b preferred (>90%)
	TRII		 <p>2b</p>	Despite no expected product, still major conversion to 2b is observed (>75% of the product)
2'-acetyl-[1,1'-biphenyl]-2-carbaldehyde			2b	

 <p>1c</p>	TRI	 <p>(R)-3c</p>	 <p>2c</p>	Under redox-neutral conditions no products are found, but with added isopropanol the expected formation of 3c is increased over 91%
	TRII			As expected, no conversion is detected
2'-(2,2,2-trifluoroacetyl)-[1,1'-biphenyl]-2-carbaldehyde				
 <p>1d</p>	TRI	 <p>(R)-2d</p>	 <p>4d</p>	Small amounts of 4d are detected under redox-neutral conditions that can be increased to over 93% conversion by exchanging the cosolvent to isopropanol
	TRII	 <p>(S)-2d</p>		No substrate consumption is detected
2'-benzoyl-[1,1'-biphenyl]-2-carbaldehyde				

The experimental data differs in many cases from predictions made by the docking study. Since the expected product is formed for the substrate **1a** that contains two aldehyde moieties, the problems of the other compounds **1b-1d** could be based on the ketone functionalities in these molecules. The influence of the substituents could be gauged in a wrong way, what could lead to predict the hydride attack on the aldehyde instead of the ketone and vice versa. Furthermore, using YASARA and PyMol did not consider the difference in reactivity of ketones and aldehydes as well the influence of the substituents on the ketone. The CF₃ and the Ph should serve to activate the carbonyl group by withdrawing electrons and so making the carbon more electrophilic and likely to be reduced. However, effects regarding the activity of the different ketones and aldehyde are considered in the calculation, but the calculations are solely based on structure.

3.1.1. [1,1'-biphenyl]-2,2'-dicarbaldehyde

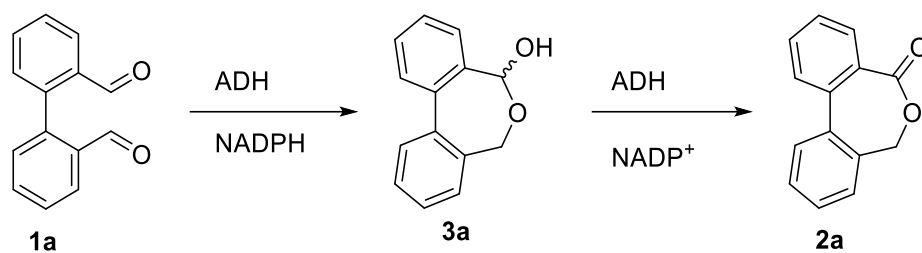


Figure 33 reaction route to **2a**

[1,1'-biphenyl]-2,2'-dicarbaldehyde or **1a** is one of the less demanding substrates since it possesses 2 equivalent aldehyde moieties and is symmetrical. Hence, only one final product **2a** is expected as seen in Figure 33. This lactone also does not possess any chirality. But on the other hand, two different enantiomers of the intermediate (*R*)-**3a** and (*S*)-**3a** could serve as an intermediate. Previous works have already shown that the secondary hydroxy group racemises due to having the possibility to reopen the lactol **3a** and reclose to yield the other enantiomer.

TR I

Step 1: Reduction

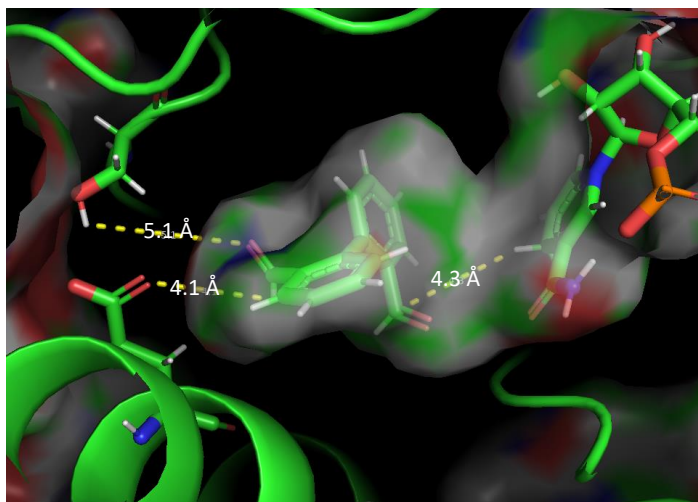


Figure 34 Substrate **1a** in TR I with oxidised cofactor and amino acid side chains that can stabilize the substrate

As seen in Figure 34 TR I possess a binding pocket large enough for **1a** and the aldehyde functionality of the substrate is orientated in proximity of 4.3 Å to the cofactor allowing the transfer of the Hydride. In the binding pocket are Serine on position 167 and Glutamic acid on position 222 positioned that could interact with the aldehyde to give a positive effect on the substrate orientation. The carboxylic acid moiety of the sidechain of the glutamic acid (Glu 222) has a distance of 4.1 Å to the proton of the aldehyde moiety of the substrate and could delocalise this proton, while the serine (Ser 167) is 5.1 Å away and oriented towards the oxygen and could act as a acid to protonate.

TR I

Step 2: Oxidation

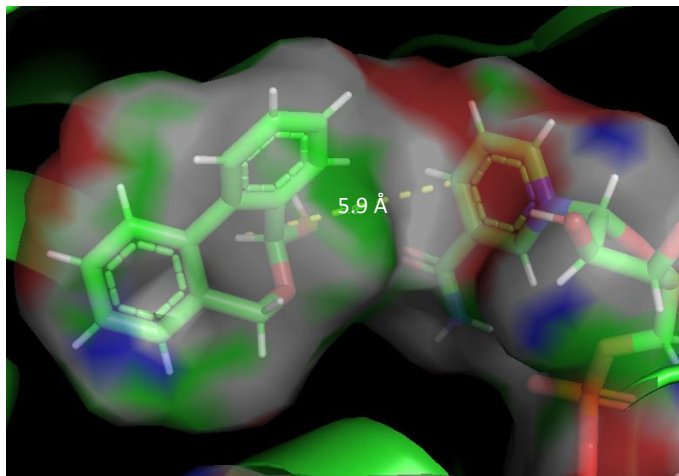


Figure 35 Intermediate **3a** in TR I with oxidised cofactor and amino acid side chains that can stabilize the intermediate

After the reduction of the aldehyde moiety to the alcohol and spontaneous ring closure, the formed lactol **3a** is present as a racemate, because the reduced aldehyde produces a primary alcohol that cannot possess any chiral information. Since the axis was already determined in previous works to be unhindered and is allowed to change chirality. All this should enable a dynamic kinetic resolution for converting 100% of the substrate. The distance between the hydride of the substrate and the cofactor displayed in Figure 35 is 5.9 Å for **3a** and the substrate is directed in the opposite direction of the NADPH. All calculated fits for **3a** have long distance between the hydride to remove the intermediate lactol and the cofactor and are facing away from the cofactor. Nevertheless, experimental data shows a high conversion to **2a**, indicating that the oxidation occurs and eventual problems with the model exist.

TR II

Step 1: Reduction

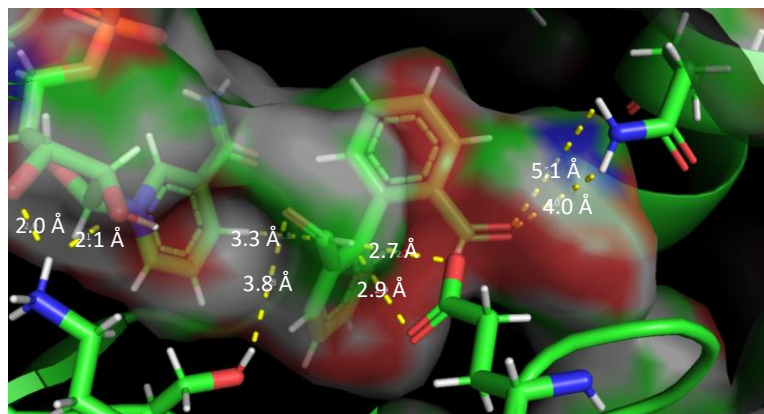


Figure 36 Substrate **1a** in TRII with oxidised cofactor and amino acid side chains that can stabilize the substrate

TRII also shows a binding pocket large enough to fit **1a** easily inside and can be orientated with the aldehyde moiety towards the NADP⁺ as seen in Figure 36 above. The resulting distance between the Hydride and carbonyl carbon is 3.3 Å. This distance indicates a very likely reduction of substrate.

TR II

Step 2: Oxidation

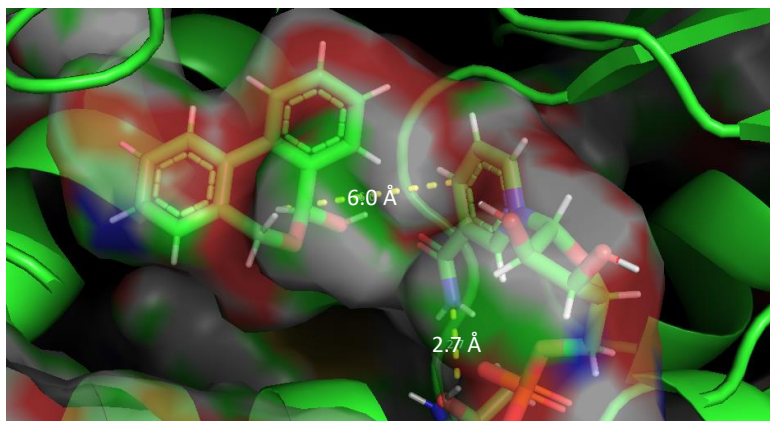


Figure 37 Intermediate **3a** in TRII with reduced cofactor and amino acid side chains that can stabilize the intermediate

Since the ring should be able to alter the chirality of the hydroxy group and the axis producing different enantiomers, all conformations need to be considered for this step. The oxidation of the lactone intermediate seems to be more demanding, but the size of the binding pocket is still large enough for the compound as illustrated in Figure 37. The orientation of the Hydroxy group of **2a** seems more tilted away of the cofactor what leads to a distance of 6.0 Å for **3a**. Therefore, the oxidation to the lactone does not seem likely, but nevertheless, the formation of **3a** can be experimentally observed.

Keto-aldehyde containing substrates (substrates: **1b-d**)

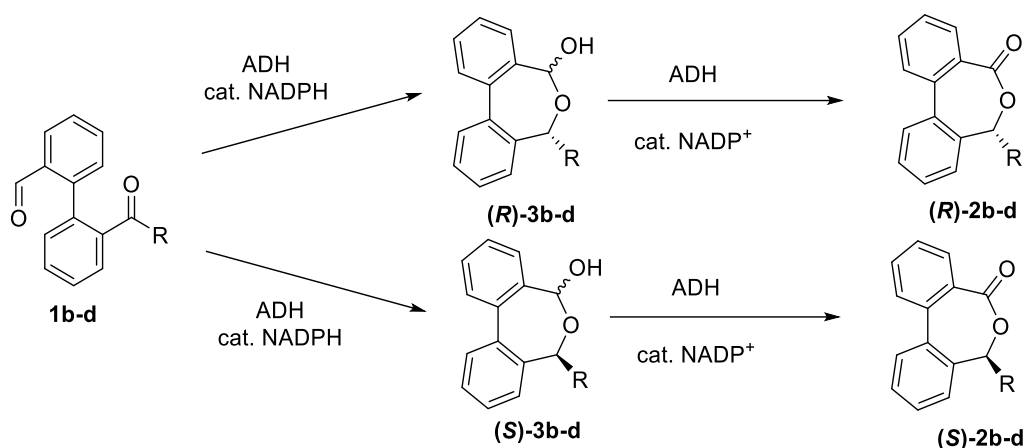


Figure 38 Reaction routes to **(R)-2b-d** and to **(S)-2b-d**

A specific reduction of the ketone moiety of **1b-d** introduces a chiral alcohol in the intermediate **3b-d** that should be retained during the oxidation to the final product **2b-d**. Since both are chiral compounds, they are referred to as **(R)-3b-d**, **(S)-3b-d** and **(R)-2b-d**, **(S)-2b-d** respectively, when discussing chirality of the substituents and in regard to the potential chirality of the axis the compounds are referred to as **(aR)-3b-d**, **(aS)-3b-d** and **(aR)-2b-d**, **(aS)-2b-d**. The produced chirality in **3b-d** and therefore, also in **2b-d** is predicted by the site (*re* or *si*) where the hydride attacks the substrate. Possible products and intermediates are displayed in Figure 38.

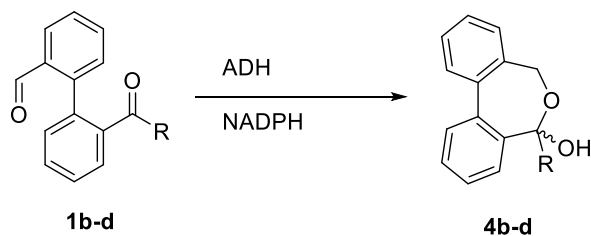


Figure 39 Side reaction to **4b-d**

When the aldehyde moiety of **1b-d** is reduced first the formation of **4b-d** is expected as visible in Figure 39. Since a primary alcohol is formed a racemate of **4b-d** is expected. The conformation of axis cannot be predicted based on this model, but the atropoisomers possibly directed by the chirality of the substituent (*R*) cannot be ruled out. Since a racemate is expected, there would be probable two enantiomers: **(aR,S)-4b-d**, **(aS,R)-4b-d**

3.1.2. 2'-acetyl-[1,1'-biphenyl]-2-carbaldehyde

TR I

Step 1: Reduction

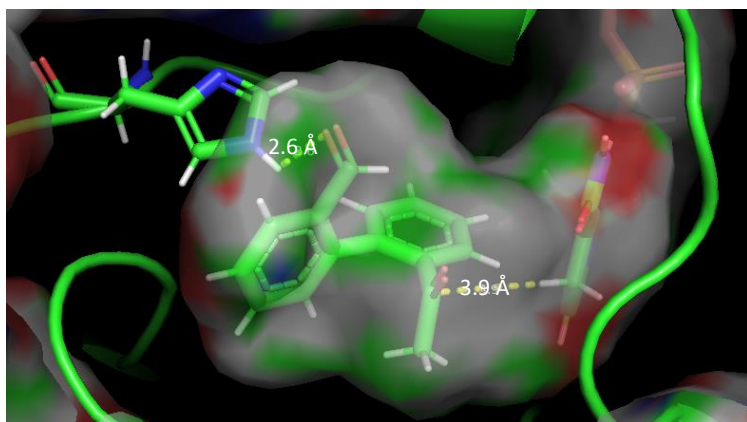


Figure 40 Substrate **1b** in TRI with oxidised cofactor and amino acid side chains that can stabilize the substrate (Orientation of the ketone towards the cofactor)

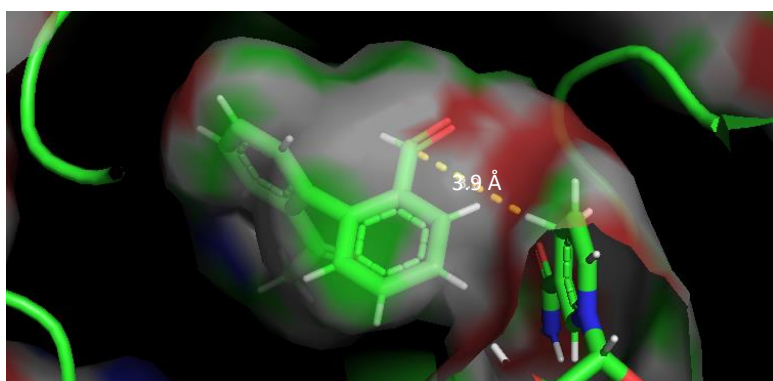


Figure 41 Substrate **1b** in TRI with oxidised cofactor and amino acid side chains that can stabilize the substrate (Orientation of the aldehyde towards the cofactor)

Tropinone reductase I is predicted to be equal likely to oxidise both the ketone and the aldehyde moiety of **1b**, due to a distance of 3.9 Å to the hydride. Both fits are seen in Figure 40 and 41. This model also predicts the attack of the hydride on the *si* site of the substrate. Therefore, the formation of both (*S*)-**3b** and **4b** approximately equally likely, but (*S*)-**3b** may be slightly more probable due to fixation by the histidine (His 112)

TR I

Step 2: Oxidation

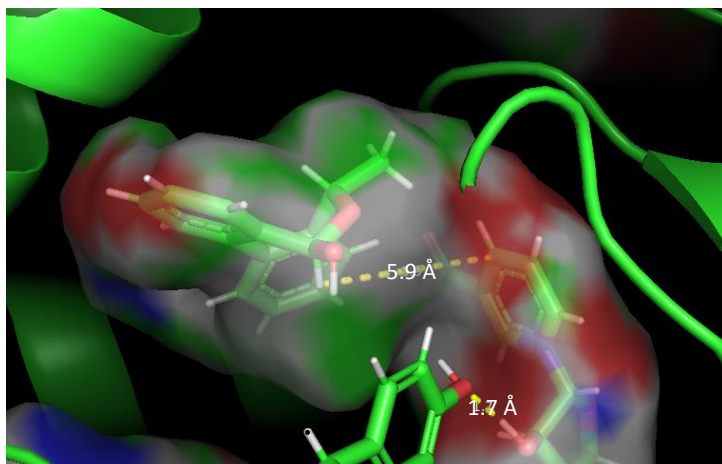


Figure 42 Intermediate **3b** in TR I with reduced cofactor and amino acid side chains that can stabilize the intermediate

The distance of 5.9 Å of the hydride to the cofactor shown in Figure 42 seems far, making the oxidation reaction quite unlikely, but the space and orientation of the intermediate in the binding pocket still seem to fit. The best fitting molecule is **(S)-3b**, the molecule most probable to be the product of a reduction of **1b**, displaying the hydroxyl group having *R* chirality. The conformation is shown in Figure 43 below. Therefore, under non reducing conditions a formation of **(S)-3b** could be expected with also **4b** been produced.

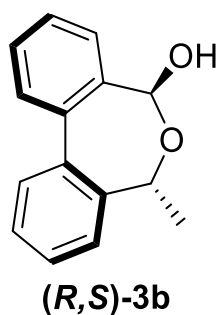


Figure 43 Structure of **(R,S)-3b**

Experimentally mainly oxidation on aldehyde is observed, since **2b** is formed and the oxidation is predicted with no change in chirality, but the formation of the hemiketal **4b** is preferred in a reductive environment.

TR II

Step 1: Oxidation

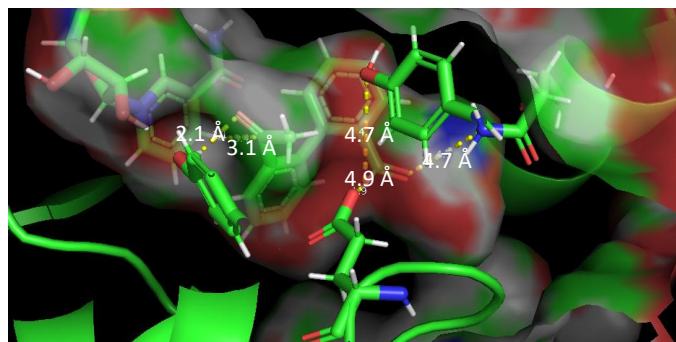


Figure 44 Substrate **1b** in TRII with oxidised cofactor and amino acid side chains that can stabilize the substrate (Orientation of the ketone towards the cofactor)

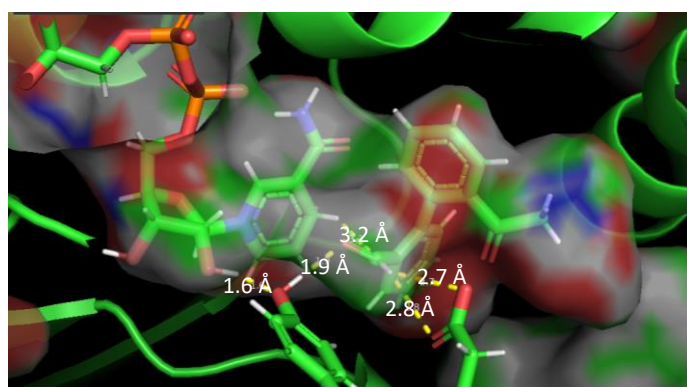


Figure 45 Substrate **1b** in TRII with oxidised cofactor and amino acid side chains that can stabilize the substrate (Orientation of the aldehyde towards the cofactor)

Reduction on the ketone or the aldehyde functionality seems almost equally probable, due to having nearly an equal distance to the hydride donor with 3,4 Å for the ketone and 3,3 Å for the aldehyde. Both fits are shown in Figure 44 and 45. However, the reduction of the ketone moiety seems difficult, due to the orientation of **1b**. The substrate is neither facing the *si* or the *re* site of the molecule, but rather between the carbonyl carbon and the aryl ring. An attack from both calculated angles should be impossible.

Nevertheless, the reduction of **1b** occurs on the ketone since the formation of **2b** can be observed experimentally. Therefore, also the oxidation reaction from **3b** to **2b** must occur.

3.1.3. 2'-(2,2,2-trifluoroacetyl)-[1,1'-biphenyl]-2-carbaldehyde

TR I

Step 1: Reduction

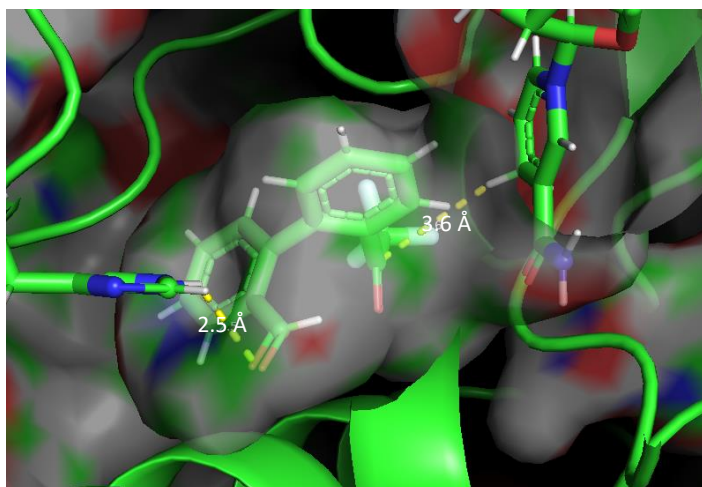


Figure 46 Substrate **1c** in TR I with oxidised cofactor and amino acid side chains that can stabilize the substrate

The model, displayed in Figure 46 predicts a probable and selective reduction of **1c** with a cofactor-substrate distance of 3.6 Å. The *re* site of the substrate faces the cofactor and should therefore selectively produce the (**R**)-**3c**, while no possible for fit for reducing the aldehyde or the *si* site of the compound. The binding pocket is calculated to be spacious enough for fitting **1c** inside. Furthermore, the calculated fit could be aided by a histidine (His 112) that can interact with the aldehyde on the opposite side of the molecule.

Step 2: Oxidation

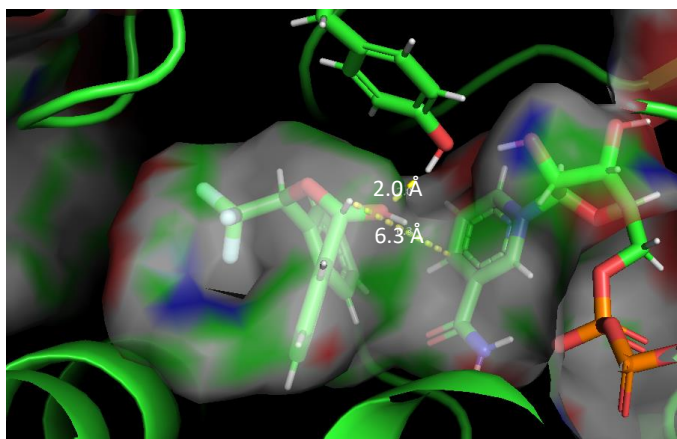


Figure 47 Intermediate **3c** in TRI with reduced cofactor and amino acid side chains that can stabilize the intermediate

The best possible calculated fit for any of the possible intermediates **3c** with all chirality and in all possible configurations is seen Figure 47 and exhibits still more than 6.0 Å distance to the hydride and is facing away from the cofactor. This orientation could be favoured, due to a tyrosine (Try 171) interacting with and fixing the hydroxy group of the lactol in a position that forces the hydride pointing away from the NADP⁺.

Experimentally tropinone reductase I is able to yield **3c** under reductive conditions, like in the model predicted and no oxidation of **3c** to **2c** using tropinone reductase I can be detected.

TR II

Step 1: Reduction

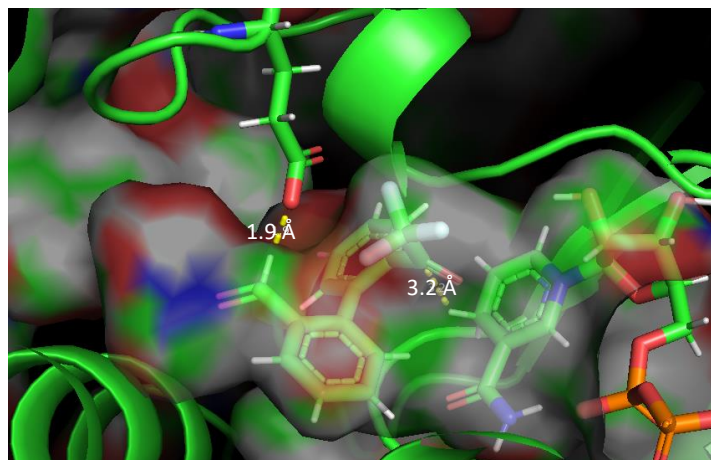


Figure 48 Substrate **1c** in TRII with oxidised cofactor and amino acid side chains that can stabilize the substrate (Orientation of the ketone towards the cofactor)

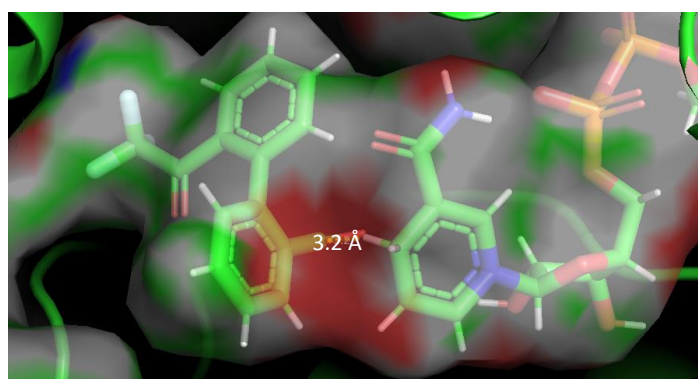


Figure 49 Substrate **1c** in TRII with oxidised cofactor and amino acid side chains that can stabilize the substrate (Orientation of the aldehyde towards the cofactor)

The distance between the cofactor and the carbonyl carbon of the ketone and aldehyde moiety of the substrate should be with 3.2 Å in both cases equally likely to perform a reduction. Both are displayed in Figure 48 and 49. However, the glutamate (Glu 156) is with 1.9 Å in proximity to the aldehyde to bind and orient **1c** in a position that allow the ketone moiety to face towards the NADPH as shown in Figure 49. This could potentially favour the reduction of this group, but the position of **1c** towards the cofactor is in a disfavoured angle to each other. The only possible way for an attack hydride would be directly between the carboxyl and the aryl group. This angle should not allow any reduction of the substrate in either case. No formation of **2c**, **3c** or **4c** can be quantified in any experiment, like expected based on the model.

3.1.4 2'-benzoyl-[1,1'-biphenyl]-2-carbaldehyde

TR I

Step 1: Reduction

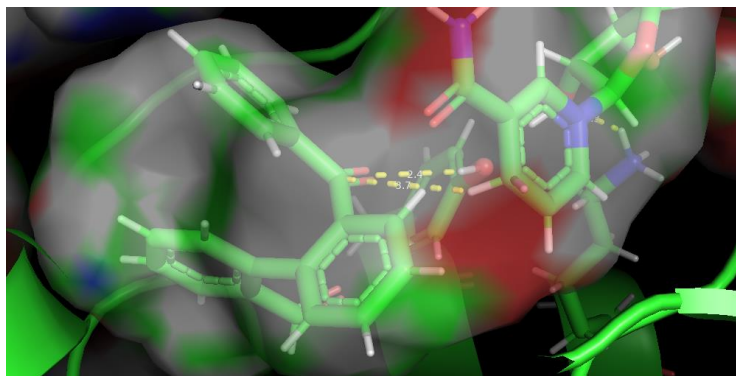


Figure 50 Substrate **1d** in TRI with oxidised cofactor and amino acid side chains that can stabilize the substrate (Orientation of the ketone towards the cofactor)

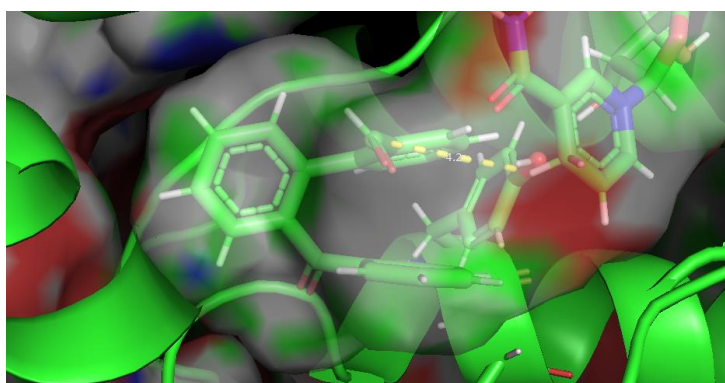


Figure 51 Substrate **1d** in TRI with oxidised cofactor and amino acid side chains that can stabilize the substrate (Orientation of the aldehyde towards the cofactor)

Even **1d** having with a phenyl group one of the most demanding substituent modelled the substrate still seems to fit easily in the pocket within close proximity of 3.7 Å to ketone the NADPH. In Figure 50 a Tyr 171 is with 2.4 Å in position to fix and possible protonate **1d** after the reduction. The model predicts the attack of the hydride on the *re* site of the molecule. Reduction of the aldehyde shown in Figure 51 does not display such help. The formation of **4d** cloud also be possible, since the distance to the aldehyde moiety is with 4.2 Å still in the right range to be reduced.

Step 2: Oxidation

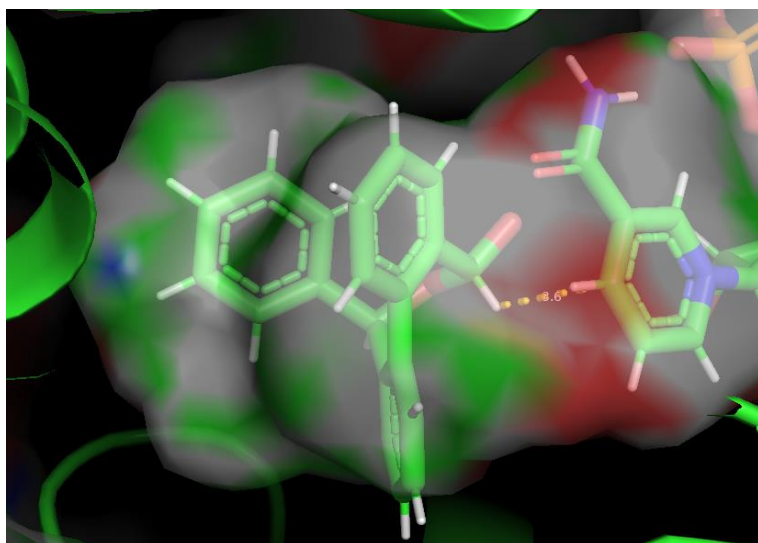


Figure 52 Intermediate **3d** in TRII with reduced cofactor and amino acid side chains that can stabilize the intermediate

(aR)-3d is the most probable product of the reduction and with a distance of 3.6 Å the intermediate is **(aR,R)-3d** shown in Figure 52 below the most likely substrate for the oxidation reaction. The axis is in a disfavoured position regarding the phenyl substituent, but the ring exhibits in the model still position in a way that should not cause to grave interaction in the molecule and could still allow the oxidation reaction.

Based on this model the expected main product would be **(R)-2b**, most likely **(aR,R)-2d** displayed in Figure 53, if the energy barrier is too high to allow isomerisation.

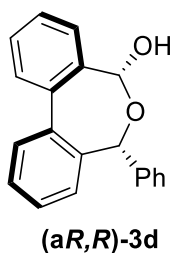


Figure 53 Structure of **(aR,R)-3d**

Nevertheless, in experiments **4b** is the main product formed by tropinone reductase I. The formation of **4b** is not predicted as improbable but was expected to be less favoured than **2b**.

TR II

Step 1: Reduction

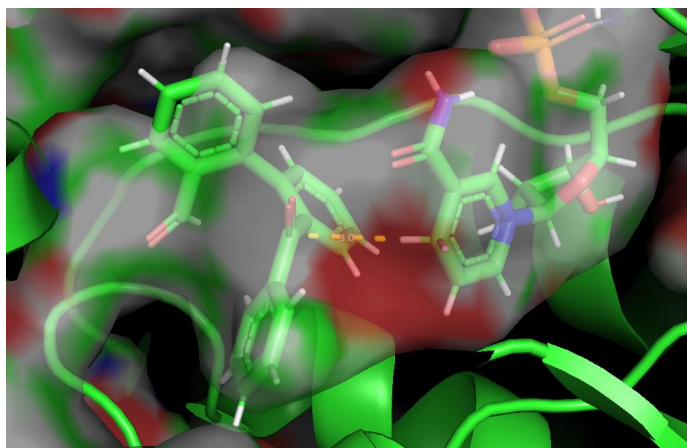


Figure 54 Substrate **1d** in TRII with oxidised cofactor and amino acid side chains that can stabilize the substrate (Orientation of the ketone towards the cofactor)

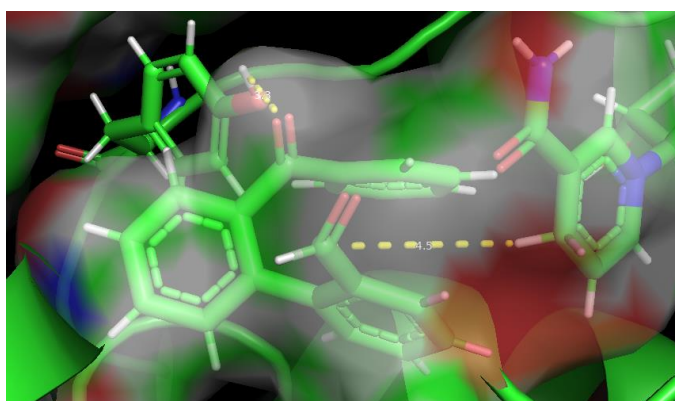


Figure 55 Substrate **1d** in TRII with oxidised cofactor and amino acid side chains that can stabilize the substrate (Orientation of the aldehyde towards the cofactor)

With 3.0 Å the ketone moiety is closest to the cofactor, but a part of the aryl ring containing the aldehyde clashes with the boundaries of the binding pocket, making this fit and also the reduction of **1d** in this case unlikely. However, if possible, the hydride would attack on the *si* site as seen displayed in Figure 54, due possible deformation of the substrate or the pocket that cannot be calculated based on the models used. The angle of the hydride attack would also fit for a hydride transfer. The docking displayed in Figure 55 possesses with 4.5 Å still a possible hydride transfer to the aldehyde forming **4d** and a tyrosine (Try 100) might even aid to stabilise the substrate **1d** and place it facing with the aldehyde group towards the NADPH.

Step 2: Oxidation

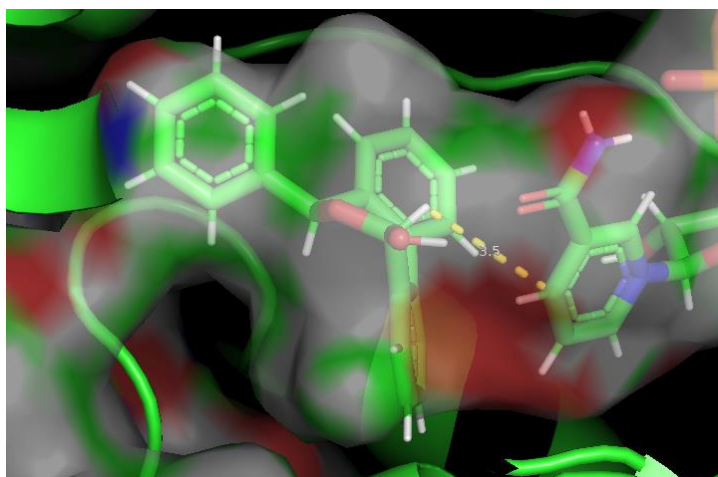


Figure 56 Intermediate **3d** in TRII with reduced cofactor and amino acid side chains that can stabilize the intermediate

The lactol **(S)-3d** is the most probable intermediate produced if the clashing with the boundaries of the pocket are not considered to completely hinder the reduction on the ketone. The fit is displayed in Figure 56. The best fitting substrate being oxidised is also a conformer of **(aR,S)-3d** as displayed in Figure 57 below. The axis and the substituents are in this case also oriented to maximise the space between them resulting in a stable compound that fits in the binding pocket with only slight clashes of the boundary with a few hydrogens from two of the aryl-rings. The distance and orientation of the hydride to the NADP⁺ seems with 3.5 Å fit for a transfer. So, either the formation of **(S)-2d** or **4d** would be predicted based on the docking.

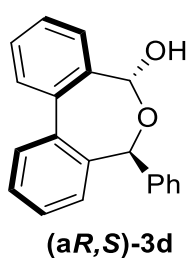


Figure 57 Structure of **(aR,S)-3d**

The conducted experiments tropinone reductase II does not reveal any reaction at all with the substrate **1d** indicating the substrate being probable too demanding. Furthermore, the channel leading to the binding pocket was not investigated in this modelling. This channel could be in general too small to allow the substrate to reach the active site.

3.2 Screening

3.2.1. [1,1'-biphenyl]-2,2'-dicarbaldehyde

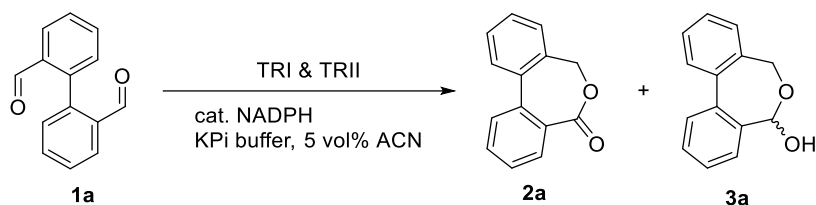


Figure 58 Biotransformation of **1a** using TR I and TR II with 5 vol% CH₃CN

Since **1a** was the simplest molecule of the investigated substrates and did not exhibit neither chirality nor selectivity issues, this compound serves as a model substrate to test the substrate capabilities of tropinone reductase I and II. The reaction scheme is displayed in Figure 58.

Table 6 Reaction conditions: 10 mM of **1a**, 20 mg/mL TR I/TR II, 0.5 mM NADPH, KPi buffer (50 mM, pH 7.0, 2 mM MgCl₂), 5 vol% CH₃CN, 30 °C, 150 rpm, overnight.

Conversion based on GC (HP-5) peak areas

ADH	2a [%]	3a [%]
TRI	78	5
TRII	86	n.d.

1a was converted using stoichiometric amounts of NADPH to yield **2a** as a product by using both TRI and TR II. While TR I produced the lactol **3a** as a side product, TRII produced no detectable amounts of **3a**. Conversion is listed in Table 6.

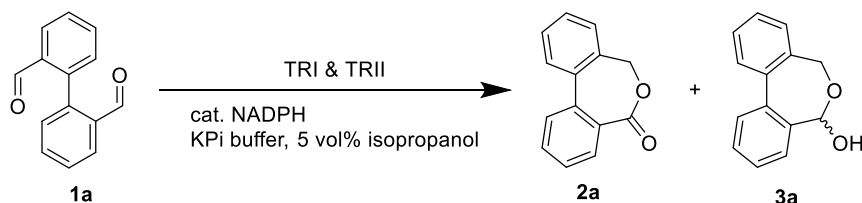


Figure 59 Biotransformation of **1a** using TR I and TR II with 5 vol% propan-2-ol

Table 7 Reaction conditions: 10 mM of **1a**, 20 mg/mL TR I/TR II, 0.5 mM NADPH, KPi buffer (50 mM, pH 7.0, 2 mM MgCl₂), 5 vol% propan-2-ol, 30 °C, 150 rpm, overnight.

Conversion based on GC (HP-5) peak areas

ADH	2a [%]	3a [%]
TRI	6	94
TRII	89	n.d.

By using catalytic amounts of NADPH with isopropanol as cosolvent the main product of TR I was shifted to **3a**, while TR II still was able to produce the lactone **3b** with no traceable amounts of **3a**. This result could indicate that TRII is not able to use isopropanol as cosolvent. Relative conversions of **2a** and **3a** are shown in Table 7.

3.2.2. 2'-acetyl-[1,1'-biphenyl]-2-carbaldehyde

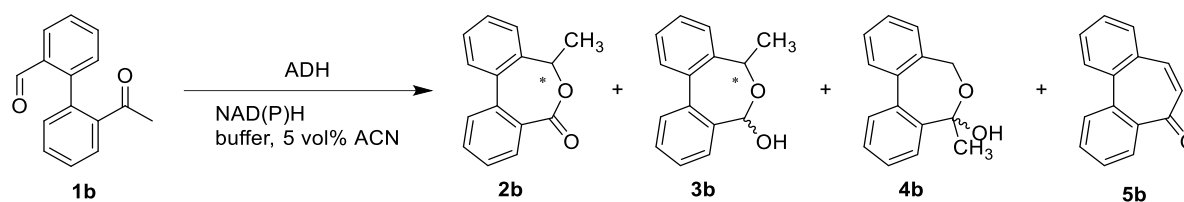
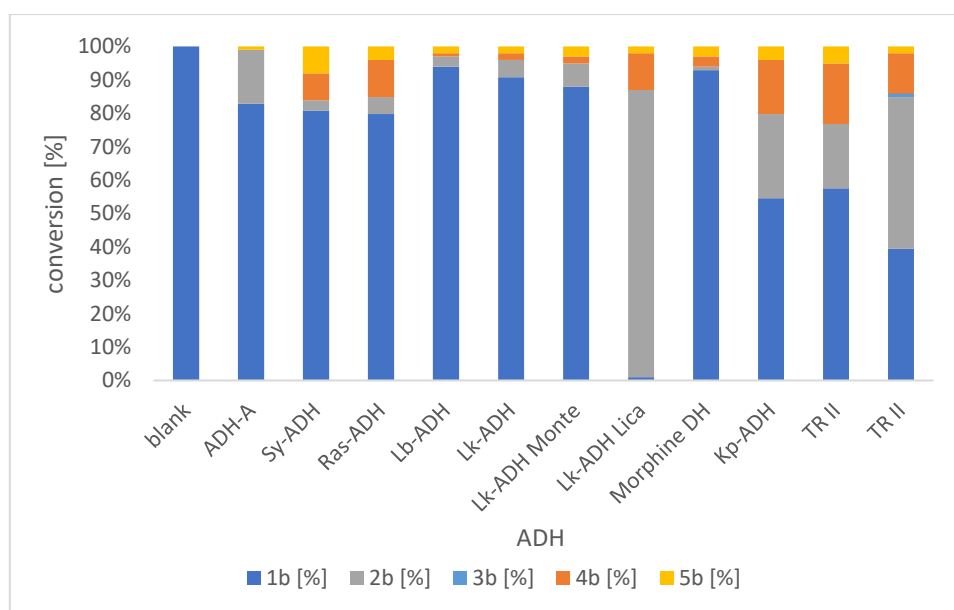
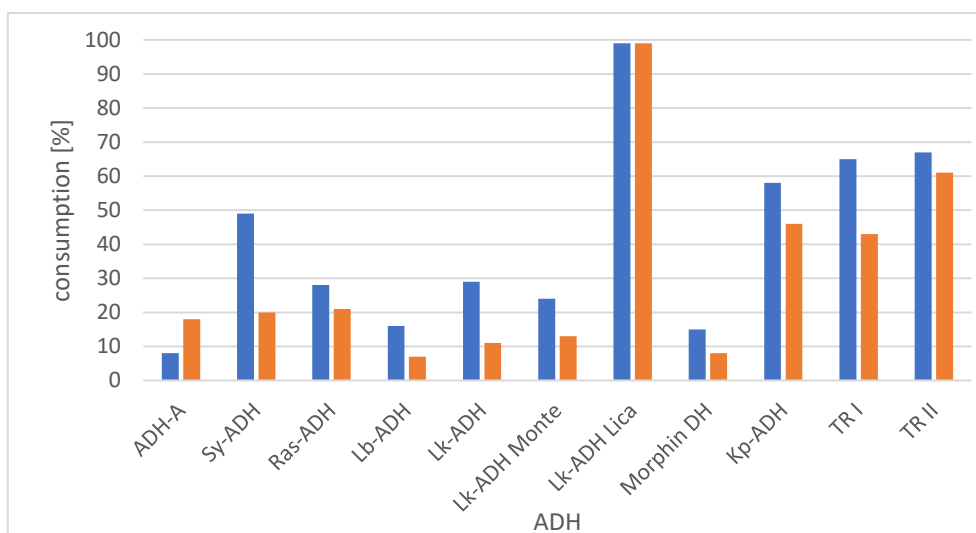


Figure 60 Biotransformation of **1b** with 5 vol% CH₃CN



Graph 1 Reaction conditions: 10 mM of **1b**, 20 mg/mL ADH, 0.5 mM NADPH, KPi buffer (50 mM, pH 7.0, 2 mM MgCl₂), 5 vol% CH₃CN, 30 °C, 150 rpm, overnight, Conversion based on GC (CB-Dex) peak areas

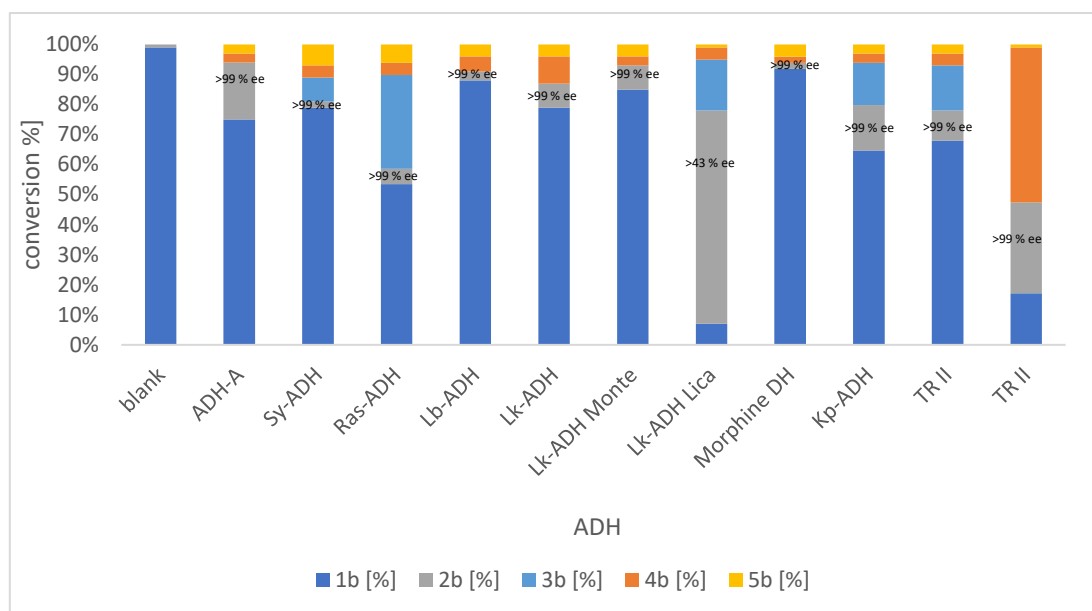
While all tested ADHs showed at least some consumption of substrate **1b** and formation of products **2b** to **5b** shown in Figure 60, the most promising conversion were exhibited by tropinone reductase I and II, Kp-ADH with at least 40 % substrate consumption and Lk-ADH Lica that was able to convert almost all **1b**. All conversions can be seen in Graph 1. The consumption of substrate was determined by an external calibration of **1b** and by relative comparison of total peak areas related to the sum of **1b** to **5b**. A comparison of both shows large differences in substrate consumption based on the used method for the determination of the concentration as seen in Graph 2. While Lk-ADH Lica showed almost total substrate consumption using both methods and most entries (ADH-A, Ras-ADH, Lb-ADH, Morphine DH and TR II) differ less than 10 %, others vary even greater. For example, Sy-ADH and Lb-ADH have 150% more consumption determined by calibration. This could indicate still to be identified or misidentified side products.



Graph 2 Substrate consumption based on calibration (blue) and total peak areas (orange)

Reaction conditions: 10 mM of **1b**, 20 mg/mL ADH, 0.5 mM NADPH, KPi buffer (50 mM, pH 7.0, 2 mM MgCl₂), 5 vol% CH₃CN, 30 °C, 150 rpm, overnight

In general, all enzymes showed substrate consumption as listed in Graph 1 and 2. Lica was also able to convert 86% to the desired lactone **2b**. Second highest formation of the product was achieved using TR II with over 40 % yield. Under experimental condition all the ADHs produced almost no traceable amounts of the intermediate product **3b**, indicating all the is oxidised to **2b**. It has to be remarked that **3b** could not be properly identified. The emiketal **4b** is produced depended on the enzyme in minor or moderate quantities to up to 18 % probably reaching the maximum conversion based on the available reducing agent. **4b** also showed several problems for identification. Furthermore, all reactions of the screening also have minor conversion to the side product **5b** as a result of aldol varying between 2 % and 8 %.



Graph 3 Reaction conditions: 10 mM of **1b**, 20 mg/mL ADH, 0.5 mM NADPH, KPi buffer (50 mM, pH 7.0, 2 mM MgCl₂), 5 vol% CH₃CN, 30 °C, 150 rpm, overnight,
Chiral analysis of products,
Conversion based on GC (CB-Dex) peak areas

Chiral analysis of **2b** showed that entry 1 to 6 (ADH-A, Sy-ADH, Ras-ADH, Lb-ADH, Lk-ADH and Lk-ADH Montelukast) and 8 to 11 (Morphine DH, Kp-ADH, TR I and TR II) all produce exclusively the same enantiomer of the product in very high enantiomeric excess. Lk-ADH Lica was the only ADH that had the ability of producing both species of the lactone. The intermediate **3b** and side product **4b** while still possessing a chirality did not show any signals in the chiral GC analysis, since the prepared references of both compounds were enantiomerically pure. This could be either explained by an unfit method that was incapable of separation of the isomers, the enzymes used for synthesis of the reference material being selective for one enantiomer or the purification of the reference removed the other enantiomer.

At direct comparison of the two screening sets, a general trend of substrate consumption stays the same with just minor changes, where most ADHs reduced the substrate consumption slightly, most likely due to enzyme degradation over time. The resulting activity loss could be a normal side effects of prolonged storage, since several months passed between the sets of reaction. However, Ras ADH and TR II both seemed to increase the consumption of **1b** by 30 and 20 % to 50 and 80%, respectively. Most curious TR II seems even with an increase of 25 % to consumption TR II produced 30 % less **2b** and four times the amount of **4b**. This is an even more interesting behaviour when considering this quantity exceeds the theoretical limit of reduced product by far, since the added amount of NADPH should allow a maximum for 5 % conversion. This limit can and was at times slightly overstepped, due to residues of cofactor remaining in the lyophilised cells used for the transformations. Also, TR I and Kp-ADH for example, yielded less **2b** according to the less consumed substrate, but moreover, both apparently had a switch in the distribution of **3b** and **4b** completely. While **3b** was hardly detectable in the first set, several enzymes such as TR I, Kp-ADH, Sy-ADH, Ras-ADH and Lk-ADH Lica showed increased conversion to lactol of up to 30 % in case of Ras-ADH. The additional 30 % of **3b** corresponded approximately to the higher substrate consumption of Ras-ADH. All data of the chiral analysis is displayed in Graph 3.

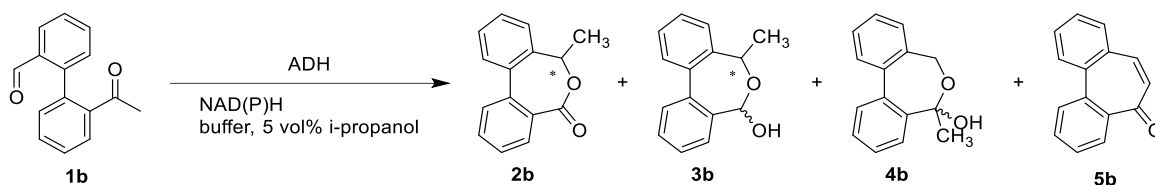
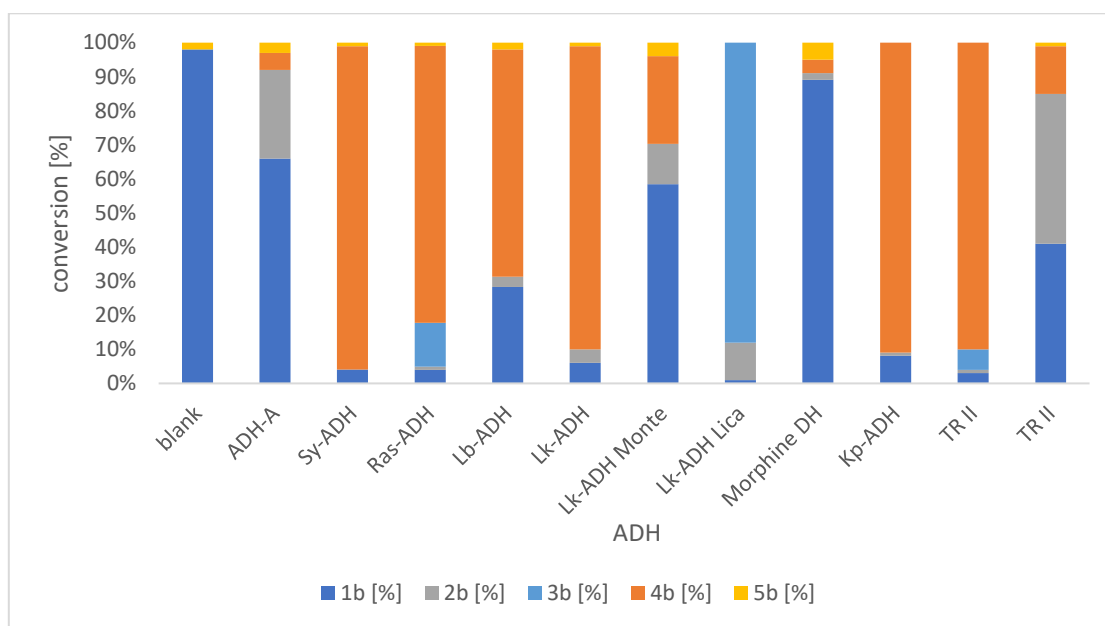
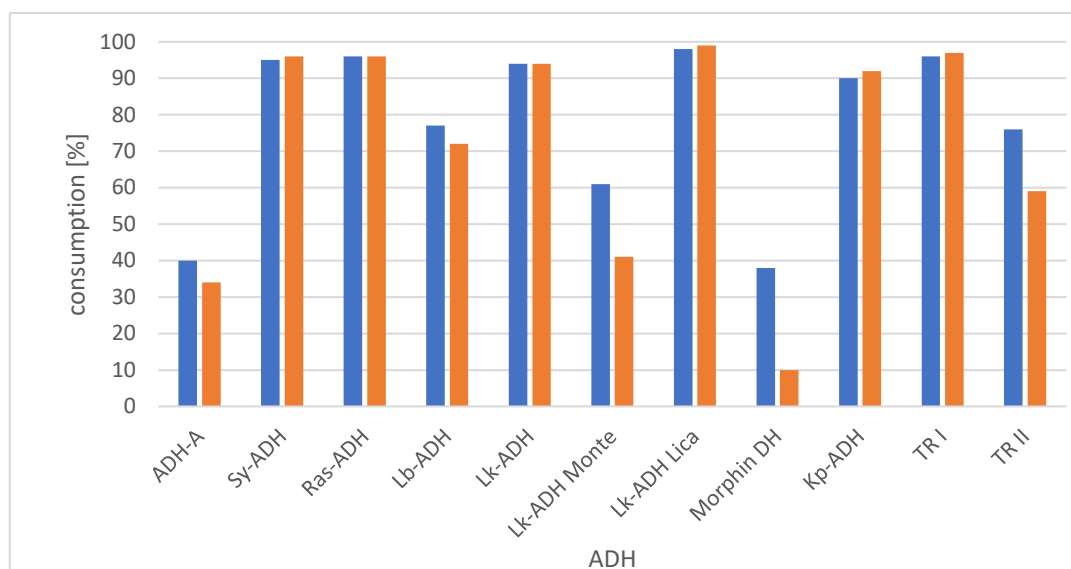


Figure 61 Biotransformation of **1b** with 5 vol% propan-2-ol



Graph 4 Reaction conditions: 10 mM of **1b**, 20 mg/mL ADH, 0.5 mM NADPH, KPi buffer (50 mM, pH 7.0, 2 mM MgCl₂), 5 vol% propan-2-ol, 30 °C, 150 rpm, overnight
Conversion based on GC (HP-5) peak areas

To push the distribution of the products to **3b** or **4b** the screening reaction were conducted under reducing conditions already established with TR I and model substrate **1a**. So, it was possible to increase the substrate consumption of entry 2, 3, 5, 9 and 10 (Sy-ADH, Ras-ADH, Lk-ADH, Kp-ADH and TR I) close to full consumption and entry 1, 4, 6, and 8 (ADH-A, Lb-ADH, Lk-ADH Montelukast and Morphine DH) significantly as shown in Graph 4 and 5. The conversion and product distribution of tropinone reductase II was not influenced by the change of cosolvent similar as established in experiments using **1a** as substrate, while entry 7, Lk-ADH Lica still showed full consumption of **1b**, but converted all to the lactol **3b** instead of the **2b** under redox neutral conditions. This was expected since **2b** was postulated to be produced by oxidising **3b**. Other ADHs like Sy-ADH, Ras-ADH, Lk-ADH, Kp-ADH and TR I showed strong preference towards building **4b** as the main product. Oddly, the chiral analysis as seen in Graph 6 showed Lk-ADH and TR II produce minor amounts of **4b** in pure fashion, while the non-chiral analysis of Graph 4 was unable to detect any traces of **4b**.

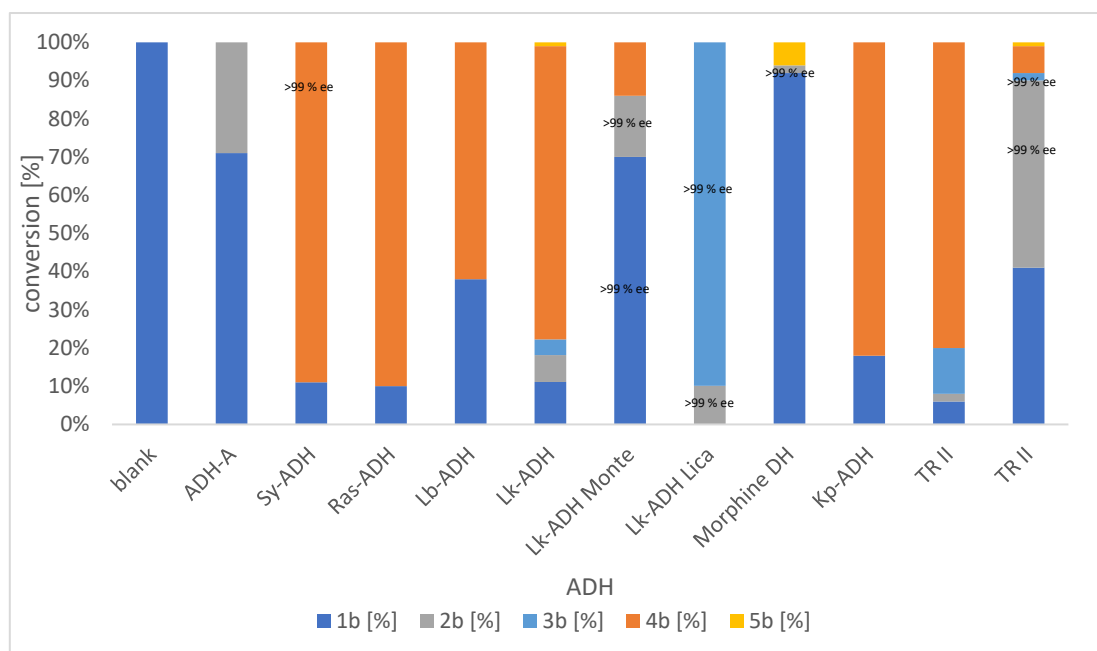


Graph 5 Substrate consumption based on calibration (blue) and total peak areas (orange)

Reaction conditions: 10 mM of **1b**, 20 mg/mL ADH, 0.5 mM NADPH, KPi buffer (50 mM, pH 7.0, 2 mM MgCl₂), 5 vol% propan-2-ol, 30 °C, 150 rpm, overnight

The comparison of substrate consumption with the calibration method and the conversion based on total peak areas seen in Graph 5, exhibits high agreement especially in lower concentrations, while higher concentrations of **1b** can lead to a greater variation in determined consumption.

For example, Morphine DH possesses around 10 % substrate consumption and 8 % under redox neutral conditions based on total peak areas, while the determination with the calibration indicates a much higher consumption of almost 40 % and 20 %, respectively. In general, the consumption based on the total peak areas appears lower than expected based on the calibration. This could indicate one or several product peaks have not been identified and therefore, reducing the apparent conversion of the substrate.



Graph 6 Reaction conditions: 10 mM of **1b**, 20 mg/mL ADH, 0.5 mM NADPH, KPi buffer (50 mM, pH 7.0, 2 mM MgCl₂), 5 vol% propan-2-ol, 30 °C, 150 rpm, overnight
 Chiral analysis of products
 Conversion based on GC (CB-Dex) peak areas

In Graph 6 above the relative peak areas are listed based on the chiral GC analytics. The enantiomeric excess was calculated based on the ratio peaks of the same compound. All produced **2b** and **3b** was determined to be highly enantiomeric pure if present. Interestingly, even the small amounts of **2b** produced by Lk-ADH Lica that had been previously analysed to produce a racemic mixture of **2b** under redox-neutral conditions, displayed only one enantiomer.

3.2.3. 2'-(2,2,2-trifluoroacetyl)-[1,1'-biphenyl]-2-carbaldehyde

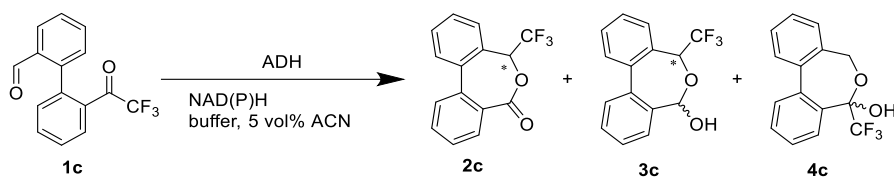
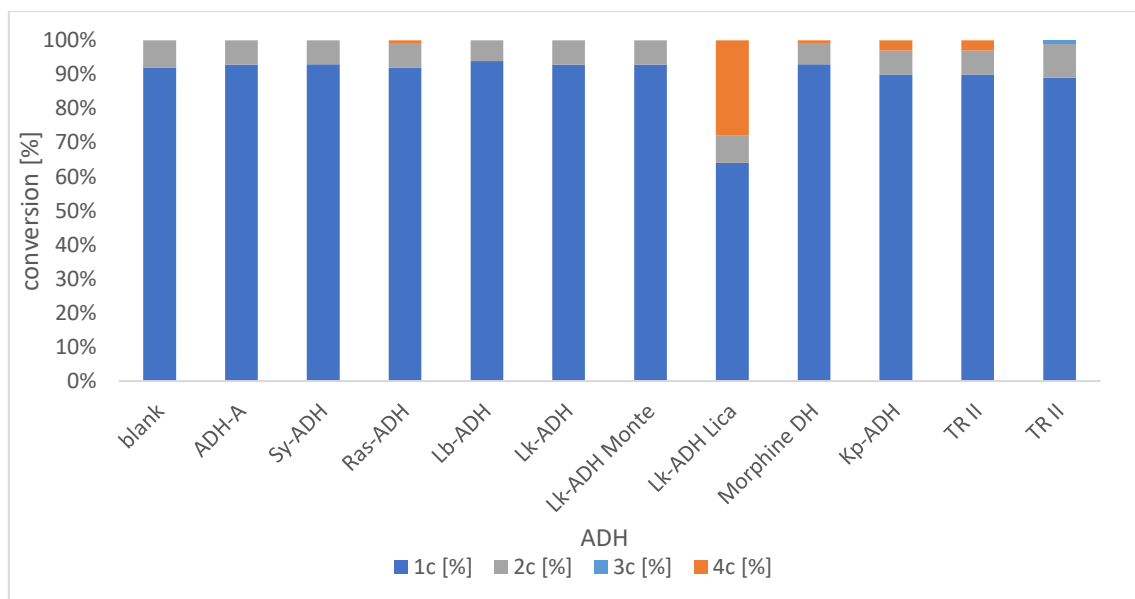
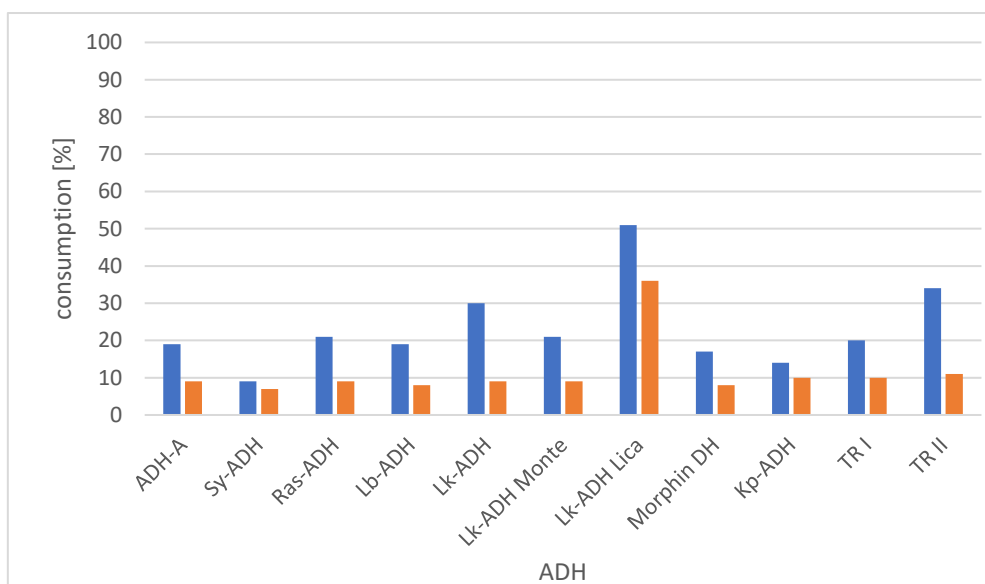


Figure 62 Biotransformation of **1c** with 5 vol% CH₃CN



Graph 7 Reaction conditions: 10 mM of **1c**, 20 mg/mL ADH, 0.5 mM NADPH, KPi buffer (50 mM, pH 7.0, 2 mM MgCl₂), 5 vol% CH₃CN, 30 °C, 150 rpm, overnight
Conversion based on GC (HP-5) peak areas

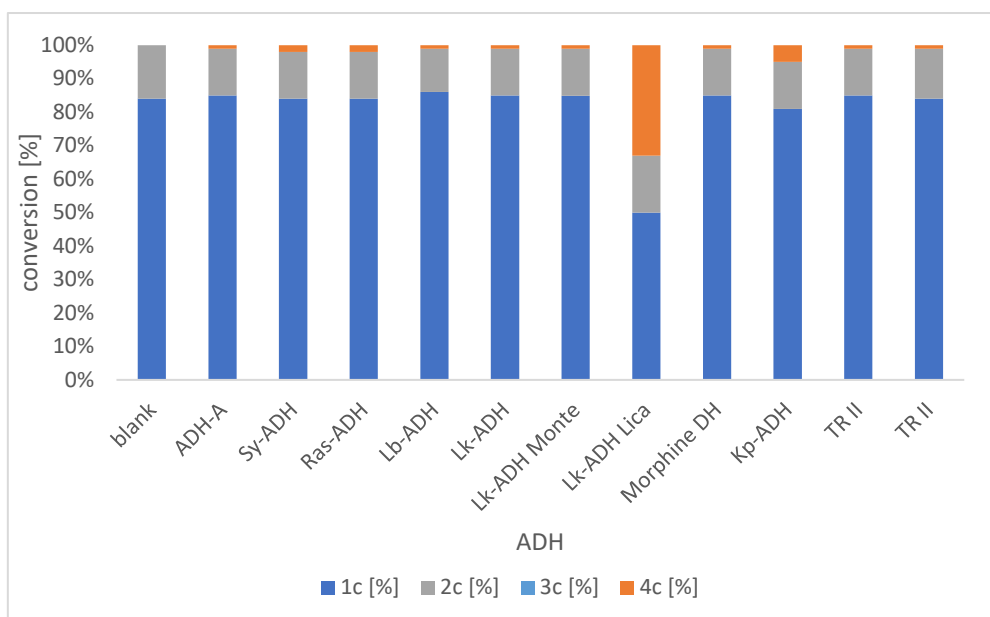
Substrate **1c** was in comparison to **1b** a much poorer substrate, despite the comparable size of both and the theoretical activation of the carbonyl group. **2c** is detectable in all samples inclusive the blanks in roughly the same concentration, indicating that **2c** is probably an impurity of the substrate from the Suzuki-coupling. Entry 7 (Lk-ADH Lica) was the only sample with considerable substrate consumption with 35 % consumption based on relative peak areas or approximately 50 % based on determination by external calibration. Nevertheless, the amount of **2c** did not increase, but all substrate was transformed to **4c** as a main product. All results of the analysis are displayed in Graph 7.



Graph 8 Substrate consumption based on calibration (blue) and total peak areas (orange)

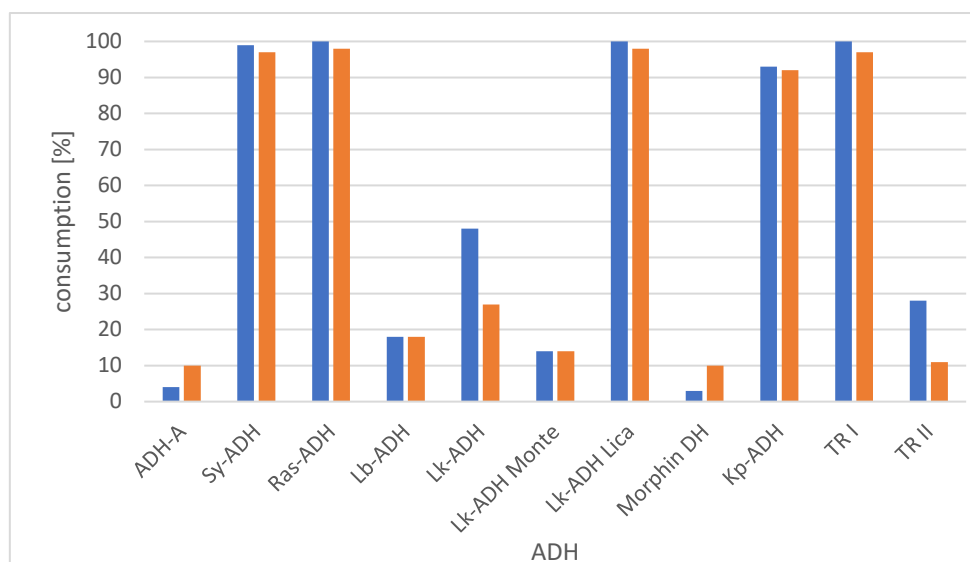
Reaction conditions: 10 mM of **1c**, 20 mg/mL ADH, 0.5 mM NADPH, KPi buffer (50 mM, pH 7.0, 2 mM MgCl₂), 5 vol% CH₃CN, 30 °C, 150 rpm, overnight

While all entries, except 7 with Lk-ADH Lica exhibited around 10 % consumption, the normalised peak areas showed consequently smaller areas than the blank implicating strongly another yet undiscovered product peak. The normalised area of the blank is over 1.2, while the areas of most other entries is in the range of 0.8 to 1.0. When compared with the consumption based on the calibration can exhibit up to 20 % more consumption. A direct comparison is visualised in Graph 8.



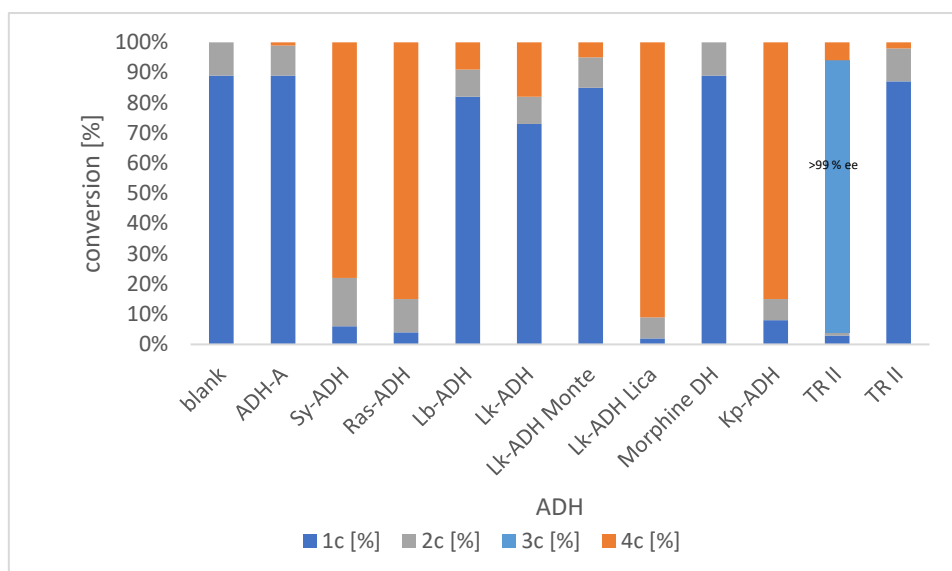
Graph 9 Reaction conditions: 10 mM of **1c**, 20 mg/mL ADH, 0.5 mM NADPH, KPi buffer (50 mM, pH 7.0, 2 mM MgCl₂), 5 vol% CH₃CN, 30 °C, 150 rpm, overnight
 Chiral analysis of products
 Conversion based on GC (CB-Dex) peak areas

Since **2c** was synthesised as a side product in the Suzuki coupling reaction, this product shows no signs of chirality. But nevertheless, **2c** could be isolated, purified and characterised and the chiral analysis showed to major peaks serving as proof of favouring 2 enantiomers, where the axis is possible directed by the chiral centre similar as described in the literature.^[67] Despite being detected in minor amounts on non-chiral column, no peaks were visible on chiral column and therefore, the enantiomeric excess could not be determined. **4c** was able to be detected in traces except in Lk-ADH Lica, where around 30% of the hemiketal are produced and all seem to be highly enantiomerically pure. All details of the chiral analysis are displayed in Graph 9.



Graph 11 Substrate consumption based on calibration (blue) and total peak areas (orange)
 Reaction conditions: 10 mM of **1c**, 20 mg/mL ADH, 0.5 mM NADPH, KPi buffer (50 mM, pH 7.0, 2 mM MgCl₂), 5 vol% propan-2-ol, 30 °C, 150 rpm, overnight

The majority of the substrate consumptions were in high agreement with each other as shown in Graph 11. Sy-ADH, Ras-ADH, Lk-ADH Lica, Kp-ADH and TR I all showed almost the same high percentages (>90%) in both cases. Enzymes with low consumptions like ADH-A, Lb-ADH, LK-ADH Monte and Morphine DH were also very similar, but Lk-ADH and tropinone reductase II showed differences larger than 10%. Again, these differences might be caused by unrecognised side reactions.



Graph 12 Reaction conditions: 10 mM of **1c**, 20 mg/mL ADH, 0.5 mM NADPH, KPi buffer (50 mM, pH 7.0, 2 mM MgCl₂), 5 vol% propan-2-ol, 30 °C, 150 rpm, overnight
 Chiral analysis of products
 Conversion based on GC (CB-Dex) peak areas

The chiral GC analysis seen in Graph 12 does not give much additional information regarding the conversion and product contribution, mainly just confirming data from the achiral analysis. Interestingly enough, even in samples where quite large quantities are measured on the achiral GC, the chirality of **3c** could not be determined. Only in entry 10 (TR I) the chirality of the lactol could be determined as basically enantiomerically pure. On the other hand, all of the **4c** produced exhibits only one peak in the data though it is not expected to have chiral information, since it is the product of ring closure with a primary alcohol.

3.2.4. 2'-benzoyl-[1,1'-biphenyl]-2-carbaldehyde

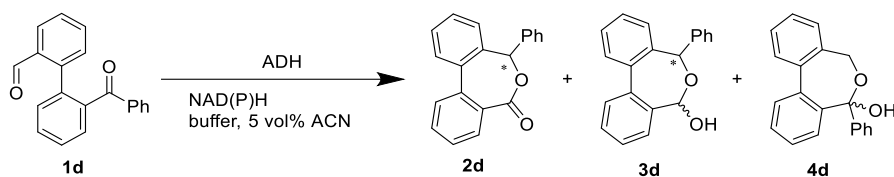
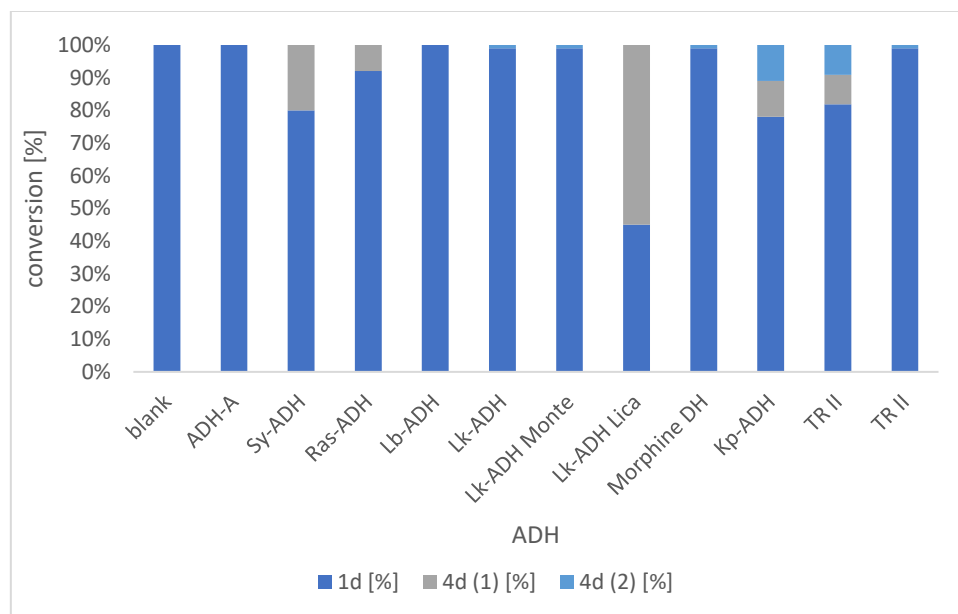


Figure 64 Biotransformation of **1d** with 5 vol% CH₃CN



Graph 13 Reaction conditions: 10 mM of **1d**, 20 mg/mL ADH, 0.5 mM NADPH, KPi buffer (50 mM, pH 7.0, 2 mM MgCl₂), 5 vol% CH₃CN, 30 °C, 150 rpm, overnight
Conversion based on GC (HP-5) peak areas

1d was expected to be the most demanding substrate due to the very bulky phenyl-group as a substituent. Nevertheless, Lk-ADH Lica that is known to be an ADH with exceptional capability of accepting bulky-bulky ketones and alcohols, was able to consume over 50% of the substrate. Oddly, the identified product was not the lactone **2b**, but rather **4b**. Since these reactions are prepared in ACN, this conversion surpassed the expected limit of 0.5 mM based on the added cofactor several times. Moreover, Sy-ADH, Ras-ADH, Kp-ADH and tropinone reductase I exhibit acceptance of the substrate at a smaller rate around 10% to 20%. In all cases **4d** was the product, so all tested enzymes prefer to reduce selectively the aldehyde moiety of this molecule, probably because the phenyl-ring on the ketone is too large of a hindrance or because the aldehyde is much more reactive than the ketone, despite the increase of the reactivity due to the phenyl substituent. Data can be seen in Graph 13.

The isolated reference material produced in a scaled-up reaction using Lica in ACN was first identified with **4d (1)** but converts spontaneously to **4d (2)** over time. After 1 to 2 weeks in organic solvent (ethyl acetate) both peaks at 16.79 and 16.95 minutes are visible. After the retention times the first peak is named **4d (1)** and the second one **4d (2)**. After longer periods only the later peak **4d (2)** could be detected and therefore, is the more stable species. Steric information of both compounds could not be determined, but since the measurement is performed in an achiral fashion, the presence of an enantiomer could still be assumed. After considering the work of Turner^[67] two possible products seen in Figure 65 below can be assumed

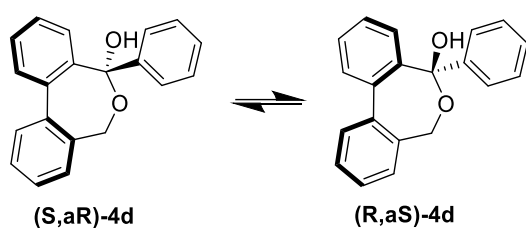
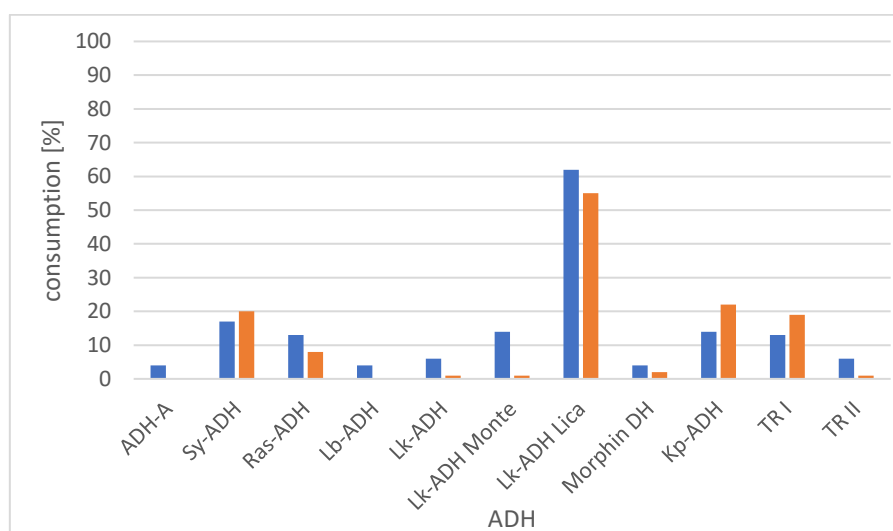


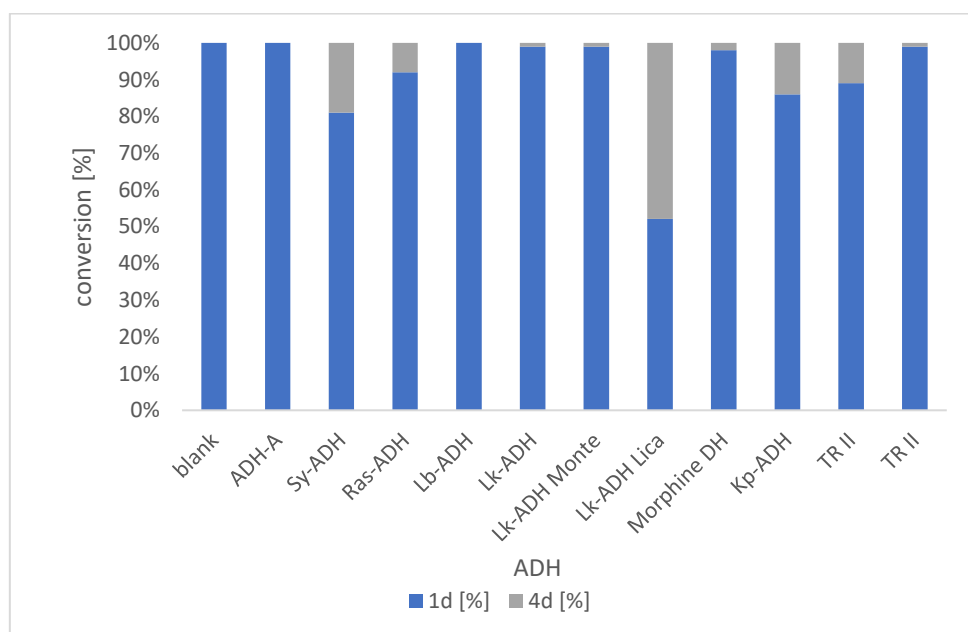
Figure 65 Possible derived chiral axis of product **4d**



Graph 14 Substrate consumption based on calibration (blue) and total peak areas (orange)

Reaction conditions: 10 mM of **1c**, 20 mg/mL ADH, 0.5 mM NADPH, KPi buffer (50 mM, pH 7.0, 2 mM MgCl₂), 5 vol% CH₃CN, 30 °C, 150 rpm, overnight

Most entries showed similar results regarding substrate consumption as displayed in Graph 14, the largest difference is exhibited in Monte with difference of 13% consumption. Since no trace of **2d** or **3d** had been identified, it might even be possible that small amounts of these products were formed but not identified as such, resulting in a higher consumption based on the external calibration. Entry 1, 4, 5, 8 and 11 (ADH-A, Lb-ADH, Lk-ADH, Morphine DH and TR II) also showed hardly visible reduction of concentration of **1d**. This minor loss in substrate could be explained by absorption of a few percentages of substrate in the lyophilised cell used as the catalyst.



Graph 15 Reaction conditions: 10 mM of **1d**, 20 mg/mL ADH, 0.5 mM NADPH, KPi buffer (50 mM, pH 7.0, 2 mM MgCl₂), 5 vol% CH₃CN, 30 °C, 150 rpm, overnight
Conversion based on chiral HPLC (chiral pack C) peak areas

For chiral analysis the samples were also measured with a chiral column on organic HPLC. Mainly the results of the GC analysis were confirmed, but no indication of another product related to **4d** could be identified. The reference product for **4d** confirms the identity of the one product peak but is unable to locate any additional isomer peaks as seen in Graph 15. Therefore, **4d** were assumed enantiomeric pure.

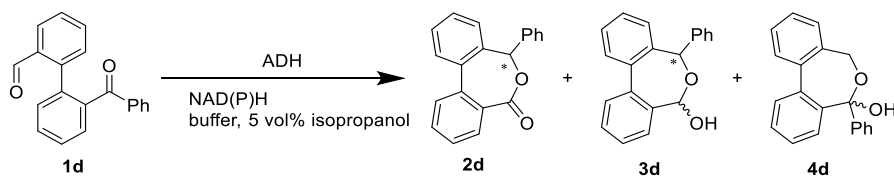
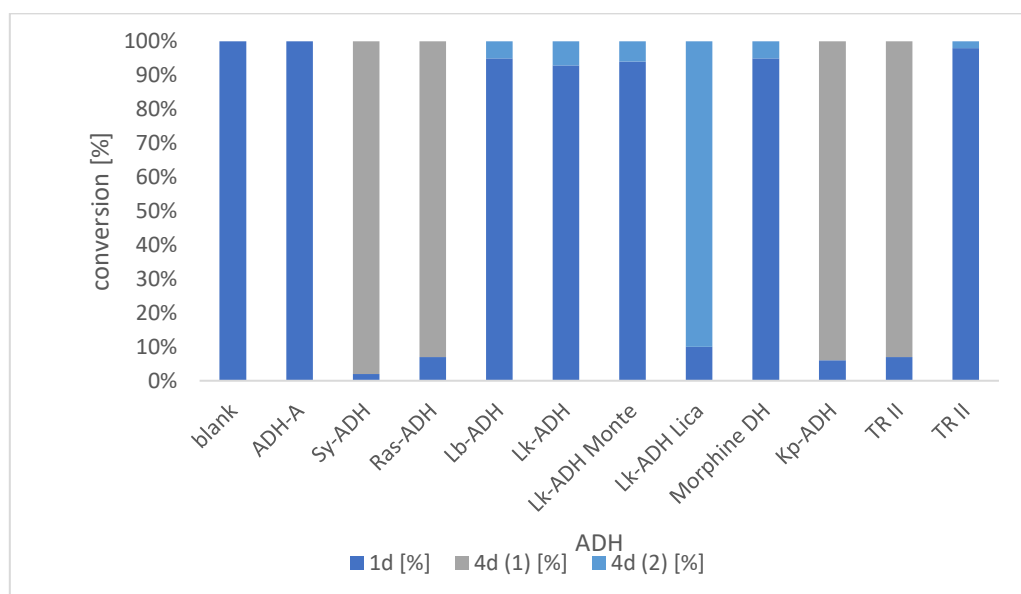


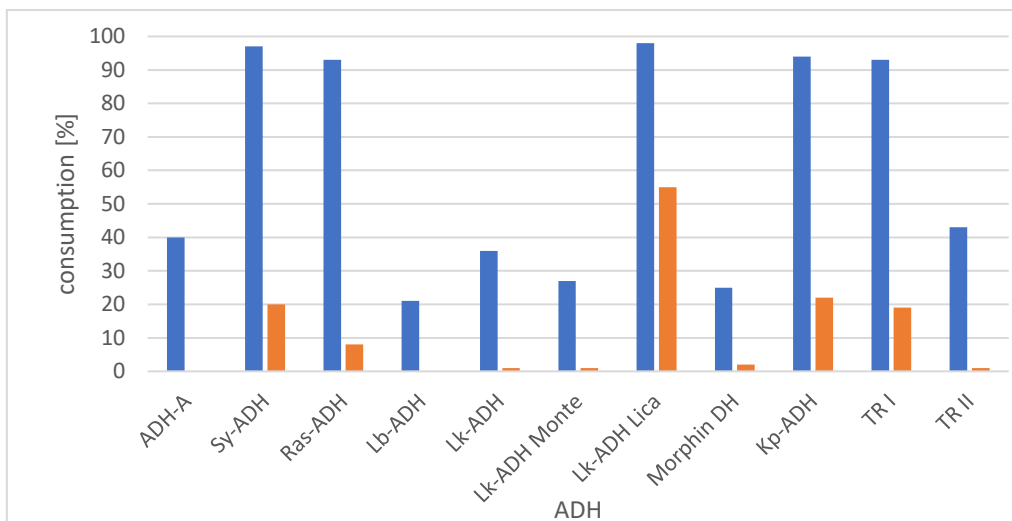
Figure 66 Biotransformation of **1d** with 5 vol% propan-2-ol



Graph 16 Reaction conditions: 10 mM of **1d**, 20 mg/mL ADH, 0.5 mM NADPH, KPi buffer (50 mM, pH 7.0, 2 mM MgCl₂), 5 vol% propan-2-ol, 30 °C, 150 rpm, overnight
Conversion based on GC (HP-5) peak areas

All enzymes exhibiting substrate consumption had increased the consumption to over 90% to one of the forms of **4d**, while the other entries showed only minor decreases in **1d** and no significant increase of any identifiable product. All results are listed in Graph 16.

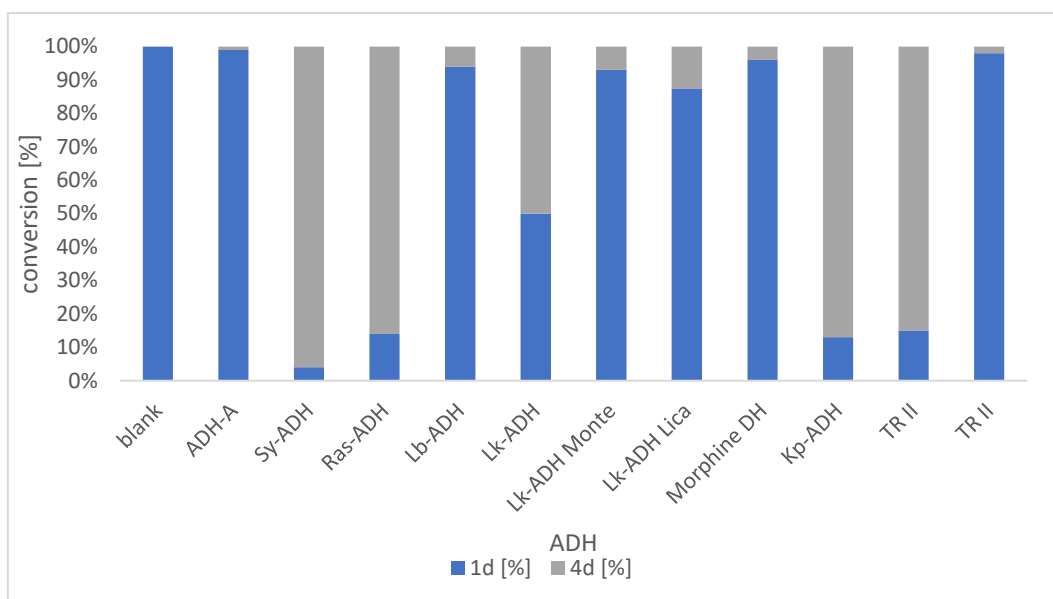
Since Lk-ADH Lica was able to reduce half of the substrate to **4b**, the increase of this yield was expected with isopropanol as a cosolvent, but while the consumption was almost complete, the normalised area of this peak showed a decline of **4d**. The product of this reaction was not identified but since the product cannot be identified as **4d**, a likely product would be **3d**.



Graph 17 Substrate consumption based on calibration (blue) and total peak areas (orange)

Reaction conditions: 10 mM of **1d**, 20 mg/mL ADH, 0.5 mM NADPH, KPi buffer (50 mM, pH 7.0, 2 mM MgCl₂), 5 vol% propan-2-ol, 30 °C, 150 rpm, overnight

The entries with Sy-ADH, Ras-ADH, Lk-ADH Lica, Kp-ADH and TR I had based on both methods over 90% substrate consumption, while the other entries 1, 4, 5, 6, 8 and 11 (ADH-A, Lb-ADH, Lk-ADH, Lk-ADH Monte, Morphine dehydrogenase and TR II) exhibited up to 40 % more decrease in **1d** and still produced hardly traceable amounts of product. In this case the product might be the hypothesised **3b** that could not be isolated and characterised. Comparison data can be found in Graph 17.



Graph 18 Reaction conditions: 10 mM of **1d**, 20 mg/mL ADH, 0.5 mM NADPH, KPi buffer (50 mM, pH 7.0, 2 mM MgCl₂), 5 vol% propan-2-ol, 30 °C, 150 rpm, overnight
Conversion based on chiral HPLC (chiral pack C) peak areas

All results of the GC could be confirmed on HPLC as seen in Graph 18, but furthermore, peaks with an area in the size range of the missing products can be identified at a retention time of 5.1 minutes in entry 7 (Lk-ADH Lica). To identify this product the reaction is scaled up and a compound with the same retention time is found in the larger scale reaction. This product was isolated, but the pure fraction still showed peaks of **4d** on HPLC, despite being purified via preparative HPLC. The compared reference is synthesised by Lk-ADH Lica in ACN. This product could not be identified via NMR or HRMS, but the GC-MS showed the expected mass for **4d** or **3d**. Interestingly, this compound possesses the same retention time as **4d** on the preparative HPLC. So, both peaks may be isomers of **4d**, but this hypothesis could not be confirmed. Moreover, this also cannot explain the lack of visible **4d** on GC, since these 2 compounds should be unable to be differentiate between and therefore, still be detectable.

3.3. Up-Scale

Several biotransformations were selected for regarding their substrate conversion and selectivity for yielding the lactone (**2**) or the lactol intermediate (**3**) or a hemiketal as a side product (**4**) and repeated in an up-scale reaction with 50 mg of substrate (**1**). Products have been extracted and were purified on preparative HPLC to isolate and characterise the products qualitatively via MS and NMR.

A detailed list of up-scale reactions and their details are shown in Table 8 below.

Table 8 predated products and the reaction conditions

entry	Substrate	ADH	5 vol% cosolvent	Main product
1	1b	Lk-ADH Lica	acetonitrile	2b
2	1b	Lk-ADH Lica	isopropanol	3b
3	1b	Kp ADH	isopropanol	4b (?)
4	1c	Lk-ADH Lica	isopropanol	4c
5	1c	TR I	isopropanol	3c
6	1c	TR II	acetonitrile	-
7	1d	Lk-ADH Lica	acetonitrile	4d
8	1d	Lk-ADH Lica	isopropanol	4d
9	1d	Sy-ADH	isopropanol	4d

The 50 mg up-scale reactions prepared under the same conditions were also compared to the biotransformation regarding conversions and favoured products to ensure the success of the up-scale as listed in Table 9.

Table 9 Up-scale reaction conditions, substrate consumption, main product and conversion

entry	Substrate	ADH	5 vol% cosolvent	Isolated crude [mg]	Main product	Substrate consumption [%]	Product [%]	Product [mg]
2	1b	Lk-ADH Lica	isopropanol	46.7	3b	>99	90	20.4
3	1b	Kp-ADH	isopropanol	38.3	4b (?)	94	79	13.1
4	1c	Lk-ADH Lica	isopropanol	42.7	4c	97	91	24.8
5	1c	TR I	isopropanol	43.6	3c	>99	94	15.9
6	1c	TR II	acetonitrile	32.6	-	n.d.	15	-
9	1d	Sy-ADH	isopropanol	35.4	4d	>99	>99	20.1

3.3.1. Up-scale entry 2-Biotransformation of **1b** with Lk-ADH Lica under reductive conditions

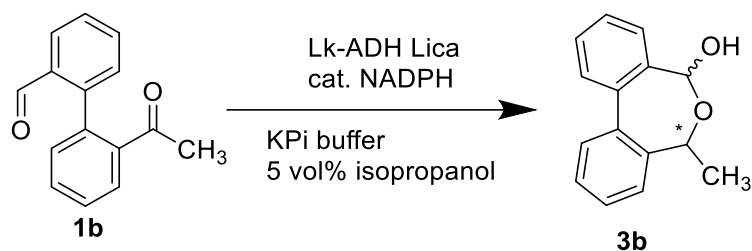


Figure 67 Scheme of up-scale biotransformation of **1b** to **3b**

Table 10 Reaction conditions: 10 mM of **1b**, 20 mg/mL ADH, 0.5 mM NADPH, KPi buffer (50 mM, pH 7.0, 2 mM MgCl₂), 5 vol% isopropanol, 30 °C, 150 rpm, overnight

Conversion based on GC peak areas

a) remeasured sample after prolonged storage at 4 °C

	1b [%]	2b [%]	3b [%]	4b [%]
Up-Scale	n.d.	8	90	2
screening	1	11	86	2
Screening ^{a)}	8	92	n.d.	n.d.

In direct comparison of the screening and the Up-scale reaction with 50mg substrate show several similarities. Lk-ADH Lica is also capable of an almost complete consumption of **1b** at a larger scale and produces the lactol **3b** as a major product (approximately. 90%), while in both cases around 10% of the lactone **2b** is produced as a side product. This confirms that the reductive environment created by the surplus of isopropanol works also in a larger scale, but more importantly the goal for this was to yield enough compound for proper identify the molecule. Results are seen in Table 10. It must be remarked that in direct comparison between both reactions the peak belonging to **3b** differs slightly in retention time and shape. While under normal circumstances the change in retention time could be caused by drift of the GC, this seems not likely, because peaks of **1b**, **2b** and the internal standard showed no such drift. Furthermore, the peak of the larger scale reaction is wider and not as narrow as in the screening. This could indicate for example, **3b** not being a stable compound that could react further or decayed under the storage conditions. Another hypothesis could be **3b** isomerising or undergoing a ring opening and therefore, be present in its open form.

However, it is proven that **3b** and **4b** are not completely stable having no traceable amounts left after several weeks of storage of the sample, but this does not necessary explain the differences between screening and up-scale, since both were measured shortly after the reaction. While the sample dissolved in ethyl acetate was decayed after long storage at 4°C, the dried isolated compound stays stable over far longer periods of time.

When determining the conversion of the reaction with an external calibration, the same ratio of **2b** to **3b** can be observed as shown in Table 11, almost no observable amounts of substrate left, around 10 % lactone and approximately 90 % lactol.

Table 11 Reaction conditions: 10 mM of **1b**, 20 mg/mL ADH, 0.5 mM NADPH, KPi buffer (50 mM, pH 7.0, 2 mM MgCl₂), 5 vol% isopropanol, 30 °C, 150 rpm, overnight
Conversion based on external calibration

	1b [%]	2b [%]	3b [%]
Up-Scale	1	9	88
screening	2	12	91

3.3.2. Up-scale entry 3-Biotransformation of **1b** with Kp-ADH under reductive conditions

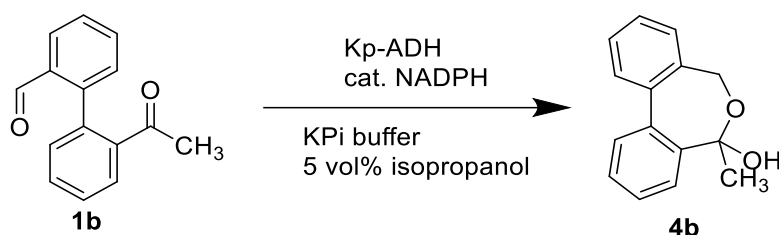
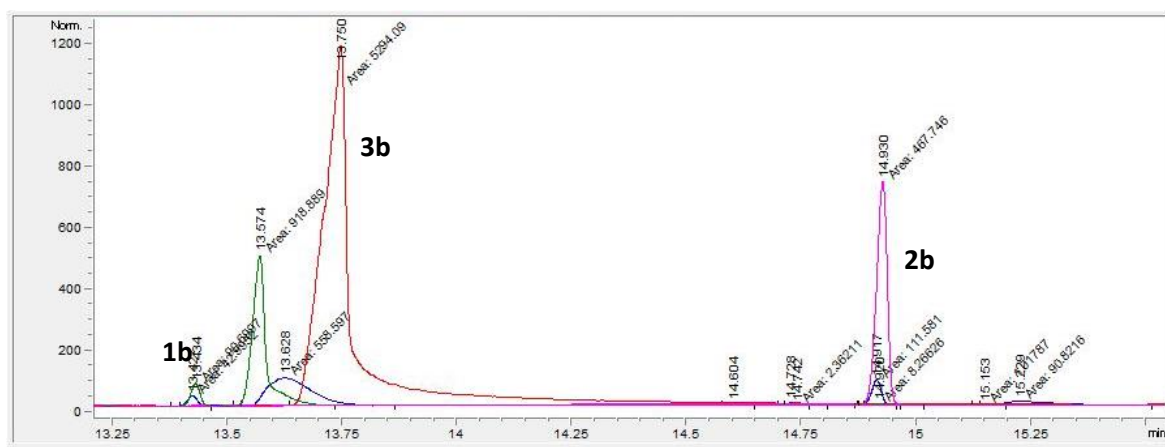


Figure 68 Scheme of up-scale biotransformation of **1b** to **4b**

Table 12 Reaction conditions: 10 mM of **1b**, 20 mg/mL ADH, 0.5 mM NADPH, KPi buffer (50 mM, pH 7.0, 2 mM MgCl₂), 5 vol% isopropanol, 30 °C, 150 rpm, overnight
Conversion based on GC peak areas

	1b [%]	2b [%]	4b [%]	4b [%]
Up-Scale	6	15	n.d.	79
screening	8	1	91	n.d.

This up-scaled reaction is a particularly interesting one, because the comparison of up-scale and screening showed vast differences as seen in Table 12. Substrate consumption stayed in a similar range and the yield of **2b** is moderately increased, but main product peak is shifted to 13.63 minutes (blue) as seen in Chromatogram 1 below, while the main product in the product peak the screening set is at 13.57 (green) and much narrower. In direct overlay with the screening and the references **1b**, **2b** and **3b**, the product peak of the up-scaled reaction cannot be linked to one of the identified peaks. Considering that **1b** and **2b** exhibit insignificant shifts, another reason than drift of the device must be assumed, but either a change in specificity of Kp-ADH or an isomerisation, conformation change or degradation of **4b** could occur. The purification and identification of this product **4b** was inconclusive, but the molecular mass determined by MS confirmed this being a reduced species.



Chromatogram 1 Overlay of screening reaction and Up scaled reaction inclusive references of **2b** and **3b**

3.3.3. Up-scale entry 4-Biotransformation of **1c** with Lk-ADH Lica under reductive conditions

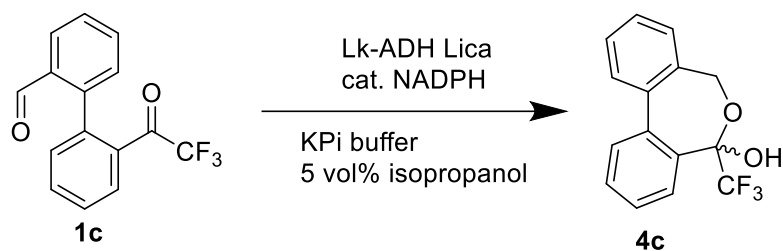


Figure 69 Scheme of up-scale biotransformation of **1c** to **4c**

Table 13 Reaction conditions: 10 mM of **1c**, 20 mg/mL ADH, 0.5 mM NADPH, KPi buffer (50 mM, pH 7.0, 2 mM MgCl₂), 5 vol% isopropanol, 30 °C, 150 rpm, overnight
Conversion based on GC peak areas

	1c [%]	2c [%]	3c [%]	4c [%]
Up-Scale	3	6	n.d.	91
screening	2	6	1	92

For the reductive transformation of **1c** with Lk-ADH Lica is the screening and the up-scaled reaction in high agreement. The results are shown in Table 14. Both show over 90 % conversion to **4c** with only trace amounts of **3c**. After considering all **2c** is most probable an impurity of the substrate, since the same concentration is also present in the blanks, the conversion to **4c** can be regarded as nearly complete.

The conversion based on an external calibration arrives at a similar conclusion, having almost complete consumption of the substrate and high percentages of **4c** that could not be exactly calculated, due being outside the range of the calibration. However, this at least confirms **4c** being near the maximum conversion. Data can be seen in Table 14 below.

Table 14 Reaction conditions: 10 mM of **1c**, 20 mg/mL ADH, 0,5 mM NADPH, KPi buffer (50 mM, pH 7.0, 2 mM MgCl₂), 5 vol% isopropanol, 30 °C, 150 rpm, overnight
Conversion based on external calibration

	1c [%]	4c [%]
Up-Scale	4	>117
screening	4	>124

3.3.4. Up-scale entry 5-Biotransformation of **1c** with TR I under reductive conditions

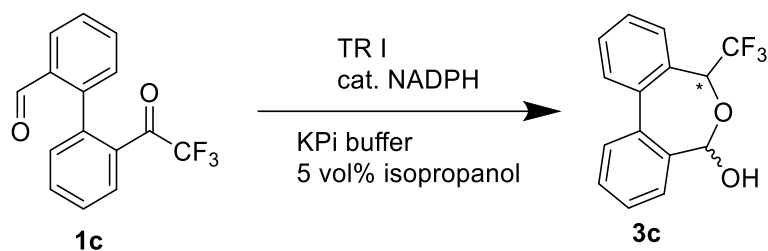


Figure 70 Scheme of up-scale biotransformation of **1c** to **3c**

Table 15 Reaction conditions: 10 mM of **1c**, 20 mg/mL ADH, 0.5 mM NADPH, KPi buffer (50 mM, pH 7.0, 2 mM MgCl₂), 5 vol% isopropanol, 30 °C, 150 rpm, overnight
Conversion based on GC peak areas

	1c [%]	2c [%]	3c [%]	4c [%]
Up-Scale	n.d.	n.d.	94	6
screening	3	1	90	7

Using tropinone reductase I as an ADH under reductive conditions shows a change in product. Instead of **4c** the favoured product is **3c**. A total consumption of **1c** can also be observed. Both the screening and the upscale have a similar distribution of products with over 90% conversion to **3c**, around 8% **4c** and only traces of **2c**. Results are seen in Table 15.

The product peak of **3c** possess a similar behaviour of **3b** changing the appearance and retention time of the peak. Since both **3c** and **3b** are analogue to each other, it is reasonable to assume both exhibiting the same process that causes this observation.

The external calibrations of **1c** and **4c** are both in high agreement with the conversion rates determined by the peak areas. Unfortunately, it was not possible to establish a calibration for the main product **3c** and therefore, could not be compared to ensure proper quantification. Comparison of both determination methods for **1c** and **4c** are shown in Table 16.

Table 16 Reaction conditions: 10 mM of **1c**, 20 mg/mL ADH, 0.5 mM NADPH, KPi buffer (50 mM, pH 7.0, 2 mM MgCl₂), 5 vol% isopropanol, 30 °C, 150 rpm, overnight
Conversion based on external calibration

	1c [%]	4c [%]
Up-Scale	n.d.	7
screening	1	7

3.3.5. Up-scale entry 6-Biotransformation of **1c** with TR II under redox-neutral conditions

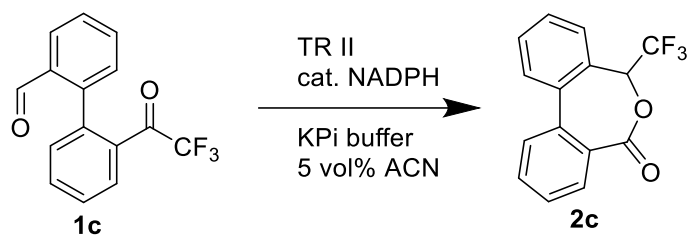


Figure 71 Scheme of up-scale biotransformation of **1c**

Table 17 Reaction conditions: 10 mM of **1c**, 20 mg/mL ADH, 0.5 mM NADPH for screening and stoichiometric NADPH for up-scale, KPi buffer (50 mM, pH 7.0, 2 mM MgCl₂), 5 vol% isopropanol, 30 °C, 150 rpm, overnight
Conversion based on GC peak areas

	1c [%]	2c [%]	4c [%]
Up-Scale	85	13	2
screening	81	9	9

In this experiment the synthesis of **2c** as a main product was attempted. Since for this reaction TR II was used as a biocatalyst, the amount of cofactor had to be increased to stoichiometric amounts, because tropinone reductase II does not show capability of using isopropanol to recycle NADPH. Unfortunately, all **2c** seems to originate from the synthesis of the substrate **1c**, so it is assumed that no detectable amounts of the lactone were produced. Results are displayed in Table 17.

3.3.6. Up-scale entry 9-Biotransformation of **1d** with Sy-ADH under reductive conditions

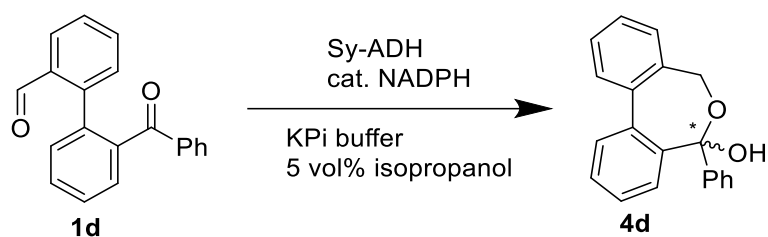


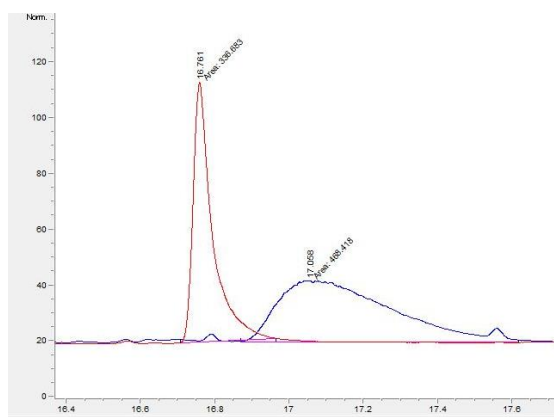
Figure 72 Scheme of up-scale biotransformation of **1d** to **4d**

Table 18 Reaction conditions: 10 mM of **1d**, 20 mg/mL ADH, 0.5 mM NADPH, KPi buffer (50 mM, pH 7.0, 2 mM MgCl₂), 5 vol% isopropanol, 30 °C, 150 rpm, overnight
Conversion based on GC peak areas

	1d [%]	4d [%]	4d [%]
Up-Scale	n.d.	100	n.d.
Up-Scale	n.d.	n.d.	100
screening	2	n.d.	98

1d has already been suspected from the start being the most sterically demanding substrate, so observing hardly any substrate consumption under redox neutral conditions was not surprising, but under reducing conditions several ADHs showed promising results. Of the most promising candidates Sy-ADH, Ras-ADH, Kp-ADH and TR I; Sy-ADH was selected, because all favoured the same product in the screening experiments and this enzyme exhibits the most conversion to **4d** and the smallest amount of side products. Results are shown in Table 18.

Like in the screening no visible amount of substrate was left in the scaled-up reaction, while all substrate is transformed to **4d** and hardly any side products could be detected. A curious observation could be made regarding the product peak on GC as displayed in chromatogram 2. The first measurement of the reaction control directly after the biotransformation showed a much narrower peak after 16.76 (red) minutes, while at a remeasurement 24 days later exhibits a new broader peak after 17.06 (blue) minutes. Both peaks can also be found in screening reactions in varying concentrations.



Chromatogram 2 Overlay of **4d** (in red) and **4d** (in blue) after storage

A confirmation that a reaction occurs is a remeasure of the isolated product of this reaction, where after 13 days of storage in ethyl acetate two peaks at both positions have been visible if the initial peak was only present in traces anymore. Therefore, a change in conformation, an isomerisation or even a ring opening has likely occurred to give rise to a more stable product. The dried product **4d** on the other hand could be stored for prolonged time without changes of the structure. This is confirmed by remeasuring the compound with NMR after storage at 4°C, furthermore, the NMR sample was stored at room temperature for over a week, before remeasuring again. Therefore, it can be assumed that the changes of the compound are caused by prolonged storage in certain organic solvents such as ethyl acetate, but not chloroform. The kind of transformation that the product undergoes was not yet properly explained. However, MS measurements show no change in molecular mass of the product.

4. Experimental section

4.1 General information

All chemicals and solvent were purchased from Sigma Aldrich, Fluorochem, Acros Organics, Honeywell Fluka™ and Roth and were used as received. Competent *E. coli* (BL21 DE3, Arctic Express and Lemo 21) cultivation, overnight culture and enzyme expression were done in an HT Infors Unitron AJ 260 Shaker. Biotransformations were done in an HT Infors Unitron AJ 260 Shaker at 120 rpm and 30°C. Centrifugation was done in Hettich Rotina 420, Hitachi CR22N, Heraeus Biofuge primo or Eppendorf 5424. NMR spectra were recorded on a Bruker AVANCE III 300 spectrometer unit at 300 (1H) and 75 (13C) MHz, shifts are given in ppm and coupling constants (J) in Hz. GC-FID analysis was performed on Agilent Technologies 7890A GC system, equipped with Agilent HP-5 (30 m x 0.25 mm x 0.25 µm) and DB-1701 (30 m x 0.25 mm x 0.25 µm) using He as carrier gas. GC-MS analysis was performed on Agilent Technologies 7890A GC system, equipped with mass detector Agilent Technologies 5975C inert XL mSD, column HP-5ms (30 m x 0.25 mm x 0.25 µm) and an Agilent 7697A headspace autosampler using He as carrier gas at a flow of 0.7 mL/min. SDS page was stained and washed in an ELMI DRS-12 Digital Rocking Shaker.

4.2. Synthesis General

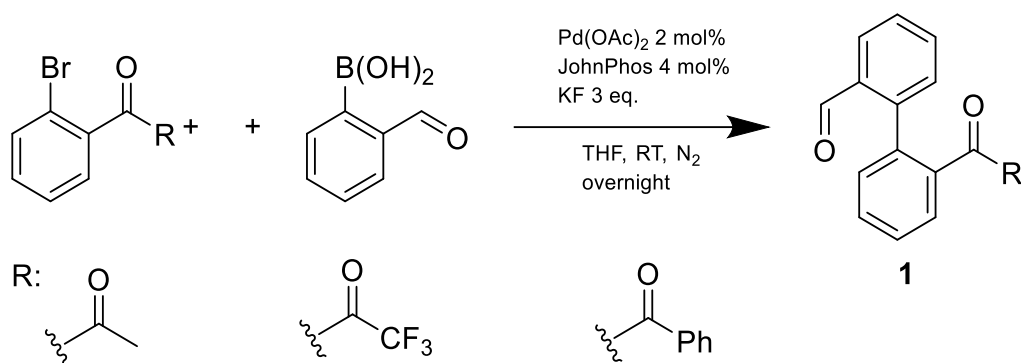


Figure 73 General synthesis of substrates **1b-1d**

To the bromo compound were added 1.5 equivalent of the boronic acid, 2 mol% of Pd(OAc)₂, 4 mol% of bipyridine and 3 equivalents of KF as a base in a round bottom flask under inert gas and suspended in dry THF. The mixture was vigorously stirred at room temperature overnight. Reaction scheme is shown in Figure 73.

The reaction was filtered over celite to remove catalyst, ligands, and the base. Solvent was removed under reduced pressure. The crude product was purified by flash chromatography, if necessary. (eluent: cyclohexane: ethyl acetate 19:1) Alternatively the product can be extracted from the reaction mixture with ethyl acetate and washed with water/ brine. Biotransformation were also be prepared directly from the crude without further purification as a reaction cascade.

4.3. Biotransformation

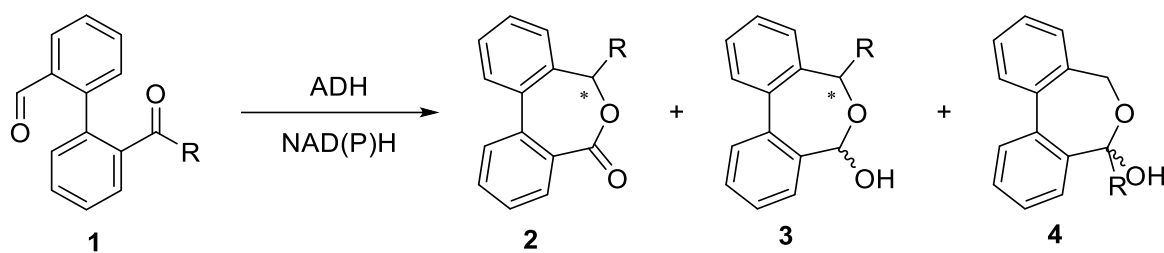


Figure 74 General scheme of a biotransformation for bio-Tishchenko-like reactions

Reactions were performed in 1.5 mL Eppendorf vials with 500 μ L total volume in KPi buffer (phosphate buffer pH=7.0; 50 mM; 2 mM $MgCl_2$) and 5 vol% cosolvent. Reactions were prepared with 10 mg lyophilised whole cells containing the ADH (20 mg/mL) and 0.5 mM NAD(P)H depending on the ADHs. Reaction were incubated at 30 $^{\circ}C$ at 120 rpm for at least 12 h (overnight). Scheme of the biotransformation is displayed in Figure 74 above.

The reaction was extracted twice with 300 μ L EtOAc spiked with IS (internal standard: 10 mM (*R*)-(+)-limonene), centrifuged for 1 minute, after each extraction at maximum rpm. The collected organic fractions were dried over anhydrous Na_2SO_4 , the sample was centrifuged again to separate the organic phase and the Na_2SO_4 .

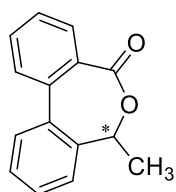
Dried organic phases were measured via GC-FID and organic HPLC.

Up-Scale Biotransformation

Analogous to the screening reaction, up-scaled reactions were prepared based on 50 mg substrate. For this the reactions were performed in 50 mL tubes in KPi buffer (phosphate buffer pH=7.0; 50 mM; 2 mM $MgCl_2$) and 5vol% cosolvent. Reactions were prepared with lyophilised whole cells with a total concentration of 20 mg ADH/mL and 0.5 mM NAD(P)H depending on the used enzyme. Reaction were incubated at 30 $^{\circ}C$ at 120 rpm for at least 12 h (overnight).

The reaction was extracted twice with EtOAc, the organic phases were combined and dried over Na_2SO_4 . The excess solvent is removed under reduced pressure to give rise of the crude product that is dissolved in a small amount of ACN (100–400 μ L depending on amount on solubility) to isolate products and intermediates via preparative HPLC. Solvents are removed under reduced pressure and isolated compounds are dried under vacuum. Isolated products were used as reference material to characterises the structure via H-NMR and C-NMR and to conform the retention time on GC and HPLC measurements of the performed up-scale and non-up-scale biotransformations.

4.4. Product characterisation



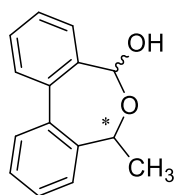
2b

2b was fully characterised by NMR and HRMS.

HRMS: calculated m/z : 225.091006, found m/z : 225.09125 (Diff: 1.084ppm / Agilent Algorithm: 1.09ppm)

^1H NMR (300 MHz, Chloroform-*d*) δ 8.01 (dd, $J = 7.8, 1.4$ Hz, 1H), 7.72 – 7.46 (m, 7H), 5.31 (q, $J = 6.6$ Hz, 1H), 1.88 (d, $J = 6.6$ Hz, 3H).

^{13}C NMR (75 MHz, Chloroform-*d*) δ 170.00, 138.68, 137.55, 137.36, 132.53, 131.34, 130.90, 129.59, 128.98, 128.81, 128.57, 128.38, 123.96, 73.13, 16.89.



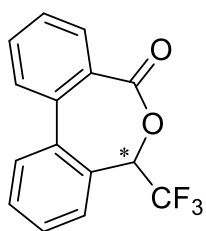
3b

3b has much more difficulties for characterisation, since the NMR data is inconclusive, and the molecular mass could not be found on HRMS. The calculated mass of 226.0994 g/mol was not found, closes masses found was 228.1379 in positive mode and 227.1078 in negative mode. These masses are not fit for any of the expected products or intermediates, but the confirmed higher mass than the substrate could still indicate a reduction of **1b** to this compound.

Product identity is not able to be confirmed by HRMS.

^1H NMR (300 MHz, Chloroform-*d*) δ 7.67 – 7.60 (m, 1H), 7.49 – 7.30 (m, 5H), 7.19 – 7.07 (m, 2H), 4.58 (q, $J = 6.5$ Hz, 1H), 4.31 (d, $J = 7.0$ Hz, 1H), 1.39 (d, $J = 6.5$ Hz, 3H)

^{13}C NMR (75 MHz, Chloroform-*d*) δ 143.40, 140.47, 138.80, 138.24, 129.87, 129.54, 129.18, 128.27, 127.97, 127.73, 127.07, 125.52, 65.71, 62.90, 23.12.



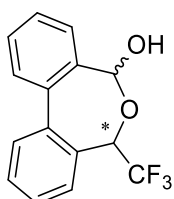
2c

The lactone **2c** is properly identified with NMR and HRMS but was only produced as a side product originating from the synthesis of **1c**. Therefore, this compound can be directly isolated from the substrate, but nevertheless, it is also able to be isolated from biotransformations such as in entry 9.

Product identity is confirmed by HRMS; calculated m/z : 279.062741, found m/z : 279.062829 (Diff: 0.315 ppm / Agilent Algorithm: 0.15 ppm)

^1H NMR (300 MHz, Chloroform- d) δ 8.02 – 7.97 (m, 3H), 7.92 (dd, J = 7.8, 1.4 Hz, 1H), 7.88 – 7.82 (m, 1H), 7.78 (ddd, J = 7.9, 7.4, 1.5 Hz, 1H), 7.52 (dtd, J = 23.0, 7.5, 1.3 Hz, 3H), 4.77 (s, 1H).

^{13}C NMR (75 MHz, Chloroform- d) δ 136.35, 130.39, 129.33, 128.76, 127.85, 124.27, 123.49.



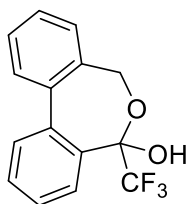
3c

Similar to **3b**, **3c** possess unclear NMR data and the expected molecular masses have also not been found. As observed in **3b** the found masses are with 282.1104 in positive mode and 281.0790 in negative mode around 2 ppm and 1 ppm higher respectively, as the calculated 280.0711. These striking similarities in mass distribution in 2 related molecules is probably more than coincident and could confirm both identities.

Product identity is not able to be confirmed by HRMS.

^1H NMR (300 MHz, Chloroform- d) δ 7.84 – 7.77 (m, 1H), 7.63 – 7.37 (m, 5H), 7.27 – 7.21 (m, 1H), 7.20 – 7.15 (m, 1H), 4.77 (q, J = 7.3 Hz, 1H), 4.45 – 4.17 (m, 2H).

^{13}C NMR (75 MHz, Acetonitrile- d_3) δ 135.19, 134.57, 131.91, 129.10, 125.10, 124.22, 123.98, 123.56, 123.18 (d, J = 3.4 Hz), 122.26 (d, J = 2.0 Hz), 63.56, 63.14, 57.95.



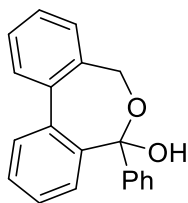
4c

4c was isolated and purified in good amounts, and the identity could be confirmed by NMR. However, this substance is only detected in the negative of the HRMS.

Product identity is confirmed by HRMS; calculated m/z : 279.063838, found m/z : 279.064182 (Diff: 1.233 ppm / Agilent Algorithm: 1 ppm)

^1H NMR (300 MHz, Acetonitrile- d_3) δ 7.99 (dp, $J = 7.0, 0.9$ Hz, 1H), 7.80 – 7.74 (m, 1H), 7.68 – 7.59 (m, 2H), 7.53 (dddd, $J = 7.2, 5.1, 2.8, 1.5$ Hz, 2H), 7.46 – 7.36 (m, 2H), 5.31 (s, 1H), 4.85 – 4.57 (m, 2H).

^{13}C NMR (75 MHz, Acetonitrile- d_3) δ 139.08, 138.54, 137.98, 132.70, 131.47, 130.68, 130.45, 129.09, 128.41, 127.88, 127.55, 127.07, 124.71, 117.34, 66.23.



4d

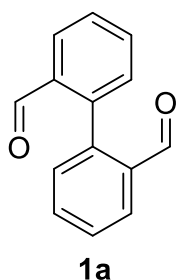
Identity of **4d** is identified with NMR and HRMS as a product of **1d**.

Product identity is confirmed by HRMS; calculated m/z : 289.122306, found m/z : 289.122182 (Diff: -0.429 ppm / Agilent Algorithm: -0.32 ppm)

^1H NMR (300 MHz, Chloroform- d) δ 7.79 – 7.70 (m, 2H), 7.61 – 7.25 (m, 9H), 7.14 (td, $J = 7.5, 1.4$ Hz, 1H), 6.99 (dd, $J = 7.5, 1.4$ Hz, 1H), 4.71 – 4.36 (m, 2H), 3.66 – 2.61 (m, 1H).

^{13}C NMR (75 MHz, Chloroform- d) δ 198.59, 140.22, 139.26, 138.97, 138.79, 137.24, 133.45, 130.85, 130.35, 130.08, 129.26, 129.02, 128.52, 127.29, 126.85, 63.37.

4.5. Synthesis



2-Bromobenzaldehyde (50 mg; 0.27 mmol; 32 μ L), 2-Formylphenyl boronic acid (45 mg; 0.297 mmol) and the Pd catalyst [1,1'-Bis(diphenylphosphino)ferrocene]palladium(II)dichloride (Pd(dppf)Cl₂) (4 mg; 0.05 mmol) were added to 1 mL degassed deionised water with Na₂CO₃ (85 mg; 0.81 mmol) in a 5 mL vial. The resulting mixture is stirred at 90°C for 6 hours to yield [1,1'-biphenyl]-2,2'-dicarbaldehyde. Afterwards directly used in dilution with acetonitrile

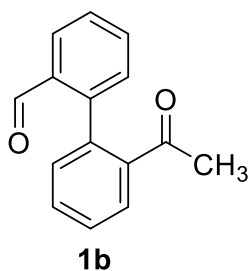
to the desired substrate concentration. (maximum of 10 vol% cosolvent)

The crude was used further in the enzymatic step of the one-pot cascade.

NMR was achieved by isolation of **1a** as side product of the synthesis of **1b**.

NMR: ¹H NMR (300 MHz, Chloroform-*d*) δ 9.86 (s, 2H), 8.09 (dd, *J* = 7.6, 1.6 Hz, 2H), 7.66 (ddd, *J* = 14.0, 7.1, 1.3 Hz, 4H), 7.38 (dd, *J* = 7.4, 1.4 Hz, 2H).

¹³C NMR (75 MHz, Chloroform-*d*) δ 191.06, 141.23, 134.57, 133.44, 131.72, 128.84, 128.57.



2-Bromoacetophenone (199 mg, 1 mmol), 2-Formylphenyl boronic acid (226 mg, 1.5 mmol), 2 mol% Pd(OAc)₂, 4 mol% JohnPhos and KF (174 mg, 3 mmol) were combined in a round bottom flask under inert gas (nitrogen) and suspended in dry THF. The mixture was vigorously stirred at room temperature overnight. The reaction is filtered, and the solvent is removed under reduced pressure. The crude product is purified by flash chromatography (eluent:

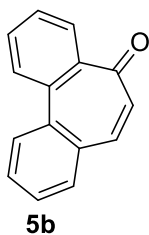
Cyclohexane: Ethyl acetate 19:1) to yield 2'-acetyl-[1,1'-biphenyl]-2-carbaldehyde.

Isolated yield: 59 %

HRMS: calculated *m/z*: 225.091006, found *m/z*: 225.091072 (Diff: 0.293 ppm / Agilent Algorithm: 0.3 ppm)

NMR: ¹H NMR (300 MHz, Chloroform-*d*) δ 9.85 (s, 1H), 8.03 (dd, *J* = 7.7, 1.5 Hz, 1H), 7.81 (dd, *J* = 7.2, 1.9 Hz, 1H), 7.67 – 7.50 (m, 6H), 7.33 – 7.23 (m, 3H), 2.27 (s, 4H).

¹³C NMR (75 MHz, Chloroform-*d*) δ 201.11, 191.58, 144.64, 139.42, 137.30, 133.85, 133.48, 131.84, 131.06, 130.54, 128.68, 128.33, 128.16 (d, *J* = 4.5 Hz).

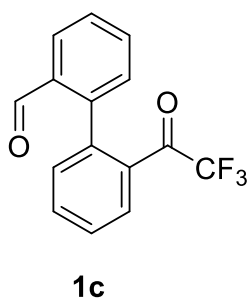


2-Bromoacetophenone (54 mg, 0.27 mmol), 2-Formylphenyl boronic acid (46 mg, 0.30 mmol), and the Pd catalyst [1,1'-Bis(diphenylphosphino)ferrocene]palladium(II) dichloride (Pd(dppf)Cl₂) (4 mg; 0.05 mmol) were added to 1 mL degassed deionised water with Na₂CO₃ (85 mg; 0.81 mmol) in a 5 mL vial. The resulting mixture is stirred at 90 °C overnight to yield 5H-dibenzo[a,c][7]annulen-5-one. The product is extracted with Ethyl acetate and the organic phase is dried over Na₂SO₄. The product was purified by preparative HPLC.

Isolated yield: 38 %

NMR: ¹H NMR (300 MHz, Chloroform-*d*) δ 8.01 – 7.90 (m, 3H), 7.70 (td, *J* = 7.7, 1.6 Hz, 1H), 7.64 – 7.48 (m, 4H), 7.39 (d, *J* = 12.2 Hz, 1H), 6.70 (d, *J* = 12.2 Hz, 1H).

¹³C NMR (75 MHz, Chloroform-*d*) δ 192.63, 141.18, 139.91, 138.26, 137.03, 133.57, 133.06, 131.52 (d, *J* = 1.7 Hz), 131.11, 130.25, 129.38, 129.02, 128.54, 128.22.



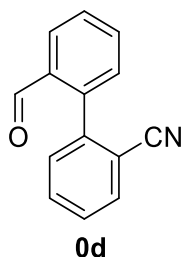
2'-Bromo-2,2,2-trifluoro-acetophenone (253 mg, 1 mmol), 2-Formylphenyl boronic acid (226 mg, 1.5 mmol), 2mol% Pd(OAc)₂, 4 mol% JohnPhos and KF (174 mg, 3 mmol) were combined in a round bottom flask under inert gas (nitrogen) and suspended in dry THF. The mixture is vigorously stirred at room temperature overnight. The reaction was filtered, and the solvent is removed under reduced pressure. The crude product was purified by flash chromatography (eluent: Cyclohexane: Ethyl acetate 19:1) to yield 2'-(2,2,2-trifluoroacetyl)-[1,1'-biphenyl]-2-carbaldehyde.

Isolated yield: 65 %

HRMS: calculated *m/z*: 279.062741, found *m/z*: 279.062997 (Diff: 0.917 ppm / Agilent Algorithm: 1.28 ppm)

NMR: ¹H NMR (300 MHz, Chloroform-*d*) δ 9.83 (s, 1H), 8.00 (ddd, *J* = 7.9, 2.9, 1.6 Hz, 2H), 7.73 (td, *J* = 7.5, 1.4 Hz, 1H), 7.68 – 7.52 (m, 4H), 7.39 (dd, *J* = 7.5, 1.4 Hz, 1H), 7.23 – 7.18 (m, 1H).

¹³C NMR (75 MHz, Chloroform-*d*) δ 191.35, 142.65, 140.94, 133.77, 133.56, 133.40, 132.46, 130.56, 130.19, 129.55 (d, *J* = 3.3 Hz), 129.48, 128.41, 128.27.

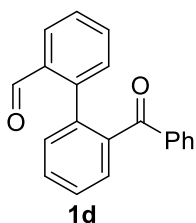


2-bromobenzonitrile (182 mg, 1 mmol), 2-Formylphenyl boronic acid (226 mg, 1.5 mmol), 2 mol% Pd(OAc)₂, 4mol% JohnPhos and KF (174 mg, 3 mmol) were combined in a round bottom flask under inert gas (nitrogen) and suspended in dry THF. The mixture is vigorously stirred at room temperature overnight. The reaction was filtered, and the solvent was removed under reduced pressure. The crude product purified by flash chromatography (eluent: Cyclohexane: Ethyl acetate 19:1) to yield 2'-formyl-[1,1'-biphenyl]-2-carbonitrile.

Isolated yield: 35 %

NMR: ¹H NMR (300 MHz, Chloroform-*d*) δ 9.89 (s, 1H), 8.08 (dd, *J* = 7.7, 1.5 Hz, 1H), 7.82 (dd, *J* = 7.8, 1.3 Hz, 1H), 7.77 – 7.66 (m, 3H), 7.58 (dd, *J* = 7.7, 1.3 Hz, 1H), 7.45 (ddd, *J* = 7.7, 3.5, 1.2 Hz, 2H).

¹³C NMR (75 MHz, Chloroform-*d*) δ 190.78, 142.15, 140.83, 133.86 (d, *J* = 2.0 Hz), 133.11, 132.47, 131.10 (d, *J* = 8.3 Hz), 129.42, 128.56, 117.70, 113.05.



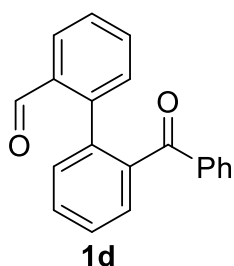
2'-formyl-[1,1'-biphenyl]-2-carbonitrile (207 mg, 1 mmol), phenylboronic acid (122 mg, 1 mmol), 6 mol% Pd(OAc)₂, 12 mol% bipyridine were suspended in 10 mL H₂O with 10 equivalent of TFA. The mixture was stirred overnight at 90°C under reflux. The reaction is filtered, and the solvent is removed under reduced pressure. The crude product is purified by flash chromatography (eluent: Cyclohexane: Ethyl acetate 19:1) to yield 2'-benzoyl-[1,1'-biphenyl]-2-carbaldehyde.

Isolated yield: 44 %

NMR: ¹H NMR (300 MHz, Chloroform-*d*) δ 9.94 (s, 1H), 7.88 (dd, *J* = 7.6, 1.6 Hz, 1H), 7.83 – 7.77 (m, 2H), 7.67 – 7.55 (m, 7H), 7.52 – 7.21 (m, 19H), 6.99 (d, *J* = 7.6 Hz, 1H).

¹³C NMR (75 MHz, Chloroform-*d*) δ 198.66, 191.58, 143.45, 140.57, 139.05, 138.71, 137.25, 133.62, 130.55, 128.41, 128.02, 126.39, 71.69, 60.42, 21.08, 14.22.

Direct synthesis of **1d** with Suzuki coupling:



2-Bromobenzophenone (261 mg, 1 mmol), 2-Formylphenyl boronic acid (226 mg, 1.5 mmol), 2mol% Pd(OAc)₂, 4 mol% JohnPhos and KF (174 mg, 3 mmol) were combined in a round bottom flask under inert gas (nitrogen) and suspended in dry THF. The mixture is vigorously stirred at room temperature overnight. The reaction is filtered, and the solvent is removed under reduced pressure to 2'-benzoyl-[1,1'-biphenyl]-2-carbaldehyde.

Isolated yield: 90 % (with 2 mmol substrate)

HRMS: calculated m/z: 287.106656, found m/z: 287.106647 (Diff: -0.031 ppm / Agilent Algorithm 0 ppm)

NMR: ¹H NMR (300 MHz, Chloroform-*d*) δ 9.94 (d, *J* = 0.7 Hz, 1H), 7.93 – 7.84 (m, 1H), 7.65 – 7.59 (m, 4H), 7.57 (dd, *J* = 6.5, 1.4 Hz, 1H), 7.50 – 7.42 (m, 2H), 7.41 – 7.37 (m, 2H), 7.36 – 7.29 (m, 2H), 7.25 – 7.20 (m, 1H).

¹³C NMR (75 MHz, Chloroform-*d*) δ 197.50, 191.58, 143.45, 139.38, 137.50, 133.88, 133.08 (d, *J* = 3.2 Hz), 131.69, 131.07, 130.11, 129.77, 128.97, 128.25, 128.10, 127.83 (d, *J* = 3.8 Hz).

4.6. Enzyme expression

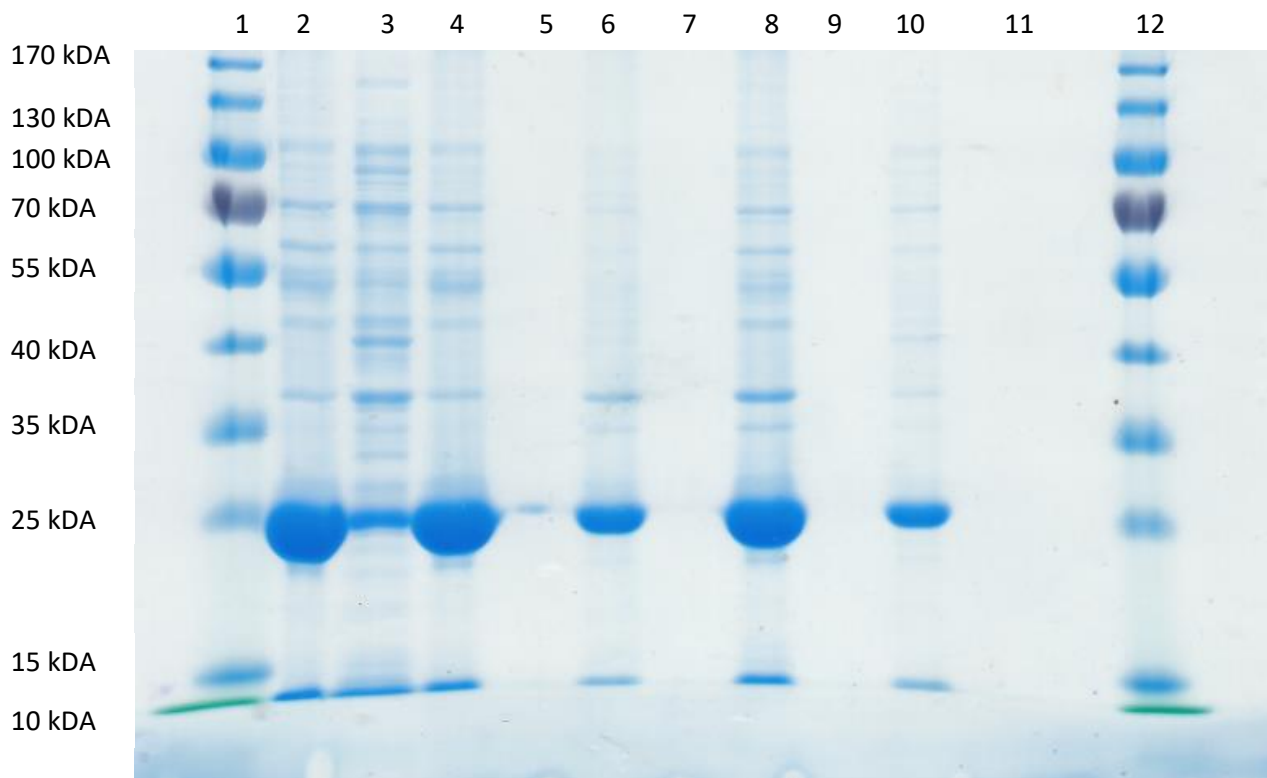
For enzyme expression of TR I and TR II BL21(DE3) cells are used. 3 µL plasmid is added to 100 µL BL21(DE3) for 30 minutes on ice. Afterward it is heated for 10 seconds at 42 °C. To this mixture 250 µL LB-medium is added and is shook for 1 hour at 37 °C and 350 rpm. Afterwards this mixture is plated on a LB/Amp (100 mM) plate that grows overnight at 30 °C in a drying oven. 10 mL of LB medium, 10 µL ampicillin and one colony are cultivated overnight at 30 °C and 120 rpm. To 100 mL of LB medium with 100 µL of Amp stock (100 mM) are added 1 vol% of the overnight culture (ONC) and cultivated at 30/37 °C at 120 rpm till their OD600 is above 0.6. Afterwards the flasks are induced with 0.1 mM IPTG and expressed at different conditions, shown in the Table 19 below.

Table 19 used condition for cultivation and expression of TR II in BL21 DE3

Sample	Overnight culture (ONC)	expression	Time [h]
1	30 °C 120 rpm	18 °C	16
2	30 °C 120 rpm	20 °C	16
3	37 °C 120 rpm	37 °C	3
4	37 °C 120 rpm	18 °C	16
5	37 °C 120 rpm	20 °C	3

4.6.1. Enzyme solubility test of TRII

For exploring the part of soluble and insoluble enzyme 2 mL of the culture are centrifuged to yield a pellet that is resuspended to be sonicated to break the cells. The amount of expressed enzymes is controlled via SDS-Page. (enzyme MW: 28.311 kDa)

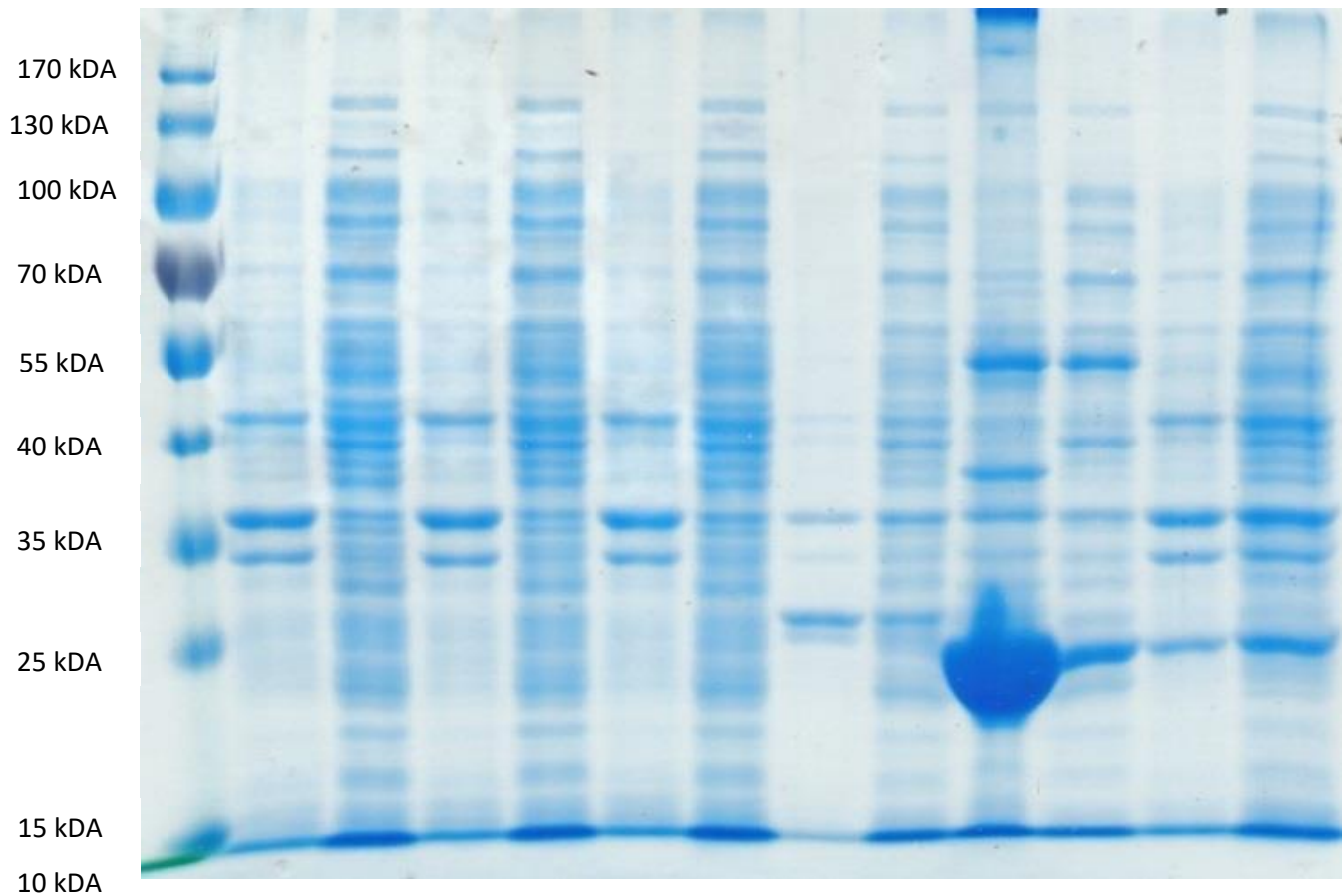


1) Page ruler, 2) 1 pellet, 3) 1 supernatant, 4) 2 pellet, 5) 2 supernatant, 6) 3 pellet, 7) 3 supernatant, 8) 4 pellet, 9) 4 supernatant, 10) 5 pellet, 11) 5 supernatant, 12) Page ruler

A preference for lower temperatures is seen in this test regarding enzyme solubility correlating with better solubility. Hence, following this trend the expression is redone with Arctic Express, Lemo 21 and 5 different BL21(DE3) containing each another chaperone, and are repeated at lower temperature conditions while expressing.

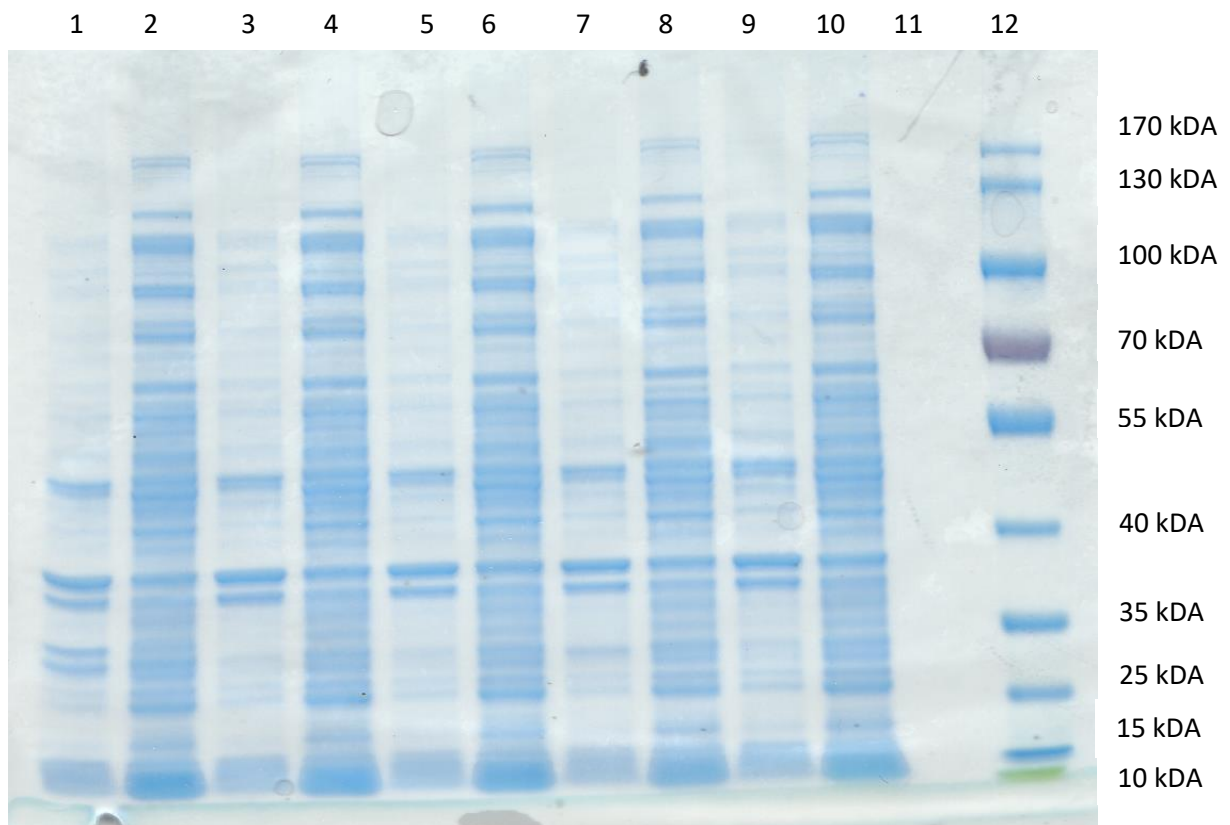
Table 20 used condition for cultivation and expression of TRII

Sample	ONC	expression
Chaperone 1	37 °C 130 rpm	18 °C
Chaperone 2	37 °C 130 rpm	18 °C
Chaperone 3	37 °C 130 rpm	18 °C
Chaperone 4	37 °C 130 rpm	18 °C
Chaperone 5	37 °C 130 rpm	18 °C
Lemo 21	30 °C 130 rpm	18 °C
Arctic Express	37 °C 130 rpm	16 °C

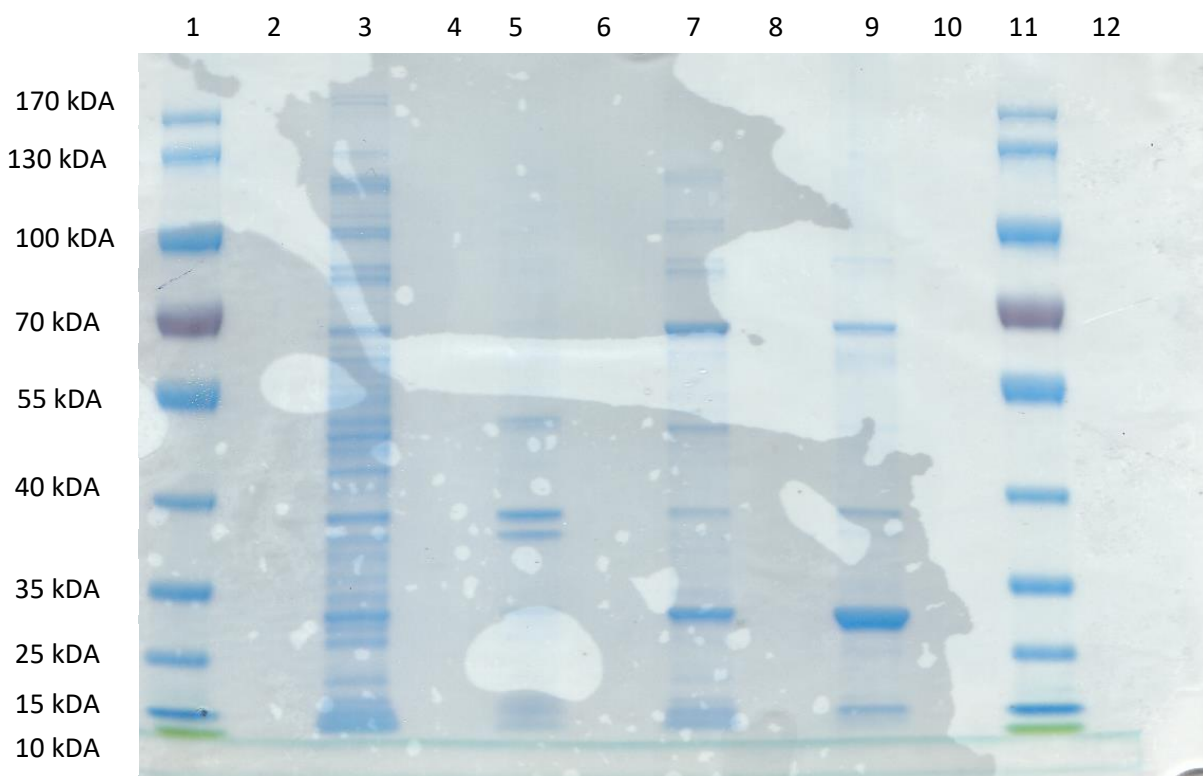


1) Page ruler, 2) Chaperone 1 pellet, 3) Chaperone 1 supernatant, 4) Chaperone 2 pellet, 5) Chaperone 2 supernatant, 6) Chaperone 3 pellet, 7) Chaperone 3 supernatant, 8) Chaperone 4 pellet, 9) Chaperone 4 supernatant, 10) Chaperone 5 pellet, 11) Chaperone 5 supernatant, 12) Lemo 21 pellet, 13) Lemo 21 supernatant

In this first set of trials regarding different organism for expression Arctic express was not able to be cultivated during the overnight culture and furthermore, several of the cells showed no sign of enzyme expression. Therefore, the test was repeated with the same conditions. SDS-Pages are shown below.

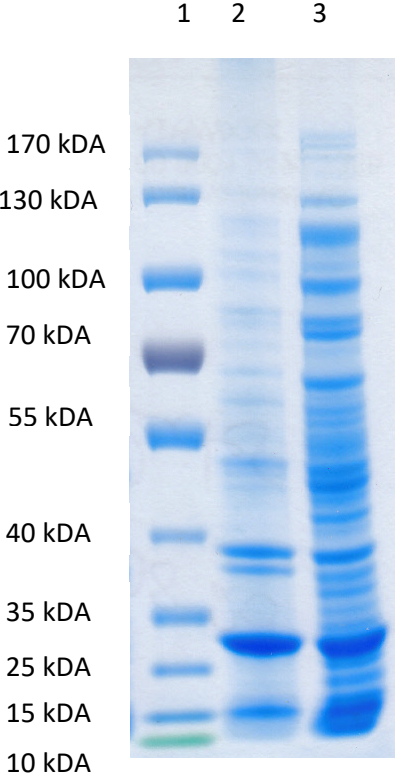


1) Chaperone 1 pellet, 2) Chaperone 1 supernatant, 3) Chaperone 2 pellet, 4) Chaperone 2 supernatant, 5) Chaperone 3 pellet, 6) Chaperone 3 supernatant, 7) Chaperone 4 pellet, 8) Chaperone 4 supernatant, 9) Chaperone 5 pellet, 10) Chaperone 5 supernatant, 12) Page ruler



1) Page ruler, 3) Arctic Express pellet, 5) Arctic Express supernatant, 7) Lemo 21 pellet, 9) Lemo 21 supernatant, 11) Page rulers

Lemo 21 seem likely to be the most suitable candidate for expression of tropinone reductase II in moderate soluble amounts. Lemo 21 were cultivated, incubated and the enzymes were expressed as described.



1) Page ruler, 2) Lemo 21 pellet, 3) Lemo 21 supernatant

4.6.2. Activity test of TRI and TRII

The activity of the alcohol dehydrogenases tropinone reductase I and II is tested with compounds similar to the natural substrate tropinone such as 4-methylcyclohexanone, cyclohexanone and cycloheptanone. Furthermore, *o*-phthalaldehyde and acetophenone are investigated as possible substrates.

Table 21 Reaction conditions: 10 mM of substrate, 20 mg/mL ADH, 10 mM NADPH, KPi buffer (50 mM, pH 7.0, 2 mM MgCl₂), 5 vol% CH₃CN, 30 °C, 150 rpm, overnight.

Conversion based on peak areas; products are identified by GC-MS; n.d. not detected.

Substrate	TRI Conversion [%]	TRII Conversion [%]
<i>o</i> -phthalaldehyde	n.d.	n.d.
4-methylcyclohexanone	26	19
Cyclohexanone	12	9
Cycloheptanone	n.d.	n.d.
Acetophenone	9	n.d.

TRI and TRII possess both an activity with 4-methylcyclohexanone and cyclohexanone, two non-native substrates, similar to tropinone. However, another similar compound cycloheptanone does not show any activity. Acetophenone can only be reduced by TRI and *o*-phthalaldehyde is not transformed by neither enzymes.

To increase yield and reduce cofactor to catalytic amounts a cofactor recycling system is implemented.

Table 22 Reaction conditions: 10 mM of substrate, 20 mg/mL ADH, 10 mM NADPH, KPi buffer (50 mM, pH 7.0, 2 mM MgCl₂), 5 vol% propan-2-ol, 30 °C, 150 rpm, overnight

Conversion based on peak areas; n.d. not detected.

Substrate	TRI Conversion [%]	TRII Conversion [%]
<i>o</i> -phthalaldehyde	n.d.	n.d.
4-methylcyclohexanone	100	21
Cyclohexanone	100	8
Cycloheptanone	n.d.	n.d.
Acetophenone	98	n.d.

A successful recycling system based on the coupled-substrate approach was implemented by using an oxidizable cosolvent such as isopropanol and showed an almost quantitative conversion of 4-methylcyclohexanone, cyclohexanone and acetophenone for TR I, while the usage of stoichiometric amounts of cofactor just show moderate conversion. The implementation of a recycling system to TRII could not increase the conversion of any product.

5. Conclusion & Outlook

Three different substrates (**1b**, **1c** and **1d**) containing one aldehyde and one ketone with various substituents on the ketone moiety and eleven ADHs were investigated for developing a biocatalytic formal hydroacylation platform and are listed in Figure 75 and Table 23, respectively.

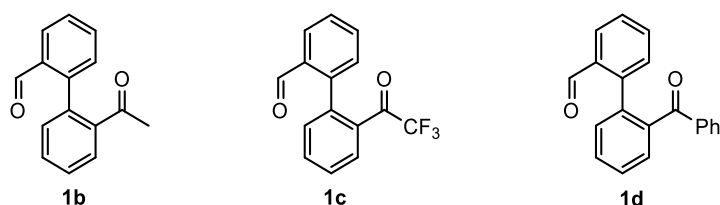


Figure 75 Used keto-aldehyde containing substrates

Table 23 Used ADHs

PEG	Name	Organism	Cofactor
10	ADH-A	<i>Rhodococcus ruber</i> DSM 44541	NADH
53	Sy-ADH	<i>Sphingobium yanoikuyae</i> DSM 6900	NADPH
105	Ras-ADH	<i>Ralstonia</i> sp. DSM 6428	NADPH
180	Lb-ADH	<i>Lactobacillus brevis</i>	NADPH
326	Lk-ADH	<i>Lactobacillus kefir</i> DSM 20587	NADPH
474	Lk-ADH Montelukast	<i>Lactobacillus kefir</i> DSM 20587	NADPH
475	Lk-ADH Lica	<i>Lactobacillus kefir</i> DSM 20587	NADPH
478	Morphine dehydrogenase	<i>Pseudomonas putida</i>	NADH
587	Kp-ADH 50C10	<i>Kluyveromyces polysporus</i>	NADPH
585	Tropinone reductase I	<i>Datura stramonium</i>	NADPH
586	Tropinone reductase II	<i>Datura stramonium</i>	NADPH

A functioning system for substrate **1b** was successfully developed that is able to produce the corresponding lactone in high quantities. The best product yield was achieved with Lk-ADH Lica. Furthermore, by changing the cosolvent from acetonitrile to isopropanol (5 vol%) the product shift to the corresponding lactol was achieved with the same enzyme. Other ADHs such as Sy-ADH and Kp-ADH can be used to reduce the aldehyde and form the hemiketal.

For the substrate **1c** no platform for lactone synthesis was established since all enzymes were incapable of oxidising the intermediate or reducing the aldehyde moiety before the ketone. Under reductive conditions large quantities of lactol and hemiketal were produced.

Similar to the case of **1c** no conversion of **1d** to the desired lactone **2d** was achieved but the hemiketal **4d** was yielded in between 85 and 96 % under reductive conditions with Sy-ADH, Ras-ADH, Lk-ADH, Lk-ADH Lica, Kp-ADH and TR I.

This work contributed to enhance the understanding in several aspects regarding the use of ADHs as biocatalyst, especially for lactone formation using bio Tishchenko-like reactions, and the application of tropinone reductase I and II. The substrate scope of several other enzymes could also be expanded. Furthermore, several new compounds have been synthesised as substrates via Suzuki-coupling and as products of the biotransformation. In the scope of this work the identity and chirality of all products could not be properly identified and are therefore, in need to be completely characterised.

Outlook

The docking study with YASARA and PyMOL is also a point that could get further investigation since several predictions were not matching the experimental data. With adjustments of parameters or different data interpretation such as consideration of the way the substrate must enter the active site, or the angle of the hydride attack the study could produce more accurate result. An additional study is also suggested to enhance activity and selectivity of the tested enzymes tropinone reductase I and II by introducing mutations in critical positions in the binding pocket. Based on the results mutant variants of TR I and TR II could be design and investigated.

To further examine the capabilities of the wild type TR I and TR II more screenings and experiments like a time study should be made to determine important key features for application like TOF and k_{cat} . Additional screening can also serve to optimise reaction conditions and to lower the key parameters such as the used amount of ADH and cofactor. An increase of substrate is also parameter worth of further investigations.

Additional experiments with novel substrates for TR I, TR II and other ADHs could be done to expand their substrate scope. Several well-suited substrates would be compound **1e** to **1k** because these compounds showed promising results in the conducted docking study. Some like **1i** to **1k** for example are predicted to possess much better fits than **1a**, a substrate that is almost completely consumed. Moreover, these experiments could also confirm and serve to refine the data of the docking study.

In conclusion further investigations are needed to further explore the capabilities of the tested enzymes, especially TR I and TR II, regarding bio Tishchenko-like reactions under redox neutral conditions. Further examinations of TR I and TR II should be done, since it is a under investigated ADH with capability of performing several interesting reactions with promising results.

6. Reference:

- [1] X. Chen, Z.-Q. Liu, C.-P. Lin, Y.-G. Zheng, *Bioorg. Chem.* **2016**, *65*, 82.
- [2] A. A. Desai, *Angew. Chem. Int. Ed.* **2011**, *50*, 1974.
- [3] T. Furuya, M. Miura, K. Kino, *ChemBioChem* **2014**, *15*, 2248.
- [4] F. M. Menger, *Acc. Chem. Res.* **1985**, *18*, 128.
- [5] K. Faber, *Biotransformations in organic chemistry. A textbook*, Springer-Verlag Berlin Heidelberg, **2018**.
- [6] C.-S. Chen, C. J. Sih, *Angew. Chem. Int. Ed.* **1989**, *28*, 695.
- [7] W. H. de Camp, *Chirality* **1989**, *1*, 2.
- [8] P. de María, G. de Gonzalo, A. Alcántara, *Catalysts* **2019**, *9*, 802.
- [9] H. Gröger, W. Hummel, C. Rollmann, F. Chamouleau, H. Hüsken, H. Werner, C. Wunderlich, K. Abokitse, K. Drauz, S. Buchholz, *Tetrahedron* **2004**, *60*, 633.
- [10] T. M. Penning, *Chem.-Biol. Interact.* **2015**, *234*, 236.
- [11] T. M. Penning in *Comprehensive Toxicology*, Elsevier, **2018**, S.164–189.
- [12] H. Jörnvall, *Eur. J. Biochem.* **1970**, *14*, 521.
- [13] B. L. Vallee, T. J. Bazzone, *Isozymes* **1983**, *8*, 219.
- [14] R. Bühler, J. Hempel, R. Kaiser, J. P. von Wartburg, B. L. Vallee, H. Jörnvall, *Proc. Natl. Acad. Sci. U. S. A.* **1984**, *81*, 6320.
- [15] S. T. Rao, M. G. Rossmann, *J. Mol. Biol.* **1973**, *76*, 241.
- [16] H. Eklund, B. V. Plapp, J. P. Samama, C. I. Brändén, *J. Biol. Chem.* **1982**, *257*, 14349.
- [17] A. Karlsson, M. El-Ahmad, K. Johansson, J. Shafqat, H. Jörnvall, H. Eklund, S. Ramaswamy, *Chem.-Biol. Interact.* **2003**, *143-144*, 239.
- [18] S. B. Raj, S. Ramaswamy, B. V. Plapp, *Biochemistry* **2014**, *53*, 5791.
- [19] C. Bukh, P. H. Nord-Larsen, S. K. Rasmussen, *J. Exp. Bot.* **2012**, *63*, 6223.
- [20] H. Gröger, W. Hummel, S. Borchert, M. Kraußer in *Enzyme Catalysis in Organic Synthesis, Third Edition*, Wiley - VCH Verlag GmbH & Co. KGaA, **2012**.
- [21] B. Persson, J. Jeffery, H. Jörnvall, *Biochem. Biophys. Res. Commun.* **1991**, *177*, 218.
- [22] S. Krahulec, G. C. Armao, P. Bubner, M. Klimacek, B. Nidetzky, *Chem.-Biol. Interact.* **2009**, *178*, 274.
- [23] K. L. Kavanagh, M. Klimacek, B. Nidetzky, D. K. Wilson, *J. Biol. Chem.* **2002**, *277*, 43433.
- [24] W. Stampfer, B. Kosjek, W. Kroutil, K. Faber, *Biotechnol. Bioeng.* **2003**, *81*, 865.
- [25] B. Kosjek, W. Stampfer, M. Pogorevc, W. Goessler, K. Faber, W. Kroutil, *Biotechnol. Bioeng.* **2004**, *86*, 55.
- [26] G. de Gonzalo, I. Lavandera, K. Faber, W. Kroutil, *Org. Lett.* **2007**, *9*, 2163.

- [27] I. Lavandera, G. Oberdorfer, J. Gross, S. de Wildeman, W. Kroutil, *Eur. J. Org. Chem.* **2008**, 2008, 2539.
- [28] H. Man, K. Kędziora, J. Kulig, A. Frank, I. Lavandera, V. Gotor-Fernández, D. Rother, S. Hart, J. P. Turkenburg, G. Grogan, *Top. Catal.* **2014**, 57, 356.
- [29] J. Liang, J. Lalonde, B. Borup, V. Mitchell, E. Mundorff, N. Trinh, D. A. Kochrekar, R. Nair Cherat, G. G. Pai, *Org. Process Res. Dev.* **2010**, 14, 193.
- [30] N. K. Modukuru, J. Sukumaran, S. J. Collier, A. S. Chan, A. Gohel, G. W. Huisman, R. Keledjian, K. Narayanaswamy, S. J. Novick, S. M. Palanivel et al., *Org. Process Res. Dev.* **2014**, 18, 810.
- [31] Q. Chen, Y. Hu, W. Zhao, C. Zhu, B. Zhu, *Appl. Biochem. Biotechnol.* **2010**, 160, 19.
- [32] N. H. Schlieben, K. Niefind, J. Müller, B. Riebel, W. Hummel, D. Schomburg, *J. Mol. Biol.* **2005**, 349, 801.
- [33] N. C. Bruce, C. J. Wilmot, K. N. Jordan, L. D. Stephens, C. R. Lowe, *J. Mol. Biol.* **1991**, 274 (Pt 3), 875.
- [34] D. L. Willey, D. A. Caswell, C. R. Lowe, N. C. Bruce, *Biochem J.* **1993**, 290 (Pt 2), 539.
- [35] G.-C. Xu, Y. Wang, M.-H. Tang, J.-Y. Zhou, J. Zhao, R.-Z. Han, Y. Ni, *ACS Catal.* **2018**, 8, 8336.
- [36] K. Nakajima, A. Yamashita, H. Akama, T. Nakatsu, H. Kato, T. Hashimoto, J. Oda, Y. Yamada, *Proc. Natl. Acad. Sci. U. S. A.* **1998**, 95, 4876.
- [37] K. Tauber, M. Hall, W. Kroutil, W. M. F. Fabian, K. Faber, S. M. Glueck, *Biotechnol. Bioeng.* **2011**, 108, 1462.
- [38] T. Eguchi, Y. Kuge, K. Inoue, N. Yoshikawa, K. Mochida, T. Uwajima, *Biosci. Biotechnol. Biochem.* **1992**, 56, 701.
- [39] W. Zhang, K. O'Connor, D. I. C. Wang, Z. Li, *Appl. Environ. Microbiol.* **2009**, 75, 687.
- [40] V. Prachayasittikul, S. Ljung, C. Isarankura-Na-Ayudhya, L. Bülow, *Int. J. Biol. Sci.* **2006**, 2, 10.
- [41] M. Le, G. E. Means, *Enzyme Microb. Technol.* **1998**, 23, 49.
- [42] J. Rocha-Martín, D. Vega, J. M. Bolivar, C. A. Godoy, A. Hidalgo, J. Berenguer, J. M. Guisán, F. López-Gallego, *BMC Biotech.* **2011**, 11, 101.
- [43] M. Nič, J. Jiráč, B. Košata, A. Jenkins, A. McNaught, *IUPAC Compendium of Chemical Terminology*, IUPAC, Research Triangle Park, NC, **2009**.
- [44] S. Cannizzaro, *Justus Liebigs Ann. Chem.* **1853**, 88, 129.
- [45] Z. Wang in *Comprehensive organic name reactions and reagents*, John Wiley & Sons, Hoboken, N.J., **2009**.
- [46] T. Laue, A. Plagens in *Namen- und Schlagwort-Reaktionen der Organischen Chemie*, Vieweg+Teubner Verlag, Wiesbaden, **1998**, S.56–58.
- [47] E. Tassano, K. Faber, M. Hall, *Adv. Synth. Catal.* **2018**, 360, 2742.
- [48] C. Wuensch, H. Lechner, S. M. Glueck, K. Zangger, M. Hall, K. Faber, *ChemCatChem* **2013**, 5, 1744.

- [49] T. Seki, T. Nakajo, M. Onaka, *Chem. Lett.* **2006**, *35*, 824.
- [50] S. A. Morris, D. G. Gusev, *Angew. Chem. Int. Ed.* **2017**, *56*, 6228.
- [51] M. Nielsen, H. Junge, A. Kammer, M. Beller, *Angew. Chem. Int. Ed.* **2012**, *51*, 5711.
- [52] Y. Ogata, A. Kawasaki, *Tetrahedron* **1969**, *25*, 929.
- [53] E. Tassano, K. Merusic, I. Buljubasic, O. Laggner, T. Reiter, A. Vogel, M. Hall, *Chem. Commun.* **2020**, *56*, 6340.
- [54] T. Y. Zhang, M. J. Allen, *Tetrahedron Lett.* **1999**, *40*, 5813.
- [55] L. Liu, Y. Zhang, Y. Wang, *J. Org. Chem.* **2005**, *70*, 6122.
- [56] A. L. Casado, P. Espinet, *Organometallics* **1998**, *17*, 954.
- [57] J. K. Stille, K. S. Y. Lau, *Acc. Chem. Res.* **1977**, *10*, 434.
- [58] B. H. Ridgway, K. A. Woerpel, *J. Org. Chem.* **1998**, *63*, 458.
- [59] M. C. Willis, *Chem. Rev.* **2010**, *110*, 725.
- [60] N. R. Vautravers, D. D. Regent, B. Breit, *Chem. Commun.* **2011**, *47*, 6635.
- [61] D. H. T. Phan, B. Kim, V. M. Dong, *J. Am. Chem. Soc.* **2009**, *131*, 15608.
- [62] B. Bosnich, *Acc. Chem. Res.* **1998**, *31*, 667.
- [63] Z. Shen, H. A. Khan, V. M. Dong, *J. Am. Chem. Soc.* **2008**, *130*, 2916.
- [64] H. A. Khan, K. G. M. Kou, V. M. Dong, *Chem. Sci.* **2011**, *2*, 407.
- [65] H. Land, M. S. Humble, *Methods Mol. Biol.* **2018**, *1685*, 43.
- [66] S. Yuan, H. S. Chan, Z. Hu, *WIREs Comput. Mol. Sci.* **2017**, *7*, e1298.
- [67] S. P. France, G. A. Aleku, M. Sharma, J. Mangas-Sanchez, R. M. Howard, J. Steflik, R. Kumar, R. W. Adams, I. Slabu, R. Crook et al., *Angew. Chem. Int. Ed.* **2017**, *56*, 15589.

List of Figures

Figure 1 Mechanism of reduction (left) and oxidation (right) of an aldehyde or ketone by an Aldo-keto reductase.....	13
Figure 2 Mechanism of reduction of an aldehyde or ketone by an SDR.....	14
Figure 3 The Prelog's rule in the reduction of carbonyl by dehydrogenases.....	18
Figure 4 Concept of a general cofactor recycling system for reducing ketones/ aldehydes	19
Figure 5 Concept of a cofactor recycling system for reducing ketones/ aldehydes using isopropanol as a reducing agent.....	19
Figure 6 Concept of a cofactor recycling system for reducing ketones/ aldehydes using glucose as a reducing agent.....	20
Figure 7 Concept of a cofactor recycling system for reducing ketones/ aldehydes using formate as a reducing agent.....	21
Figure 8 Concept of a cofactor recycling system for reducing ketones/ aldehydes using phosphite as a reducing agent.....	21
Figure 9 Concept of a general cofactor recycling system for oxidising alcohols.....	21
Figure 10 Concept of a cofactor recycling system for reducing ketones/aldehydes using pyruvate as an oxidising agent.....	22
Figure 11 Concept of a cofactor recycling system for reducing ketones/ aldehydes using α -ketoglutarate as an oxidising agent	22
Figure 12 Concept of a cofactor recycling system for reducing ketones/ aldehydes using oxygen as an oxidising agent.....	22
Figure 13 General scheme of a disproportionation	24
Figure 14 The Cannizzaro reaction	24
Figure 15 Mechanism of the Cannizzaro reaction.....	24
Figure 16 Biocatalytic Cannizzaro reaction catalysed by alcohol dehydrogenase (ADH)	25
Figure 17 The Tishchenko reaction	26
Figure 18 Mechanism and catalytic cycle of a general Tishchenko reaction after the Ogata–Kawasaki model The Tishchenko Reaction: A Classic and Practical Tool for Ester Synthesis	27
Figure 19 Biocatalytic Tishchenko reaction catalysed by alcohol dehydrogenase (ADH).....	28
Figure 20 Biocatalytic intermolecular Tishchenko reaction.....	28
Figure 21 The Suzuki-Miyaura reaction.....	29
Figure 22 Mechanism/ Catalytic cycle of a Suzuki-Miyaura reaction.....	29
Figure 23 The cis/trans isomerisation of the palladium complex	30
Figure 24 Conservation of cis/trans configuration in Suzuki-Miyaura reactions	30

Figure 25 The hydroacylation reaction(left) and intramolecular hydroacylation reaction(right).....	31
Figure 26 The intramolecular hydroacylation reaction forming a lactone	31
Figure 27 Mechanism and catalytic cycle of hydroacylation reactions.....	32
Figure 28 Mechanism of intramolecular hydroacylation reaction with a long chain on the ketone (top) and a short chain on the ketone (bottom).....	32
Figure 29 Reaction system for a keto-aldehyde substrate with reduction of the aldehyde(left) and the ketone(right) including the cofactor recycling system.....	33
Figure 30 Substrates 1b , 1c and 1d	34
Figure 31 Tested substrates 1b , 1c and 1d	35
Figure 32 Aldol-condensation of 1b to side product 5b	35
Figure 33 reaction route to 2a	44
Figure 34 Substrate 1a in TRI with oxidised cofactor and amino acid side chains that can stabilize the substrate.....	45
Figure 35 Intermediate 3a in TRI with oxidised cofactor and amino acid side chains that can stabilize the intermediate	46
Figure 36 Substrate 1a in TRII with oxidised cofactor and amino acid side chains that can stabilize the substrate.....	47
Figure 37 Intermediate 3a in TRII with reduced cofactor and amino acid side chains that can stabilize the intermediate	48
Figure 38 Reaction routes to (R) - 2b-d and to (S) - 2b-d	49
Figure 39 Side reaction to 4b-d	49
Figure 40 Substrate 1b in TRI with oxidised cofactor and amino acid side chains that can stabilize the substrate (Orientation of the ketone towards the cofactor)	50
Figure 41 Substrate 1b in TRI with oxidised cofactor and amino acid side chains that can stabilize the substrate (Orientation of the aldehyde towards the cofactor)	50
Figure 42 Intermediate 3b in TRI with reduced cofactor and amino acid side chains that can stabilize the intermediate	51
Figure 43 Structure of (R,S) - 3b	51
Figure 44 Substrate 1b in TRII with oxidised cofactor and amino acid side chains that can stabilize the substrate (Orientation of the ketone towards the cofactor)	52
Figure 45 Substrate 1b in TRII with oxidised cofactor and amino acid side chains that can stabilize the substrate (Orientation of the aldehyde towards the cofactor)	52
Figure 46 Substrate 1c in TRI with oxidised cofactor and amino acid side chains that can stabilize the substrate.....	53

Figure 47 Intermediate 3c in TRI with reduced cofactor and amino acid side chains that can stabilize the intermediate	54
Figure 48 Substrate 1c in TRII with oxidised cofactor and amino acid side chains that can stabilize the substrate (Orientation of the ketone towards the cofactor)	55
Figure 49 Substrate 1c in TRII with oxidised cofactor and amino acid side chains that can stabilize the substrate (Orientation of the aldehyde towards the cofactor)	55
Figure 50 Substrate 1d in TRI with oxidised cofactor and amino acid side chains that can stabilize the substrate (Orientation of the ketone towards the cofactor)	56
Figure 51 Substrate 1d in TRI with oxidised cofactor and amino acid side chains that can stabilize the substrate (Orientation of the aldehyde towards the cofactor)	56
Figure 52 Intermediate 3d in TRII with reduced cofactor and amino acid side chains that can stabilize the intermediate	57
Figure 53 Structure of (aR,R)-3d	57
Figure 54 Substrate 1d in TRII with oxidised cofactor and amino acid side chains that can stabilize the substrate (Orientation of the ketone towards the cofactor)	58
Figure 55 Substrate 1d in TRII with oxidised cofactor and amino acid side chains that can stabilize the substrate (Orientation of the aldehyde towards the cofactor)	58
Figure 56 Intermediate 3d in TRII with reduced cofactor and amino acid side chains that can stabilize the intermediate	59
Figure 57 Structure of (aR,S)-3d	59
Figure 58 Biotransformation of 1a using TR I and TR II with 5 vol% CH ₃ CN.....	60
Figure 59 Biotransformation of 1a using TR I and TR II with 5 vol% propan-2-ol	60
Figure 60 Biotransformation of 1b with 5 vol% CH ₃ CN.....	61
Figure 61 Biotransformation of 1b with 5 vol% propan-2-ol	65
Figure 62 Biotransformation of 1c with 5 vol% CH ₃ CN	68
Figure 63 Biotransformation of 1c with 5 vol% propan-2-ol.....	71
Figure 64 Biotransformation of 1d with 5 vol% CH ₃ CN.....	74
Figure 65 Possible dericted chiral axis of product 4d	75
Figure 66 Biotransformation of 1d with 5 vol% propan-2-ol	77
Figure 67 Scheme of up-scale biotransformation of 1b to 3b	81
Figure 68 Scheme of up-scale biotransformation of 1b to 4b	83
Figure 69 Scheme of up-scale biotransformation of 1c to 4c	84
Figure 70 Scheme of up-scale biotransformation of 1c to 3c	85
Figure 71 Scheme of up-scale biotransformation of 1c	86
Figure 72 Scheme of up-scale biotransformation of 1d to 4d	87

Figure 73 General synthesis of substrates 1b-1d	90
Figure 74 General scheme of a biotransformation for bio-Tishchenko-like reactions	91
Figure 75 Used keto-aldehyde containing substrates	105

List of Tables

Table 1 Information of ADHs used in this work.....	16
Table 2 Specificity regarding the Prelog's rule of several prominent ADHs.....	18
Table 3 List of used enzymes.....	36
Table 4 Overview of reaction prediction for substrates 1a-k based on docking using YASARA and PyMOL Distance of substrate to cofactor is measured between the carbonyl carbon and the hydride of the cofactor (NADPH)	38
Table 5 Comparison of the predicted and experimental data of substrates 1a to 1d	42
Table 6 Reaction conditions: 10 mM of 1a , 20 mg/mL TR I/TR II, 0.5 mM NADPH, KPi buffer (50 mM, pH 7.0, 2 mM MgCl ₂), 5 vol% CH ₃ CN, 30 °C, 150 rpm, overnight. Conversion based on GC (HP-5) peak areas	60
Table 7 Reaction conditions: 10 mM of 1a , 20 mg/mL TR I/TR II, 0.5 mM NADPH, KPi buffer (50 mM, pH 7.0, 2 mM MgCl ₂), 5 vol% propan-2-ol, 30 °C, 150 rpm, overnight. Conversion based on GC (HP-5) peak areas	60
Table 8 predated products and the reaction conditions.....	80
Table 9 Up-scale reaction conditions, substrate consumption, main product and conversion.....	80
Table 10 Reaction conditions: 10 mM of 1b , 20 mg/mL ADH, 0.5 mM NADPH, KPi buffer (50 mM, pH 7.0, 2 mM MgCl ₂), 5 vol% isopropanol, 30 °C, 150 rpm, overnight.....	81
Table 11 Reaction conditions: 10 mM of 1b , 20 mg/mL ADH, 0.5 mM NADPH, KPi buffer (50 mM, pH 7.0, 2 mM MgCl ₂), 5 vol% isopropanol, 30 °C, 150 rpm, overnight.....	82
Table 12 Reaction conditions: 10 mM of 1b , 20 mg/mL ADH, 0.5 mM NADPH, KPi buffer (50 mM, pH 7.0, 2 mM MgCl ₂), 5 vol% isopropanol, 30 °C, 150 rpm, overnight.....	83
Table 13 Reaction conditions: 10 mM of 1c , 20 mg/mL ADH, 0.5 mM NADPH, KPi buffer (50 mM, pH 7.0, 2 mM MgCl ₂), 5 vol% isopropanol, 30 °C, 150 rpm, overnight.....	84
Table 14 Reaction conditions: 10 mM of 1c , 20 mg/mL ADH, 0,5 mM NADPH, KPi buffer (50 mM, pH 7.0, 2 mM MgCl ₂), 5 vol% isopropanol, 30 °C, 150 rpm, overnight.....	84
Table 15 Reaction conditions: 10 mM of 1c , 20 mg/mL ADH, 0.5 mM NADPH, KPi buffer (50 mM, pH 7.0, 2 mM MgCl ₂), 5 vol% isopropanol, 30 °C, 150 rpm, overnight.....	85
Table 16 Reaction conditions: 10 mM of 1c , 20 mg/mL ADH, 0.5 mM NADPH, KPi buffer (50 mM, pH 7.0, 2 mM MgCl ₂), 5 vol% isopropanol, 30 °C, 150 rpm, overnight.....	85
Table 17 Reaction conditions: 10 mM of 1c , 20 mg/mL ADH, 0.5 mM NADPH for screening and stoichiometric NADPH for up-scale, KPi buffer (50 mM, pH 7.0, 2 mM MgCl ₂), 5 vol% isopropanol, 30 °C, 150 rpm, overnight	86
Table 18 Reaction conditions: 10 mM of 1d , 20 mg/mL ADH, 0.5 mM NADPH, KPi buffer (50 mM, pH 7.0, 2 mM MgCl ₂), 5 vol% isopropanol, 30 °C, 150 rpm, overnight.....	87

Table 19 used condition for cultivation and expression of TR II in BL21 DE3	99
Table 20 used condition for cultivation and expression of TR II	100
Table 21 Reaction conditions: 10 mM of substrate, 20 mg/mL ADH, 10 mM NADPH, KPi buffer (50 mM, pH 7.0, 2 mM MgCl ₂), 5 vol% CH ₃ CN, 30 °C, 150 rpm, overnight Conversion based on peak areas; products are identified by GC-MS; n.d. not detected.	104
Table 22 Reaction conditions: 10 mM of substrate, 20 mg/mL ADH, 10 mM NADPH, KPi buffer (50 mM, pH 7.0, 2 mM MgCl ₂), 5 vol% propan-2-ol, 30 °C, 150 rpm, overnight Conversion based on peak areas; n.d. not detected.	104
Table 23 Used ADHs	105
Table 25 Norm values Reaction conditions: 10 mM of 1b , 20 mg/mL ADH, 0.5 mM NADPH, KPi buffer (50 mM, pH 7.0, 2 mM MgCl ₂), 5 vol% CH ₃ CN, 30 °C, 150 rpm, overnight Norm. value based relation of peak areas of compounds to peak area of IS Areas are measured on GC (HP-5)	120
Table 26 Norm values (chiral analysis) Reaction conditions: 10 mM of 1b , 20 mg/mL ADH, 0.5 mM NADPH, KPi buffer (50 mM, pH 7.0, 2 mM MgCl ₂), 5 vol% CH ₃ CN, 30 °C, 150 rpm, overnight. Norm. value based relation of peak areas of compounds to peak area of IS Areas are measured on GC (CB-Dex).....	120
Table 27 Norm values Reaction conditions: 10 mM of 1b , 20 mg/mL ADH, 0.5 mM NADPH, KPi buffer (50 mM, pH 7.0, 2 mM MgCl ₂), 5 vol% propan-2-ol, 30 °C, 150 rpm, overnight Norm. value based relation of peak areas of compounds to peak area of IS Areas are measured on GC (HP-5)	121
Table 28 Norm values (chiral analysis) Reaction conditions: 10 mM of 1b , 20 mg/mL ADH, 0.5 mM NADPH, KPi buffer (50 mM, pH 7.0, 2 mM MgCl ₂), 5 vol% propan-2-ol, 30 °C, 150 rpm, overnight. Norm. value based relation of peak areas of compounds to peak area of IS Areas are measured on GC (CB-Dex).....	121
Table 29 Norm values Reaction conditions: 10 mM of 1c , 20 mg/mL ADH, 0.5 mM NADPH, KPi buffer (50 mM, pH 7.0, 2 mM MgCl ₂), 5 vol% CH ₃ CN, 30 °C, 150 rpm, overnight Norm. value based relation of peak areas of compounds to peak area of IS Areas are measured on GC (HP-5)	122
Table 30 Norm values (chiral analysis) Reaction conditions: 10 mM of 1c , 20 mg/mL ADH, 0.5 mM NADPH, KPi buffer (50 mM, pH 7.0, 2 mM MgCl ₂), 5 vol% CH ₃ CN, 30 °C, 150 rpm, overnight. Norm. value based relation of peak areas of compounds to peak area of IS Areas are measured on GC (CB-Dex).....	122
Table 31 Norm values Reaction conditions: 10 mM of 1c , 20 mg/mL ADH, 0.5 mM NADPH, KPi buffer (50 mM, pH 7.0, 2 mM MgCl ₂), 5 vol% propan-2-ol, 30 °C, 150 rpm, overnight. Norm. value based relation of peak areas of compounds to peak area of IS Areas are measured on GC (HP-5)	123
Table 32 Norm values (chiral analysis) Reaction conditions: 10 mM of 1c , 20 mg/mL ADH, 0.5 mM NADPH, KPi buffer (50 mM, pH 7.0, 2 mM MgCl ₂), 5 vol% propan-2-ol, 30 °C, 150 rpm, overnight Norm.	

value based relation of peak areas of compounds to peak area of IS Areas are measured on GC (CB-Dex).....	123
Table 33 Norm values Reaction conditions: 10 mM of 1c , 20 mg/mL ADH, 0.5 mM NADPH, KPi buffer (50 mM, pH 7.0, 2 mM MgCl ₂), 5 vol% propan-2-ol, 30 °C, 150 rpm, overnight Norm. value based relation of peak areas of compounds to peak area of IS Areas are measured on GC (HP-5)	124
Table 34 Norm values Reaction conditions: 10 mM of 1c , 20 mg/mL ADH, 0.5 mM NADPH, KPi buffer (50 mM, pH 7.0, 2 mM MgCl ₂), 5 vol% CH ₃ CN, 30 °C, 150 rpm, overnight Norm. value based relation of peak areas of compounds to peak area of IS Areas are measured on GC (HP-5)	124

List of Graphs

Graph 1 Reaction conditions: 10 mM of 1b , 20 mg/mL ADH, 0.5 mM NADPH, KPi buffer (50 mM, pH 7.0, 2 mM MgCl ₂), 5 vol% CH ₃ CN, 30 °C, 150 rpm, overnight, Conversion based on GC (CB-Dex) peak areas	61
Graph 2 Substrate consumption based on calibration (blue) and total peak areas (orange) Reaction conditions: 10 mM of 1b , 20 mg/mL ADH, 0.5 mM NADPH, KPi buffer (50 mM, pH 7.0, 2 mM MgCl ₂), 5 vol% CH ₃ CN, 30 °C, 150 rpm, overnight.....	62
Graph 3 Reaction conditions: 10 mM of 1b , 20 mg/mL ADH, 0.5 mM NADPH, KPi buffer (50 mM, pH 7.0, 2 mM MgCl ₂), 5 vol% CH ₃ CN, 30 °C, 150 rpm, overnight, Chiral analysis of products, Conversion based on GC (CB-Dex) peak areas	63
Graph 4 Reaction conditions: 10 mM of 1b , 20 mg/mL ADH, 0.5 mM NADPH, KPi buffer (50 mM, pH 7.0, 2 mM MgCl ₂), 5 vol% propan-2-ol, 30 °C, 150 rpm, overnight Conversion based on GC (HP-5) peak areas	65
Graph 5 Substrate consumption based on calibration (blue) and total peak areas (orange) Reaction conditions: 10 mM of 1b , 20 mg/mL ADH, 0.5 mM NADPH, KPi buffer (50 mM, pH 7.0, 2 mM MgCl ₂), 5 vol% propan-2-ol, 30 °C, 150 rpm, overnight.....	66
Graph 6 Reaction conditions: 10 mM of 1b , 20 mg/mL ADH, 0.5 mM NADPH, KPi buffer (50 mM, pH 7.0, 2 mM MgCl ₂), 5 vol% propan-2-ol, 30 °C, 150 rpm, overnight Chiral analysis of products Conversion based on GC (CB-Dex) peak areas	67
Graph 7 Reaction conditions: 10 mM of 1c , 20 mg/mL ADH, 0.5 mM NADPH, KPi buffer (50 mM, pH 7.0, 2 mM MgCl ₂), 5 vol% CH ₃ CN, 30 °C, 150 rpm, overnight Conversion based on GC (HP-5) peak areas	68
Graph 8 Substrate consumption based on calibration (blue) and total peak areas (orange) Reaction conditions: 10 mM of 1c , 20 mg/mL ADH, 0.5 mM NADPH, KPi buffer (50 mM, pH 7.0, 2 mM MgCl ₂), 5 vol% CH ₃ CN, 30 °C, 150 rpm, overnight.....	69
Graph 9 Reaction conditions: 10 mM of 1c , 20 mg/mL ADH, 0.5 mM NADPH, KPi buffer (50 mM, pH 7.0, 2 mM MgCl ₂), 5 vol% CH ₃ CN, 30 °C, 150 rpm, overnight Chiral analysis of products Conversion based on GC (CB-Dex) peak areas.....	70
Graph 10 Reaction conditions: 10 mM of 1c , 20 mg/mL ADH, 0.5 mM NADPH, KPi buffer (50 mM, pH 7.0, 2 mM MgCl ₂), 5 vol% propan-2-ol, 30 °C, 150 rpm, overnight Conversion based on GC (HP-5) peak areas	71
Graph 11 Substrate consumption based on calibration (blue) and total peak areas (orange) Reaction conditions: 10 mM of 1c , 20 mg/mL ADH, 0.5 mM NADPH, KPi buffer (50 mM, pH 7.0, 2 mM MgCl ₂), 5 vol% propan-2-ol, 30 °C, 150 rpm, overnight.....	72

Graph 12 Reaction conditions: 10 mM of 1c , 20 mg/mL ADH, 0.5 mM NADPH, KPi buffer (50 mM, pH 7.0, 2 mM MgCl ₂), 5 vol% propan-2-ol, 30 °C, 150 rpm, overnight Chiral analysis of products Conversion based on GC (CB-Dex) peak areas	73
Graph 13 Reaction conditions: 10 mM of 1d , 20 mg/mL ADH, 0.5 mM NADPH, KPi buffer (50 mM, pH 7.0, 2 mM MgCl ₂), 5 vol% CH ₃ CN, 30 °C, 150 rpm, overnight Conversion based on GC (HP-5) peak areas	74
Graph 14 Substrate consumption based on calibration (blue) and total peak areas (orange) Reaction conditions: 10 mM of 1c , 20 mg/mL ADH, 0.5 mM NADPH, KPi buffer (50 mM, pH 7.0, 2 mM MgCl ₂), 5 vol% CH ₃ CN, 30 °C, 150 rpm, overnight.....	75
Graph 15 Reaction conditions: 10 mM of 1d , 20 mg/mL ADH, 0.5 mM NADPH, KPi buffer (50 mM, pH 7.0, 2 mM MgCl ₂), 5 vol% CH ₃ CN, 30 °C, 150 rpm, overnight Conversion based on chiral HPLC (chiral pack C) peak areas.....	76
Graph 16 Reaction conditions: 10 mM of 1d , 20 mg/mL ADH, 0.5 mM NADPH, KPi buffer (50 mM, pH 7.0, 2 mM MgCl ₂), 5 vol% propan-2-ol, 30 °C, 150 rpm, overnight Conversion based on GC (HP-5) peak areas	77
Graph 17 Substrate consumption based on calibration (blue) and total peak areas (orange) Reaction conditions: 10 mM of 1d , 20 mg/mL ADH, 0.5 mM NADPH, KPi buffer (50 mM, pH 7.0, 2 mM MgCl ₂), 5 vol% propan-2-ol, 30 °C, 150 rpm, overnight.....	78
Graph 18 Reaction conditions: 10 mM of 1d , 20 mg/mL ADH, 0.5 mM NADPH, KPi buffer (50 mM, pH 7.0, 2 mM MgCl ₂), 5 vol% propan-2-ol, 30 °C, 150 rpm, overnight Conversion based on chiral HPLC (chiral pack C) peak areas.....	79

7. Appendix

Table 24 Norm values

Reaction conditions: 10 mM of **1b**, 20 mg/mL ADH, 0.5 mM NADPH, KPi buffer (50 mM, pH 7.0, 2 mM MgCl₂), 5 vol% CH₃CN, 30 °C, 150 rpm, overnight.

Norm. value based relation of peak areas of compounds to peak area of IS

Areas are measured on GC (HP-5)

entry	1b Norm	2b Norm	3b Norm	4b Norm	5b Norm
blank	1,120	0,000	0,000	0,000	0,000
ADH-A	1,074	0,212	0,005	0,000	0,018
Sy-ADJ	0,589	0,023	0,003	0,061	0,056
Ras-ADH	0,841	0,057	0,005	0,114	0,044
Lb-ADH	0,978	0,029	0,005	0,010	0,024
Lk-ADH	0,831	0,050	0,004	0,023	0,022
Lk-ADH Monte	0,894	0,074	0,005	0,021	0,028
Lk-ADH Lica	0,007	0,585	0,003	0,076	0,012
Morphine DH	0,990	0,012	0,005	0,029	0,038
Kp-ADH	0,483	0,226	0,003	0,143	0,037
TR I	0,403	0,136	0,002	0,131	0,037
TR II	0,383	0,440	0,006	0,121	0,021

Table 25 Norm values (chiral analysis)

Reaction conditions: 10 mM of **1b**, 20 mg/mL ADH, 0.5 mM NADPH, KPi buffer (50 mM, pH 7.0, 2 mM MgCl₂), 5 vol% CH₃CN, 30 °C, 150 rpm, overnight.

Norm. value based relation of peak areas of compounds to peak area of IS

Areas are measured on GC (CB-Dex)

Entry	1b Norm	2b Norm	ee	3b Norm	ee	4b Norm	5b Norm
blank	0,932	0,005	n.d.	0,000	n.d.	0,000	0,000
ADH-A	0,917	0,233	>99	0,001	n.d.	0,038	0,036
Sy-ADJ	0,572	0,011	>99	0,056	n.d.	0,031	0,053
Ras-ADH	0,383	0,032	>99	0,224	n.d.	0,031	0,046
Lb-ADH	0,650	0,023	>99	0,000	n.d.	0,037	0,029
Lk-ADH	0,494	0,052	>99	0,000	n.d.	0,054	0,023
Lk-ADH Monte	0,612	0,059	>99	0,000	n.d.	0,020	0,028
Lk-ADH Lica	0,058	0,626	43	0,153	n.d.	0,034	0,006
Morphine DH	0,637	0,016	>99	0,000	n.d.	0,017	0,031
Kp-ADH	0,591	0,141	>99	0,134	n.d.	0,032	0,026
TR I	0,456	0,070	>99	0,099	n.d.	0,026	0,020
TR II	0,148	0,263	>99	0,000	n.d.	0,442	0,009

Table 26 Norm values

Reaction conditions: 10 mM of **1b**, 20 mg/mL ADH, 0.5 mM NADPH, KPi buffer (50 mM, pH 7.0, 2 mM MgCl₂), 5 vol% propan-2-ol, 30 °C, 150 rpm, overnight.

Norm. value based relation of peak areas of compounds to peak area of IS

Areas are measured on GC (HP-5)

Entry	1b Norm	2b Norm	ee	3b Norm	ee	4b Norm	5b Norm
blank	1,190	0,000	n.d.	0,000	n.d.	0,000	0,023
ADH-A	0,706	0,276	>99	0,000	n.d.	0,050	0,031
Sy-ADJ	0,057	0,005	n.d.	0,000	n.d.	1,200	0,012
Ras-ADH	0,041	0,010	n.d.	0,149	n.d.	0,939	0,006
Lb-ADH	0,262	0,030	n.d.	0,000	n.d.	0,625	0,023
Lk-ADH	0,068	0,040	>99	0,000	>99	0,988	0,010
Lk-ADH Monte	0,450	0,090	>99	0,000	n.d.	0,198	0,029
Lk-ADH Lica	0,012	0,133	>99	1,028	>99	0,000	0,002
Morphine DH	0,730	0,014	>99	0,000	n.d.	0,029	0,041
Kp-ADH	0,107	0,012	n.d.	0,000	n.d.	1,166	0,004
TR I	0,036	0,009	>99	0,078	>99	1,144	0,003
TR II	0,279	0,302	>99	0,000	>99	0,096	0,009

Table 27 Norm values (chiral analysis)

Reaction conditions: 10 mM of **1b**, 20 mg/mL ADH, 0.5 mM NADPH, KPi buffer (50 mM, pH 7.0, 2 mM MgCl₂), 5 vol% propan-2-ol, 30 °C, 150 rpm, overnight.

Norm. value based relation of peak areas of compounds to peak area of IS

Areas are measured on GC (CB-Dex)

Entry	1b Norm	2b Norm	ee	3b Norm	ee	4b Norm	5b Norm
blank	3,891	0,000	n.d.	0,000	n.d.	0,000	0,000
ADH-A	1,034	0,418	>99	0,000	n.d.	0,000	0,000
Sy-ADJ	0,079	0,000	n.d.	0,000	n.d.	0,655	0,000
Ras-ADH	0,085	0,000	n.d.	0,000	n.d.	0,764	0,000
Lb-ADH	0,206	0,000	n.d.	0,000	n.d.	0,335	0,000
Lk-ADH	0,136	0,079	>99	0,051	>99	0,912	0,016
Lk-ADH Monte	0,780	0,174	>99	0,000	n.d.	0,151	0,003
Lk-ADH Lica	0,010	0,212	>99	1,872	>99	0,000	0,000
Morphine DH	1,382	0,030	>99	0,000	n.d.	0,000	0,092
Kp-ADH	0,153	0,000	n.d.	0,000	n.d.	0,719	0,000
TR I	0,065	0,018	>99	0,139	>99	0,893	0,000
TR II	0,489	0,591	>99	0,020	>99	0,088	0,010

Table 28 Norm values

Reaction conditions: 10 mM of **1c**, 20 mg/mL ADH, 0.5 mM NADPH, KPi buffer (50 mM, pH 7.0, 2 mM MgCl₂), 5 vol% CH₃CN, 30 °C, 150 rpm, overnight.

Norm. value based relation of peak areas of compounds to peak area of IS

Areas are measured on GC (HP-5)

Entry	1c Norm	2c Norm	3c Norm	4c Norm
blank	1,267	0,113	0,000	0,000
ADH-A	0,992	0,076	0,019	0,000
Sy-ADJ	1,112	0,078	0,000	0,004
Ras-ADH	0,971	0,072	0,014	0,009
Lb-ADH	0,991	0,070	0,017	0,000
Lk-ADH	0,856	0,064	0,017	0,000
Lk-ADH Monte	0,967	0,073	0,018	0,003
Lk-ADH Lica	0,614	0,073	0,003	0,270
Morphine DH	1,015	0,070	0,013	0,009
Kp-ADH	1,049	0,080	0,004	0,033
TR I	0,978	0,075	0,000	0,035
TR II	0,807	0,093	0,003	0,000

Table 29 Norm values (chiral analysis)

Reaction conditions: 10 mM of **1c**, 20 mg/mL ADH, 0.5 mM NADPH, KPi buffer (50 mM, pH 7.0, 2 mM MgCl₂), 5 vol% CH₃CN, 30 °C, 150 rpm, overnight.

Norm. value based relation of peak areas of compounds to peak area of IS

Areas are measured on GC (CB-Dex)

Entry	1c Norm	2c Norm	ee	3c Norm	ee	4c Norm	ee
blank	1,242	0,237	n.d.	0,000	n.d.	0,000	n.d.
ADH-A	1,100	0,179	1	0,000	n.d.	0,011	>99
Sy-ADJ	1,094	0,181	n.d.	0,000	n.d.	0,020	>99
Ras-ADH	1,209	0,197	n.d.	0,000	n.d.	0,030	>99
Lb-ADH	1,033	0,160	1	0,000	n.d.	0,016	>99
Lk-ADH	1,089	0,177	1	0,000	n.d.	0,014	>99
Lk-ADH Monte	1,111	0,186	1	0,000	n.d.	0,020	>99
Lk-ADH Lica	0,543	0,183	1	0,000	n.d.	0,356	>99
Morphine DH	1,080	0,173	n.d.	0,000	n.d.	0,010	>99
Kp-ADH	1,067	0,185	1	0,000	n.d.	0,069	>99
TR I	1,140	0,188	1	0,000	n.d.	0,014	>99
TR II	1,080	0,196	1	0,000	n.d.	0,014	>99

Table 30 Norm values

Reaction conditions: 10 mM of **1c**, 20 mg/mL ADH, 0.5 mM NADPH, KPi buffer (50 mM, pH 7.0, 2 mM MgCl₂), 5 vol% propan-2-ol, 30 °C, 150 rpm, overnight.

Norm. value based relation of peak areas of compounds to peak area of IS

Areas are measured on GC (HP-5)

Entry	1c Norm	2c Norm	ee	3c Norm	ee	4c Norm	ee
blank	1,403	0,188	2	0,000	n.d.	0,000	n.d.
ADH-A	1,173	0,126	2	0,000	n.d.	0,000	>99
Sy-ADJ	0,047	0,121	2	0,694	n.d.	0,600	>99
Ras-ADH	0,033	0,089	2	0,629	n.d.	0,699	>99
Lb-ADH	1,000	0,113	1	0,000	n.d.	0,103	>99
Lk-ADH	0,647	0,081	1	0,000	n.d.	0,161	>99
Lk-ADH Monte	1,049	0,122	0	0,000	n.d.	0,056	>99
Lk-ADH Lica	0,033	0,118	11	0,020	n.d.	1,879	>99
Morphine DH	1,182	0,124	1	0,000	n.d.	0,000	>99
Kp-ADH	0,118	0,104	8	0,000	n.d.	1,255	>99
TR I	0,034	0,008	36	1,115	>99	0,082	>99
TR II	0,887	0,110	1	0,002	n.d.	0,000	>99

Table 31 Norm values (chiral analysis)

Reaction conditions: 10 mM of **1c**, 20 mg/mL ADH, 0.5 mM NADPH, KPi buffer (50 mM, pH 7.0, 2 mM MgCl₂), 5 vol% propan-2-ol, 30 °C, 150 rpm, overnight.

Norm. value based relation of peak areas of compounds to peak area of IS

Areas are measured on GC (CB-Dex)

Entry	1c Norm	2c Norm	ee	3c Norm	ee	4c Norm	ee
blank	3,473	0,432	2	0,000	n.d.	0,000	n.d.
ADH-A	1,462	0,160	2	0,000	n.d.	0,019	>99
Sy-ADJ	0,107	0,265	2	0,000	n.d.	1,317	>99
Ras-ADH	0,069	0,163	2	0,000	n.d.	1,296	>99
Lb-ADH	1,950	0,224	1	0,000	n.d.	0,205	>99
Lk-ADH	1,477	0,189	1	0,000	n.d.	0,361	>99
Lk-ADH Monte	1,708	0,200	n.d.	0,000	n.d.	0,106	>99
Lk-ADH Lica	0,067	0,218	11	0,000	n.d.	2,739	>99
Morphine DH	1,442	0,174	1	0,000	n.d.	0,005	>99
Kp-ADH	0,219	0,189	8	0,000	n.d.	2,273	>99
TR I	0,056	0,017	36	1,789	>99	0,113	>99
TR II	1,235	0,152	1	0,000	n.d.	0,023	>99

Table 32 Norm values

Reaction conditions: 10 mM of **1c**, 20 mg/mL ADH, 0.5 mM NADPH, KPi buffer (50 mM, pH 7.0, 2 mM MgCl₂), 5 vol% propan-2-ol, 30 °C, 150 rpm, overnight.

Norm. value based relation of peak areas of compounds to peak area of IS

Areas are measured on GC (HP-5)

Entry	1d Norm	4d (1) Norm	4d (2) Norm
blank	2,109	0,000	0,000
ADH-A	1,893	0,005	0,000
Sy-ADJ	1,640	0,398	0,000
Ras-ADH	1,701	0,152	0,000
Lb-ADH	1,889	0,003	0,005
Lk-ADH	1,841	0,002	0,012
Lk-ADH Monte	1,684	0,002	0,010
Lk-ADH Lica	0,721	0,898	0,000
Morphine DH	1,892	0,003	0,027
Kp-ADH	1,698	0,237	0,127
TR I	1,710	0,195	0,237
TR II	1,842	0,002	0,217

Table 33 Norm values

Reaction conditions: 10 mM of **1c**, 20 mg/mL ADH, 0.5 mM NADPH, KPi buffer (50 mM, pH 7.0, 2 mM MgCl₂), 5 vol% CH₃CN, 30 °C, 150 rpm, overnight.

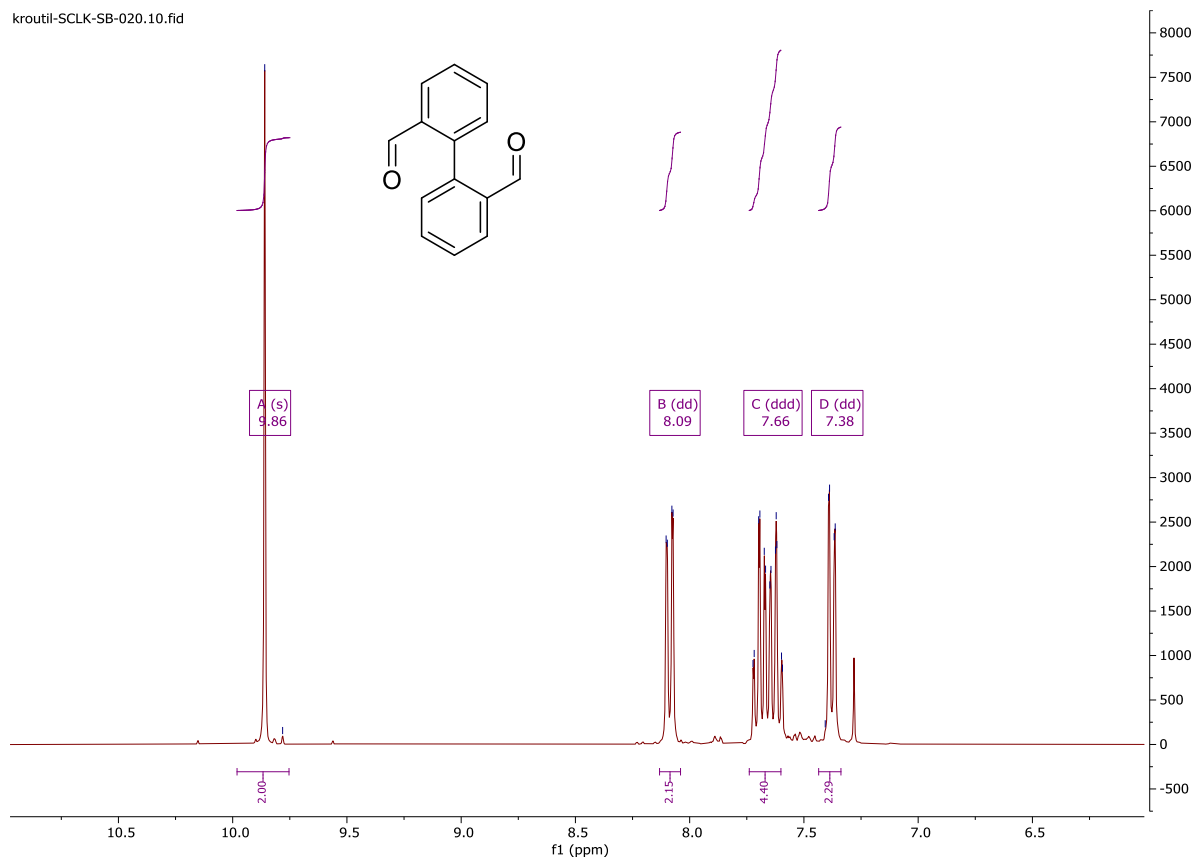
Norm. value based relation of peak areas of compounds to peak area of IS

Areas are measured on GC (HP-5)

Entry	1d Norm	4d (1) Norm	4d (2) Norm
blank	1,764	0,002	0,000
ADH-A	1,171	0,002	0,005
Sy-ADJ	0,034	1,730	0,000
Ras-ADH	0,111	1,426	0,000
Lb-ADH	1,554	0,005	0,076
Lk-ADH	1,240	0,003	0,098
Lk-ADH Monte	1,436	0,003	0,091
Lk-ADH Lica	0,015	0,000	0,120
Morphine DH	1,476	0,003	0,077
Kp-ADH	0,089	1,334	0,000
TR I	0,115	1,444	0,000
TR II	1,110	0,003	0,021

NMR data

kroutil-SCLK-SB-020.10.fid



kroutil-SCLK-SB-020.11.fid

